CORRELATION ANALYSIS ON OPTICAL AND RADIO LIGHT CURVES FOR A LARGE SAMPLE OF ACTIVE GALACTIC NUCLEI

By

SANDRA DENISE CLEMENTS

A DISSERTATION PRESENTED TO THE GRADUATE SCHOOL
OF THE UNIVERSITY OF FLORIDA IN PARTIAL FULFILLMENT
OF THE REQUIREMENTS FOR THE DEGREE OF
DOCTOR OF PHILOSOPHY

UNIVERSITY OF FLORIDA

1992

To my parents, Mary Sue and Warren Clements

ACKNOWLEDGMENTS

I would like to sincerely thank my advisor, Dr. Alex G. Smith, for providing me the opportunity to actively participate in AGN research as an observer at Rosemary Hill Observatory. In addition, I would like to thank him for his valuable suggestions and advice with regard to my research topic.

Dr. Robert Leacock has been very helpful in dealing with the technical and administrative problems that arose during my many years here. For that, I am very grateful. Thanks also go to Jeanne Kerrick, Carlon Ann Elton, and Debra Hunter for getting me through the paper jungle unscathed.

I would also like to thank the other members of my graduate committee, Dr. James Hunter, Dr. Thomas Carr, and Dr. Neil Sullivan, for their helpful advice.

Several researchers outside the Department have, in some way, provided assistance with my dissertation. Dr. Hugh Aller of the University of Michigan Radio Astronomy Observatory kindly provided unpublished radio data. The astronomers at the National Research Council of Canada also generously provided unpublished radio data from the Algonquin Radio Observatoy. I would like to thank Dr. Paul Feldman, Dr. Brian Andrew, and Dr. John MacLeod for their suggestions concerning my research. Thanks go especially to Paul Feldman for largely organizing my data gathering trip to Canada. He and his wife, Lise Jobin, were very hospitable during my visit. I would also like to thank Dr. Julian Krolik for his quick and helpful reply to questions concerning the Discrete Correlation Function. I am also grateful to Dr. Rick Edelson for giving me permission to reproduce a figure from one of his papers.

I would like to recognize Charlie Taylor for maintaining a smoothly running computing environment and for his efforts in resolving problems, especially during the weekend before first submission and the weekend before final submission.

Thanks go out to all of the former and current graduate students who provided friendship, guidance, and support. I would especially like to thank Jaydeep Mukherjee, Liz Moore, and Elaine Mahon for helping to improve my computer skills, for my own good and despite my protests. Their help was invaluable in finishing my dissertation. The cat-sitting care provided over the years by Jaydeep and Liz has also been greatly appreciated. I am indebted to Jim Webb for teaching me the ins and outs of observing. My old office mate, Greg Fitzgibbons, told many a strange and bizzare tale about former days in the Astronomy Department. My appreciation goes out to him, and to Berna Lowenstien, for their friendship and hospitality while they lived in Gainesville.

My deepest appreciation goes to my parents, Mary Sue and Warren Clements, for the loving support and encouragement they have always provided. This certainly could not have been accomplished without them. Thanks also go to my sister and brother, Karen Haworth and John Clements, and their families and to my grandmothers, Audrey Clements and Mabel Ray, for their love and support.

TABLE OF CONTENTS

ACKNOWLEDGMENTS iii

LIST OF TABLES vi

LIST OF FIGURES vii

ABSTRACT xiii

CHAPTERS

1 INTRODUCTION 1
  Background 1
  Some Models 4
  Previous Work 6

2 THE DATA 11
  Optical Data 11
  Radio Data 14
  The Objects 15

3 CORRELATION ANALYSIS 31
  Visual Inspection 31
  Classical Cross-Correlation Function Analysis 31
  Discrete Correlation Function Analysis 33
  Comparison of Classical Cross-Correlation Function and Discrete Correlation Function Analysis Results 34

4 RESULTS 41
  Optical-Radio Correlation Analysis Results 41
  A Plug for Visual Inspection 68
  Comparison of Results on Real Data with Results on Simulated Data . . . 69
  Results of Correlation Analysis on Data at Two Radio Frequencies 73

5 DISCUSSION OF RESULTS 189
  BL Lacs and QSOs in Light of the Results 189
  The Quality of the Data 193
  Summary 196

BIBLIOGRAPHY 201

BIOGRAPHICAL SKETCH 204

LIST OF TABLES

2-1 General Data 17

2-2 The Sample of Objects 20

2-3 Optical Observations 21

2-4 Radio Observations 23

4-1 Optical-Radio Correlation Analysis Results 74

4-2 Results of 14.5 GHz - 8.0 GHz Correlation Analysis 79

4-3 Results of 8.0 GHz - 4.8 GHz Correlation Analysis 83

5-1 Objects Showing Correlated Optical and Radio Events 197

5-2 Objects whose Optical and Radio Events are Not Correlated 198

5-3 Objects with Inconclusive Optical-Radio Correlation Analysis 199

LIST OF FIGURES

1-1 Broad-band Continuum Spectra of Blazars — log f_ν versus log ν 8

1-2 Broad-band Continuum Spectra for Blazars — log νf_ν versus log ν 9

1-3 Broad-band Continuum Spectra for Non-Blazars — log νf_ν versus log ν . . . 10

3-1 Comparison of Classical Cross-Correlation Function Analysis and Discrete Correlation Function Analysis on Optical and Radio Data 36

3-2 Comparison of DCF, Hole, and Interpolation Methods for III Zw 2 37

3-3 Comparison of DCF, Hole, and Interpolation Methods for 0215+015 38

3-4 Comparison of DCF, Hole, and Interpolation Methods for AO 0235+164 . . . 39

3-5 Comparison of DCF, Hole, and Interpolation Methods for OJ 287 40

4-1 0007+106 (III Zw 2) — DCF Analysis on Optical and Radio Light Curves . . 86

4-2 0048-097 — DCF Analysis on Optical and Radio Light Curves 87

4-3 0215+015 — DCF Analysis on Optical and Radio Light Curves 88

4-4 0229+131 — DCF Analysis on Optical and Radio Light Curves 89

4-5 AO 0235+164 — DCF Analysis on Optical and Radio Light Curves 90

4-6 0333+321 (NRAO 140) — DCF Analysis on Optical and Radio Light Curves . 91

4-7 0336-019 (CTA 26) — DCF Analysis on Optical and Radio Light Curves . . . 92

4-8 0420-014 — DCF Analysis on Optical and Radio Light Curves 93

4-9 0420-014 — DCF Analysis on Optical and Radio Light Curves 94

4-10 0422+004 — DCF Analysis on Optical and Radio Light Curves 95

4-11 0430+052 (3C 120) — DCF Analysis on Optical and Radio Light Curves . . . 96

4-12 0430+052 (3C 120) — DCF Analysis on Optical and Radio Light Curves — Subsets: 1971.0 to 1980.0 . . . 97

4-13 0430+052 (3C 120) — DCF Analysis on Optical and Radio Light Curves — Subsets: post-1980.0 . . . 98

4-14 0440-003 (NRAO 190) — DCF Analysis on Optical and Radio Light Curves . 99

4-15 0723-008 — DCF Analysis on Optical and Radio Light Curves . . . 100

4-16 0735+178 — DCF Analysis on Optical and Radio Light Curves . . . 101

4-17 0735+178 — DCF Analysis on Optical and Radio Light Curves — Subsets: 1978.0 to 1988.0 . . . 102

4-18 0736+017 — DCF Analysis on Optical and Radio Light Curves . . . 103

4-19 0754+100 (OI 090.4) — DCF Analysis on Optical and Radio Light Curves . 104

4-20 0829+046 — DCF Analysis on Optical and Radio Light Curves . . . 105

4-21 0851+202 (OJ 287) — DCF Analysis on Optical and Radio Light Curves . . 106

4-22 0851+202 (OJ 287) — DCF Analysis on Optical and Radio Light Curves . . 107

4-23 0953+254 (OK 290) — DCF Analysis on Optical and Radio Light Curves . 108

4-24 1101+384 (Mkn 421) — DCF Analysis on Optical and Radio Light Curves . 109

4-25 1148-001 — DCF Analysis on Optical and Radio Light Curves . . . 110

4-26 1156+295 — DCF Analysis on Optical and Radio Light Curves . . . 111

4-27 1219+285 (W Com) — DCF Analysis on Optical and Radio Light Curves . 112

4-28 1226+023 (3CR 273) — DCF Analysis on Optical and Radio Light Curves . 113

4-29 1253-055 (3C 279) — DCF Analysis on Optical and Radio Light Curves . . 114

4-30 1253-055 (3C 279) — DCF Analysis on Optical and Radio Light Curves — Subsets: 1985.0 to 1990.0 . . . 115

4-31 1308+326 — DCF Analysis on Optical and Radio Light Curves 116

4-32 1418+546 — DCF Analysis on Optical and Radio Light Curves 117

4-33 1510-089 — DCF Analysis on Optical and Radio Light Curves 118

4-34 1514-241 (AP Lib) — DCF Analysis on Optical and Radio Light Curves . . 119

4-35 1611+343 — DCF Analysis on Optical and Radio Light Curves 120

4-36 1641+399 (3CR 345) — DCF Analysis on Optical and Radio Light Curves . 121

4-37 1641+399 (3CR 345) — DCF Analysis on Optical and Radio Light Curves — Subsets: post-1970.5 122

4-38 1652+398 (Mkn 501) — DCF Analysis on Optical and Radio Light Curves . 123

4-39 1730-130 (NRAO 530) — DCF Analysis on Optical and Radio Light Curves 124

4-40 1749+701 — DCF Analysis on Optical and Radio Light Curves 125

4-41 1749+096 — DCF Analysis on Optical and Radio Light Curves 126

4-42 1807+698 (3CR 371) — DCF Analysis on Optical and Radio Light Curves . 127

4-43 1901+319 — DCF Analysis on Optical and Radio Light Curves 128

4-44 1921-293 (OV-236) — DCF Analysis on Optical and Radio Light Curves . . 129

4-45 2134+004 — DCF Analysis on Optical and Radio Light Curves 130

4-46 2144+092 — DCF Analysis on Optical and Radio Light Curves 131

4-47 2145+067 — DCF Analysis on Optical and Radio Light Curves 132

4-48 2200+420 (BL Lac) — DCF Analysis on Optical and Radio Light Curves . . 133

4-49 2200+420 (BL Lac) — DCF Analysis on Optical and Radio Light Curves — Subsets: 1971.5 to 1977.0 134

4-50 2200+420 (BL Lac) — DCF Analysis on Optical and Radio Light Curves — Subsets: post-1977.0 135

4-51 2201+315 — DCF Analysis on Optical and Radio Light Curves 136

4-52 2223-052 (3C 446) — DCF Analysis on Optical and Radio Light Curves . . 137

4-53 2230+114 (CTA 102) — DCF Analysis on Optical and Radio Light Curves . 138

4-54 2251+158 (3C 454.3) — DCF Analysis on Optical and Radio Light Curves . 139

4-55 2345-167 — DCF Analysis on Optical and Radio Light Curves 140

4-56 0851+202 (OJ 287) 141

4-57 0851+202 (OJ 287) 142

4-58 0851+202 (OJ 287) 143

4-59 0851+202 (OJ 287) 144

4-60 1156+295 145

4-61 1156+295 146

4-62 1308+326 147

4-63 1308+326 148

4-64 1641+399 (3CR 345) 149

4-65 1641+399 (3CR 345) 150

4-66 1641+399 (3CR 345) 151

4-67 1641+399 (3CR 345) 152

4-68 1901+319 153

4-69 1921-293 (OV-236) 154

4-70 2223-052 (3C 446) 155

4-71 2223-052 (3C 446) 156

4-72 0007+106 (III Zw 2) — "Perfectly correlated" — Offset: -13 months 157

4-73 0007+106 (III Zw 2) — “Perfectly uncorrelated” 158

4-74 0048-097 — “Perfectly correlated” — Offset: 0 months 159

4-75 0048-097 — “Perfectly uncorrelated” 160

4-76 0215+015 — “Perfectly correlated” — Offset: 0 months 161

4-77 0215+015 — “Perfectly correlated” — Offset: -3.3 months 162

4-78 0215+015 — “Perfectly correlated” — Offset: -5 months 163

4-79 0215+015 — “Perfectly uncorrelated” 164

4-80 AO 0235+164 — “Perfectly correlated” — Offset: 0 months 165

4-81 AO 0235+164 — “Perfectly correlated” — Offset: -2 months 166

4-82 AO 0235+164 — “Perfectly uncorrelated” 167

4-83 0430+052 (3C 120) — “Perfectly correlated” — Offset: 0 months 168

4-84 0430+052 (3C 120) — “Perfectly correlated” — Offset: -4 months 169

4-85 0430+052 (3C 120) — “Perfectly uncorrelated” 170

4-86 0851+202 (OJ 287) — “Perfectly correlated” — Offset: 0 months 171

4-87 0851+202 (OJ 287) — “Perfectly correlated” — Offset: -14 months 172

4-88 0851+202 (OJ 287) — “Perfectly uncorrelated” 173

4-89 1749+096 — “Perfectly correlated” — Offset: 0 months 174

4-90 1749+096 — “Perfectly correlated” — Offset: -3 months 175

4-91 1749+096 — “Perfectly uncorrelated” 176

4-92 1921-293 (OV-236) — “Perfectly correlated” — Offset: -10 months 177

4-93 1921-293 (OV-296) — “Perfectly uncorrelated” 178

4-94 2200+420 (BL Lac) — “Perfectly correlated” — Offset: 0 months 179

4-95 2200+420 (BL Lac) — “Perfectly correlated” — Offset: -2 months 180

4-96 2200+420 (BL Lac) — “Perfectly uncorrelated” 181

4-97 2200+420 (BL Lac) — “Perfectly correlated” — Subsets: 1971.5 to 1977.0 — Offset: 0 months 182

4-98 2200+420 (BL Lac) — “Perfectly correlated” — Subsets: 1971.5 to 1977.0 — Offset: -2 months 183

4-99 2200+420 (BL Lac) — “Perfectly uncorrelated” — Subsets: 1971.5 to 1977.0 184

4-100 AO 0235+164 — DCF Analysis on 14.5 GHz and 8.0 GHz Radio Light Curves 185

4-101 0333+321 (NRAO 140) — DCF Analysis on 14.5 GHz and 8.0 GHz Radio Light Curves 186

4-102 0420-014 — DCF Analysis on 14.5 GHz and 8.0 GHz Radio Light Curves . 187

4-103 1652+398 (Mkn 501) — DCF Analysis on 14.5 GHz and 8.0 GHz Radio Light Curves 188

Abstract of Dissertation Presented to the Graduate School
of the University of Florida in Partial Fulfillment of the
Requirements for the Degree of Doctor of Philosophy.

CORRELATION ANALYSIS ON OPTICAL AND RADIO LIGHT CURVES FOR A LARGE SAMPLE OF ACTIVE GALACTIC NUCLEI

By

Sandra Denise Clements

August, 1992

Chairman: Dr. Alex G. Smith
Major Department: Astronomy

Long-term optical and radio light curves for a large sample of active galactic nuclei were investigated in order to examine the relationship between the two emission regions. Correlation analysis using the Discrete Correlation Function was performed to determine if radio events are correlated with optical events, and if so, to determine the lag times between them. In addition, similar analysis was performed to determine lag times between events at 14.5 GHz, 8.0 GHz and 4.8 GHz.

A total of forty-six objects were examined. Nine showed correlated optical and radio events with optical leading the radio in every case. Six of these were BL Lacertids, all having lag times of less than 6 months. The one QSO which showed correlated optical and radio events had a longer lag time, on the order of a year. No difference between BL Lacs and QSOs is seen in the results of correlation analysis on two radio frequencies. Lag times between 14.5 GHz and 8.0 GHz radio data are less than 5 months in almost every case. The same is true for lag times between 8.0 GHz and 4.8 GHz data. An additional nine objects showed no correlated behavior in their optical and radio light curves. Seven of these objects were QSOs. The rest of the objects either did not have light curves with

adequate temporal coverage for reliable correlation analysis, or the analysis was confused by the number and spacing of events in one or both light curves.

This analysis was seriously hampered by inadequate temporal coverage in the optical light curves. Some variability timescales in the optical are very short, making frequent observations necessary in order to resolve events. Unavoidable constraints on ground-based observations due to the weather, the sun and the moon, make it impossible to obtain the frequent, uninterrupted observations that are necessary to obtain a light curve without yearly gaps and with well-resolved short-term events.

CHAPTER 1
INTRODUCTION

Background

An active galactic nucleus (AGN) is ". . . any extragalactic object which exhibits substantial emission in excess of normal stellar processes (starlight, H II regions, supernovae, etc.)" (Urry, 1988, p. 279). There is a veritable zoo of objects which can be categorized as AGN, including low luminosity LINERs (Low Ionization Nuclear Emission Regions), starburst systems, radio galaxies, Seyfert galaxies, radio-loud and radio-quiet quasars, BL Lac objects, and optically violent variable (OVV) quasars.

Active galactic nuclei can be subdivided into two categories, blazars and non-blazars. Blazars share the following characteristics.

1.) They are highly polarized.

2.) They exhibit large amplitude variations in intensity and polarization on short timescales.

3.) They are compact, flat-spectrum radio sources which sometimes exhibit superluminal motion.

4.) Their variability timescales vary with wavelength, being shorter at shorter wavelengths. In particular, the shortest optical variability timescales are on the order of hours to days, whereas the shortest radio timescales are usually on the order of months to years (Urry, 1988). Light travel time arguments would therefore indicate that the optical emission region is much smaller than the radio emission region. The most rapid variability seen in optical light curves suggests that the optical emitting region is on the order of 10^{-2} to 10^{-3} parsecs in extent (Bregman and Hufnagel, 1989). Studies of compact radio sources using Very Long Baseline Interferometry (VLBI) indicate that the radio emitting region is on the order of parsecs in size (Pearson and Zensus, 1987).

5.) A blazar's broad-band continuum spectrum is smooth and can be characterized as a power law of the form $f_\nu \alpha \nu^\alpha$ where f_ν is the flux at frequency ν and α is the spectral index. For AGN, a good first-order fit to the broad-band continuum is obtained with $\alpha = -1$.

Included in the blazar category are BL Lac objects, OVV quasars, high polarization quasars (HPQs), and superluminal radio sources (SLSs) (Burbidge and Hewitt, 1992). Figure 1-1 (taken from Brown et al., 1989) shows examples of two blazar broad-band continuum spectra. The top log f_ν versus log ν curve is for the BL Lacertid, OJ 287 and the bottom curve is for the OVV quasar, 3C 279. The curves are very smooth, with a slope of approximately -1 for infrared through optical frequencies. The curves flatten out in the radio region, but still join smoothly with the rest of the continuum.

The smooth power law continuum of a blazar is believed to be caused by synchrotron emission from relativistic electrons accelerating in a magnetic field (Kellerman and Pauliny-Toth, 1969). For a power law distribution of electrons,

$$N(E)dE = KE^{-\delta}dE, \tag{1-1}$$

synchrotron theory predicts that

$$f_\nu \propto \nu^{-(\delta-1)/2} \tag{1-2}$$

or

$$f_\nu \propto \nu^\alpha \tag{1-3}$$

where

$$\alpha = (1 - \delta)/2. \tag{1-4}$$

The other characteristics shared by blazars can also be explained with models incorporating synchrotron emission.

Not all AGN have such smooth broad-band continuum spectra. In Figures 1-2 and 1-3, log νf_ν versus log ν curves are shown for blazars and for non-blazars respectively. Non-blazars are, of course, all AGN other than blazars. They are not as variable as blazars and, as seen in comparing Figures 1-2 and 1-3, their broad-band continuum spectra are more complex than for blazars. In Figures 1-2 and 1-3, log νf_ν versus log ν curves were plotted instead of log f_ν versus log ν so that deviations from the smooth power law curve could be seen more easily. Broad-band continuum spectra of non-blazars have bumps and wiggles which have been attributed to a variety of physical mechanisms such as thermal emission from a hot accretion disk which shows up in the ultraviolet, thermal emission from dust seen in the infrared, radiation from stars in the underlying galaxy (Urry, 1988; Edelson and Malkan, 1986). These thermal emission processes are in addition to an underlying nonthermal synchrotron emission process.

Some reasons for thinking that optical and radio events in AGN may be correlated are given below.

a.) The smooth, continuous nature of the broad-band continuum for AGN, blazars especially, suggests that events in the optical and events in the radio may be caused by the same underlying perturbation in the object.

b.) The long-term variations in the optical are comparable in duration to the long-term radio variation.

c.) Some models proposed for these objects imply a relationship between the two regions could exist.

d.) Previous searches for correlated optical and radio events have met with some success.

Some Models

In the simple expanding source model of Shklovoskii (1960), radio emission is due to synchrotron radiation from a spherical cloud of relativistic electrons moving in a magnetic field while the cloud is expanding adiabatically. The cloud is initially optically thick, but becomes optically thin at progressively longer wavelengths as it expands. With this simple model, outbursts will be seen earlier and will have larger amplitudes and shorter durations at higher frequencies. These effects have been qualitatively observed at centimeter wavelengths for some objects, 3C 120, for example (Dent, 1968; Pauliny-Toth and Kellerman, 1966; Seielstad, 1974). Inconsistencies between theory and observations for some objects, such as lack of time delay and/or lack of amplitude change between frequencies, can be overcome by incorporating any of a large number of modifications to the simple theory. Possible modifications are continuous injection of relativistic electrons (Peterson and Dent, 1973), variable expansion of the cloud, an expanding shell instead of a sphere (van der Laan, 1962), lack of conservation of magnetic flux, non-isotropic radiation, changing electron energy distribution due to loss of energy by inverse Compton scattering, bremmstrahlung, and ionization, etc. Peterson and King (1975) extended the continuous injection model into optical wavelengths.

Jets are observed in the optical (3CR 273, for example) as well as the radio. Powerful radio jets are seen which are on the order of hundreds of kiloparsecs in extent. High resolution VLBI maps of some objects reveal structure on much smaller scales (on the order of parsecs), which is observed to be associated with the large-scale radio jets or lobes (3C 120, for example, Walker, Benson, and Unwin, 1987). The small scale structure is in the form of "blobs" in the intensity contours which are seen to move away from the central compact source when maps are made at two or more epochs. Sometimes these blobs appear to move at superluminal (faster-than-light) speeds. Superluminal motion can be explained as being the result of projection effects on an object moving at relativistic speeds at a small angle to the line of sight (Rees, 1966, 1967).

Relativistic motion at small angles to the line of sight explains not only the superluminal motion seen in VLBI maps, but also eliminates a problem which arises in synchrotron models of AGN, namely the Compton catastrophe. If their redshifts are cosmological and their radiation emitted isotropically, blazars are extremely luminous. In addition, based on light travel time arguments, the very rapid variability of these objects implies that they are very small. In synchrotron self-Compton (SSC) models, blazars are so compact and so luminous that all of their radiation should be emitted as inverse Compton scattered photons, not synchrotron photons, in contradiction to what is observed. With inverse Compton scattering, a low frequency photon is Compton scattered to a higher frequency by a high energy electron. Radio frequency photons would be Compton scattered to X-ray energies (Jones, O'Dell, and Stein, 1974). With relativistic beaming of material at small angles to the line of sight, observed luminosities are orders of magnitude larger than equivalent isotropic luminosities and observed variability timescales are much shorter than intrinsic timescales. With relativistic beaming, blazars are not so very luminous and compact, eliminating the Compton catastrophe problem.

A number of jet models have been proposed to explain the radio observations of AGN (Blandford and Rees, 1974; Blandford and Königl, 1979; Marscher, 1980; Königl, 1981; Reynolds, 1982; Ghisellini, Maraschi, and Treves, 1985; Hutter and Mufson, 1986; Hughes, Aller, and Aller, 1989a, 1989b). For example, Aller, Hughes, and Aller (1991) have successfully reproduced the variations in the University of Michigan

Radio Astronomy Observatory (UMRAO) flux density, polarization flux density, and polarization position angle for 3C 279 and BL Lac. In their model, variability in the radio is explained as being due to shocks in a relativistic jet having a tangled underlying magnetic field (Hughes, Aller, and Aller 1989a). They suggest that ". . . the IR and optical bands probe the "progenitor" flow and may be used to constrain models for evolution into the radio-emitting plasma" (Hughes, Aller, and Aller, 1989b, p. 79).

Previous Work

Several investigators have examined individual objects searching for correlated optical and radio activity. A recent example of this is the study of OJ 287 at six frequencies by Valtaoja et al. (1987). They found that radio events lagged optical events by 6 months or less. References to many other such investigations can be found in Pomphrey et al. (1976), Balonek (1982), and Valtaoja et al. (1987).

The first work which looked for correlations between optical and radio events for a large sample of AGN was that of Pomphrey et al. (1976). In that study, cross-correlation analysis was performed on the optical magnitudes and radio fluxes of 22 objects. Strong correlation was found for only one of the twenty-two, the BL Lacertid, OJ 287.

Six years later, in another extensive search for optical-radio correlations, Balonek (1982) found several sources to "unambiguously" possess correlated activity and also found that nearly a dozen others showed strong evidence favoring correlation.

In a more recent study of four objects (two BL Lacs and two OVV quasars), Bregman and Hufnagel (1989) found that the radio lagged the optical by 1 to 2 years in every case with no significant difference between the BL Lacs and the OVV quasars.

This study, with nearly a decade more data than Balonek (1982) had for his investigation, should better address the question of whether or not optical and radio events are correlated. This study also has the potential to examine differences in the relationship between optical and radio emission regions for the various types of AGN being investigated.

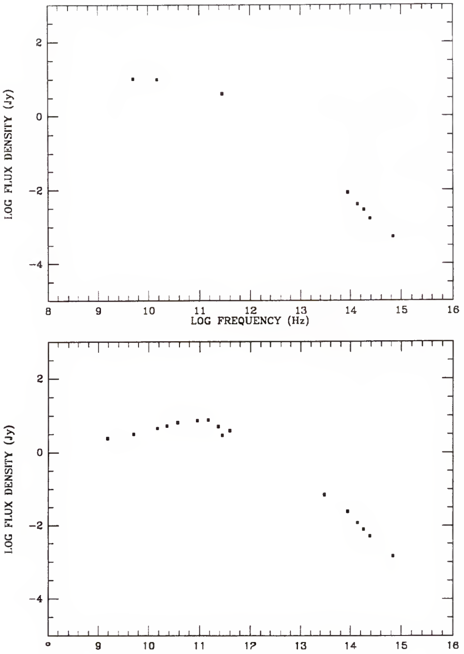

Figure 1-1: Broad-band Continuum Spectra of Blazars — log f_ν versus log ν
top) 3C 279 — OVV QSO
bottom) OJ 287 — BL Lac
(Brown et al., 1989).

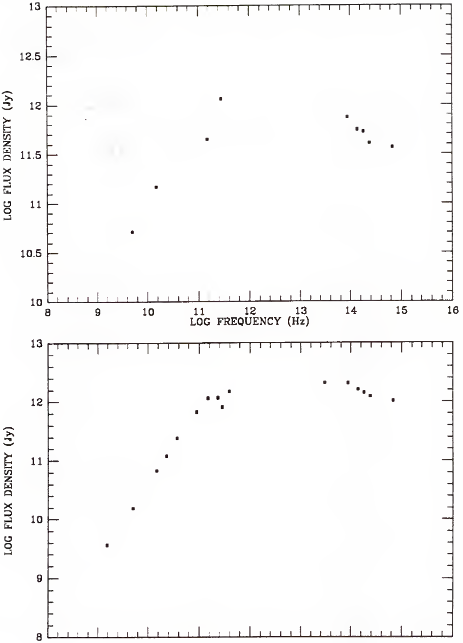

Figure 1-2: Broad-band Continuum Spectra for Blazars — log νf_ν versus log ν
top) 3C 279 — OVV QSO
bottom) OJ 287 — BL Lac
(Brown et al., 1989).

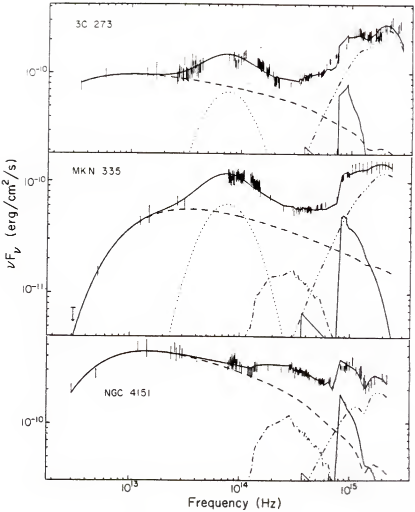

Figure 1-3: Broad-band Continuum Spectra for Non-Blazars — log νf_ν versus log ν
top) 3CR 273
middle) Mkn 335
bottom) NGC 4151
An underlying power law (the dashed line), thermal emission from dust (the dotted line), starlight from the underlying galaxy (the dot-dash line), Balmer and Paschen recombination (the solid lines), and thermal emission from a hot accretion disk (the dot-dot-dot-dash line) all contribute to the shape of the continuum of a non-blazar. (This figure was reprinted with permission from Edelson and Malkan, 1986, p. 69).

CHAPTER 2
THE DATA

Optical Data

In 1968, under the direction of Dr. Alex G. Smith, the University of Florida Department of Astronomy began a campaign to monitor the optical magnitudes of active galactic nuclei (AGN) using photographic photometry. Currently, there are 223 objects on the program. Observations are made at the f/4 Newtonian focus of the 30 inch telescope at Rosemary Hill Observatory in Bronson, Florida. Objects are monitored in either Johnson B or the International Photographic (m_{pg}) system. To reach the sky limit, five or six minute exposures are made on hypersensitized Kodak 103a-O plates. An object field is roughly 1° in diameter and contains 10 to 20 comparison stars which are used to find the magnitude of the AGN.

On a photographic emulsion, the brighter a point source (such as a star or a classical quasar), the larger the image size and the denser the silver grains will be in the image. A Cuffy Iris Astrophotometer is used to measure the image size and density and quantify these with a number called an iris reading. Iris readings are found for the comparison stars and the AGN. A second order polynomial is fit by the method of least squares to the comparison star magnitudes and iris readings. The AGN magnitude is found from this calibration curve and the AGN's iris reading. The rms scatter of the comparison star magnitudes about this calibration curve is used as the error in the AGN magnitude.

For an object whose comparison star magnitudes form a good photoelectric sequence, the error in the object's magnitude is typically about 0.08 magnitudes. The majority of objects in the monitoring program have comparison star sequences which are established by photographic transfer from a nearby calibration field. This technique is not as accurate as photoelectric photometry and objects with such comparison star sequences have typical errors slightly larger, about 0.15 magnitudes.

Variability in an object will sometimes cause it to be brighter or fainter than any of the stars in the comparison star sequence. Because the photographic emulsion is a nonlinear detector, the comparison star magnitudes should span the object's magnitude range so that the sequence never has to be extrapolated to encompass the object. If the object's magnitude varies to well beyond its comparison star magnitudes, it becomes necessary to extend the sequence so that extrapolation is no longer necessary.

Over time, the comparison star sequences are improved in a couple of ways. Sometimes, it becomes evident that a comparison star is a variable and should be dropped from the sequence. A more subtle improvement is made by "smoothing" the sequence by the method of least squares. Using several exposures, and therefore several calibration curves, the scatter of a star's magnitude about the calibration curves is minimized with least squares by adjusting the magnitude of the comparison star. This was done for the majority of objects on the program by Pollock et al., 1979. A handful of other sequences have been "smoothed" since then.

When the sequences were "smoothed" in 1979, the "smoothed" sequences were *not* used on all of the previously reduced data. With over 200 objects and many exposures of each, this would have been prohibitively time-consuming. For each object examined in this project, the earlier observations were re-reduced using the "smoothed" sequences, putting all of the magnitudes on the same sequence for a more uniform data base.

The optical data through 1987 for 22 OVVs monitored on the program were published in Webb et al. (1988). In this paper, the data were given in both tabular and graphical form. A paper on 144 non-OVVs was published by Pica et al. (1988). The observational data for these objects are summarized in Table I of this reference. Also, the light curves for a few selected objects are given there along with descriptions of a few others.

Optical magnitudes were converted to flux densities for correlation analysis with radio flux densities. The optical flux density of an object is found from its B magnitude using

$$f_B = 4.390 \times 10^6 \left(10^{-0.4B}\right) mJy. \tag{2-1}$$

The coefficient is the flux density of the star Vega at 4400Å from Hayes and Latham (1975). The B magnitude of Vega, a standard star, is defined to be zero. In the magnitude system, the relationship between the ratio of fluxes and magnitude difference is given by

$$m_1 - m_2 = -2.5 log_{10} \left(\frac{f_1}{f_2}\right) \tag{2-2}$$

or

$$\frac{f_1}{f_2} = 10^{-0.4(m_1 - m_2)}. \tag{2-3}$$

Equation 2-1 is simply Equation 2-3 with m_2 and f_2 set equal to the B magnitude and associated flux density for the standard star Vega. The error in flux density is found from the optical magnitude error and

$$\sigma_{f_B} = 0.5 f_B \left(10^{0.4\sigma_B} - 10^{-0.4\sigma_B}\right) mJy. \tag{2-4}$$

For objects monitored in m_{pg}, this conversion was used as well, without correcting from m_{pg} to B. This was done because corrections from m_{pg} to B are unknown for these objects. Flux densities found using m_{pg}'s instead of B's differ only in scale from flux densities found using m_{pg}'s corrected to B's.

Four objects were monitored in both m_{pg} and B. For these objects, the m_{pg} magnitudes were converted to B magnitudes prior to conversion to flux densities. These objects, 0735+178, OJ 287, 1354+195, and 3CR 345, had B-m_{pg} corrections of 0.33, 0.32, 0.28

and 0.29 respectively. These corrections were determined by comparing B's and m_{pg}'s taken the same night. For OJ 287, an average U-B was found from U and B exposures made on the same night. The B-m_{pg} for OJ 287 was found from Table I of Lü (1972) which lists empirically determined values of B-m_{pg} for various values of U-B.

No corrections were made for galactic extinction caused by dust in our galaxy. To make such a correction, a model for the galactic extinction as a function of galactic coordinates for the object is used. Galactic extinction models are first order approximations to the anisotropic, inhomogeneous dust distribution in our galaxy. Because corrections for extinction are so uncertain and since correcting for extinction would only change the scale of the optical flux densities for an object, not the shape, such corrections were not made.

Radio Data

The radio data used in this project are mostly from the University of Michigan Radio Astronomy Observatory (UMRAO) and are in the form of fluxes at 4.8 GHz, 8.0 GHz, and 14.5 GHz. These data are part of a campaign begun in 1965 to monitor extragalactic sources with the University of Michigan 26 meter paraboloid. Data prior to 1977 December were taken from Aller et al. (1985). Observations and data reduction techniques are discussed in this reference. The remainder of the data through 1989 December were kindly provided via private communication by Dr. H. D. Aller.

Radio data from the Algonquin Radio Observatory (ARO) were used for objects not monitored by UMRAO. Data from ARO were also used in addition to the UMRAO data to extend the baseline in some cases. The Algonquin data are part of a campaign to monitor variable extragalactic radio sources with the ARO 46 meter telescope. This campaign, sponsored by the National Research Council of Canada, lasted from 1966 July to 1983 February. Data through 1971 June were taken from Medd et al. (1972). Subsequent data through 1976 December were taken from Andrew et al. (1978). Additional data have been made available in a preliminary form by P. A. Feldman (private communication, 1991). These data may be subject to occasional small systematic errors beyond those discussed in Andrew et al. (1978) and Andrew et al. (1981) but these errors are expected to be less than the standard errors quoted for these observations in Andrew et al. (1978). Medd et al. (1972) describe observations and data reduction techniques. Additional technical points are discussed in Andrew et al. (1978).

The Objects

Table 2-1 gives general data on all of the objects examined for this project. Column 1 gives the coordinate designation for the object. An alternate name for the object is given in Column 2. The redshift and type of redshift (emission or absorption) are given in Columns 3 and 4, respectively. The redshift is uncertain if it is in parentheses. If the entry for Column 4 is "galaxy," this indicates that the redshift listed in Column 3 was determined from absorption lines and/or weak emission lines characteristic of elliptical galaxies. Columns 3 and 4 in this case are from Burbidge and Hewitt (1992). The type of object (i.e., BL Lac, Seyfert, or QSO) is given in Column 5. Columns 2 - 5 are from Hewitt and Burbidge (1987) unless noted otherwise. Column 6 lists other descriptions of the object found in the literature (BZR for blazar, HPQ for high polarization quasar, and OVV for optically violent variable). Column 7 comments on whether the object is a superluminal radio source (SLS) or if it has been detected in X-rays (XD). Columns 6 and 7 are from Burbidge and Hewitt (1992).

In order to have been selected for this project, an object must 1) be observed as part of the AGN-monitoring program at RHO, 2) have been monitored at radio frequencies by UMRAO and/or ARO, and 3) have sufficient temporal coverage in the optical and radio to make correlation analysis worthwhile. A total of 46 objects were examined – 19 BL Lacs, 24 QSOs, 2 Seyfert galaxies, and 1 NSO. Of these 46 objects, 37 are listed in the Burbidge and Hewitt (1992) compilation of blazars, high polarization variables (HPV's), and optically violent variables (OVVs). According to Burbidge and Hewitt (1992, p. 5), the term "blazar" is ". . . a pictorial term . . . applied to rapidly variable objects, some of which, but not all, can also be classified as BL Lac objects." The acronym HPQ is often seen instead of HPV and stands for high polarization quasar. According to Penston and Cannon (1970), OVVs are optically violent variables which exhibit changes in optical intensity of a magnitude or more on timescales of days to weeks. The more variability an object exhibits, the more often it is observed at RHO. It is not surprising, therefore, that such a large percentage of objects chosen for this project (and therefore thought to have sufficient temporal optical coverage for meaningful correlation analysis) are in the Burbidge and Hewitt (1992) list. Table 2-2 shows how many of the BL Lacs, QSOs, Seyferts, and the NSO in this project have been designated in the literature as blazars, HPVs, and/or OVV's as reported by Burbidge and Hewitt (1992).

In Table 2-3, the optical observations of these objects are described. Column 1 gives the coordinate name. Column 2 gives the color system used (B or m_{pg}). The total number of observations is given in Column 3. The dates of the first and last observations are given in Columns 4 and 5, respectively. The average number of observations per year is given in Column 6. Optical flux curves for all objects examined in this work are shown in the top panels of Figures 4-1 through 4-55.

Information on radio observations is given in Table 2-4. The coordinate name is given in Column 1. The radio frequency used is given in column 2. Columns 3 - 6 are the radio counterparts of Columns 3 - 6 in Table 2-3. The radio data used in the optical-radio correlation analysis are shown in the middle panels of Figures 4-1 through 4-55.

Table 2-1: General Data

1 Object	2 Other Name	3 Redshift	4 Type of Redshift	5 Type of Object	6 Names in Literature	7 Comments
0007+106	III Zw 2	0.089	emission	Seyfert[a]		
0048-097	OB-081			BL Lac	BZR	XD
0215+015	OD 026	(1.715) 1.719,etc.	emission absorption	BL Lac	BZR OVV	XD
0229+131	4C 13.14	2.065	emission	QSO		
0235+164	AO 0235+164	0.94 0.852,etc.	emission absorption	BL Lac	BZR OVV	SLS XD
0333+321	NRAO 140	1.258	emission	QSO		SLS XD
0336-019	CTA 26	0.852	emission	QSO	BZR HPQ	XD
0420-014	OF-035	0.915 0.633	emission absorption	QSO	BZR HPQ OVV	XD
0422+004	OF 038			BL Lac	BZR OVV	XD
0430+052	3C 120	0.0331	emission	radio galaxy[b] Seyfert[a]	OVV	SLS
0440-003	NRAO 190	0.844	emission	QSO	BZR OVV	XD
0723-008	OI-039	0.127	emission	NSO[c]		
0735+178	VR 17.07.02	0.424	absorption	BL Lac	BZR OVV	SLS XD
0736+017	OI 061	0.191	emission	QSO	BZR HPQ	XD
0754+100	OI 090.4			BL Lac	BZR	XD
0829+046	OJ 049			BL Lac	BZR OVV	XD
0851+202	OJ 287	0.306	emission	BL Lac	BZR OVV	SLS XD
0953+254	OK 290	0.712	emission	QSO		
1101+384	Mkn 421	0.031	galaxy	BL Lac	BZR	XD

Table 2-1: (Continued)

1 Object	2 Other Name	3 Redshift	4 Type of Redshift	5 Type of Object	6 Names in Literature	7 Comments
1148-001	4C-00.47	1.982 1.4672,etc.	emission absorption	QSO		
1156+295	4C 29.45	0.729	emission	QSO	BZR HPQ OVV	
1219+285	W Com	0.102	galaxy	BL Lac	BZR OVV	XD
1226+023	3CR 273	0.158	emission	QSO		SLS
1253-055	3C 279	0.538	emission	QSO	BZR HPQ OVV	SLS XD
1308+326	B2	0.996 0.879	emission absorption	BL Lac	BZR HPQ OVV	XD
1418+546	OQ 530	0.152	galaxy	BL Lac	BZR	XD
1510-089	OR-017	0.361 0.351	emission absorption	QSO	BZR HPQ	XD
1514-241	AP Lib	0.049	galaxy	BL Lac	BZR OVV	XD
1611+343	DA 406	1.401	emission	QSO		
1641+399	3CR 345	0.595	emission	QSO	BZR HPQ OVV	SLS XD
1652+398	Mkn 501	0.034	galaxy	BL Lac	BZR	XD
1730-130	NRAO 530	0.902	emission	QSO	OVV	
1749+701	W1	(0.770)	emission^b	BL Lac	BZR	XD SLS
1749+096	OT 081	0.322	emission^b	BL Lac	BZR	XD
1807+698	3CR 371	0.050	galaxy	BL Lac	BZR OVV	XD SLS
1901+319	3C 395	0.635	emission	QSO		SLS
1921-293	OV-236	0.352	emission	QSO	BZR HPQ OVV	XD

Table 2-1: (Continued)

1 Object	2 Other Name	3 Redshift	4 Type of Redshift	5 Type of Object	6 Names in Literature	7 Comments
2134+004	PHL 61	1.936	emission	QSO		
2144+092	OX 074[d]	1.113	emission[b]	QSO[b]	OVV	
2145+067	4C 06.69	0.99 0.7897	emission absorption	QSO		
2200+420	BL Lac	0.069	galaxy	BL Lac	BZR OVV	SLS
2201+315	4C 31.63	0.297	emission	QSO		
2223-052	3C 446	1.404 0.8472	emission absorption	BL Lac	BZR HPQ OVV	XD SLS
2230+114	CTA 102	1.037	emission	QSO	BZR HPQ	SLS XD
2251+158	3CR 454.3	0.859	emission	QSO	BZR HPQ OVV	SLS XD
2345-167	OZ-176	0.576	emission	QSO	BZR HPQ OVV	XD

[a] Pica et al. (1988)

[b] Burbidge and Hewitt (1992)

[c] Strittmatter et al. (1974)

[d] Webb et al. (1988)

Table 2-2: The Sample of Objects

Type Object	Total	Blazars	HPV's	OVV's	XD	SLS
BL Lacs	19	19	2	17	18	7
QSOs	24	12	11	10	12	7
Seyferts	2	0	0	1	0	1
NSOs	1	0	0	0	0	0
Total	46	31	13	28	30	15

Table 2-3: Optical Observations

1	2	3	4	5	6
Object	Color System	N	Date of First	Date of Last	Average N per Year
0007+106	B	72	12-11-77	11-06-90	5.6
0048-097	m_{pg}	104	11-06-70	11-13-90	5.2
0215+015	B	69	09-24-81	08-20-90	7.8
0229+131	m_{pg}	61	10-10-69	01-23-90	3.0
0235+164	B	103	09-21-77	09-05-91	7.4
0333+321	m_{pg}	53	08-29-71	01-28-90	2.9
0336-019	m_{pg}	78	12-03-69	01-19-90	3.9
0420-014	m_{pg}	152	12-03-69	02-10-91	6.9
0422+004	B	55	10-21-76	10-26-90	3.9
0430+052	B	137	10-16-71	01-26-90	7.5
0440-003	m_{pg}	99	12-08-69	01-22-90	4.9
0723-008	B	53	03-06-80	03-10-91	4.8
0735+178	B	167	04-18-74	03-10-91	9.9
0736+017	m_{pg}	112	12-11-69	03-10-91	5.3
0754+100	B	58	03-26-79	03-10-91	4.8
0829+046	B	62	11-06-80	04-17-90	6.6
0851+202	B	278	02-08-70	05-02-91	13.1
0953+254	m_{pg}	88	02-08-70	04-15-90	4.4
1101+384	B	58	04-18-77	04-16-90	4.5
1148-001	m_{pg}	30	04-13-69	03-26-90	1.4
1156+295	B	166	05-09-80	06-09-91	16.4
1219+285	B	142	02-22-72	04-15-90	7.8
1226+023	B	91	01-24-74	06-02-91	5.2
1253-055	m_{pg}	86	05-25-71	01-21-91	4.4
1308+326	B	111	04-21-76	06-18-90	7.8
1418+546	B	35	05-01-78	06-18-90	2.9
1510-089	m_{pg}	85	06-12-69	06-12-90	4.0
1514-241	m_{pg}	111	02-20-72	06-12-90	6.1

Table 2-3: (Continued)

1 Object	2 Color System	3 N	4 Date of First	5 Date of Last	6 Average N per Year
1611+343	B	35	03-22-80	07-23-90	3.4
1641+399	B	213	06-22-71	09-08-91	10.5
"	m_{pg}	27	09-19-70	07-29-71	31.6
1652+398	B	62	03-27-79	05-25-89	6.1
1730-130	m_{pg}	46	07-10-72	05-26-87	3.1
1749+701	B	41	03-29-79	09-19-90	3.6
1749+096	B	55	08-13-79	07-30-90	5.0
1807+698	m_{pg}	165	11-05-69	09-21-90	7.9
1901+319	B	43	03-22-80	11-11-88	5.0
1921-293	m_{pg}	69	05-31-71	09-18-90	3.6
2134+004	B	53	06-26-71	11-11-90	2.7
2144+092	m_{pg}	146	05-13-70	10-16-90	7.2
2145+067	m_{pg}	84	07-26-69	10-16-90	4.0
2200+420	B	321	06-24-71	10-18-90	16.6
2201+315	B	42	07-17-80	11-12-90	4.1
2223-052	B	188	09-14-71	09-18-90	9.9
2230+114	B	69	08-25-73	10-16-90	4.0
2251+158	B	110	08-20-71	09-10-91	5.4
2345-167	m_{pg}	128	10-09-69	10-26-90	6.1

Table 2-4: Radio Observations

1 Object	2 Frequency	3 N	4 Date of First	5 Date of Last	6 Average N per Year
0007+106	14.5	65	04-29-78	10-08-89	5.7
	10.6	51	03-15-76	11-03-82	7.7
	8.0	92	02-09-76	12-13-89	6.6
	4.8	32	01-24-80	11-28-89	3.2
0048-097	14.5	94	09-05-74	12-18-89	6.2
	10.6	86	04-19-71	11-03-82	7.4
	8.0	98	09-18-69	12-16-89	4.8
	4.8	48	08-29-80	12-22-89	5.2
	8.0 and 10.6	157	04-19-71	12-16-89	8.4
0215+015	14.5	52	09-04-79	09-30-89	5.2
	8.0	62	08-03-79	10-04-89	6.0
	4.8	35	02-16-80	12-25-89	3.6
0229+131	10.6	66	08-17-69	02-12-83	4.9
0235+164	14.5	148	09-29-75	12-19-89	10.4
	10.6	81	11-19-72	02-12-83	7.9
	8.0	152	08-19-74	12-09-89	9.9
	4.8	98	07-17-78	12-25-89	8.6
0333+321	14.5	82	01-17-80	12-18-89	8.3
	10.6	82	07-14-66	02-12-83	4.9
	8.0	123	06-01-78	12-09-89	10.7
	4.8	78	10-18-80	12-25-89	8.5
0336-019	14.5	95	09-17-74	12-05-89	6.2

Table 2-4: (Continued)

1 Object	2 Frequency	3 N	4 Date of First	5 Date of Last	6 Average N per Year
	10.6	134	07-14-66	11-03-82	8.2
	8.0	127	07-16-66	10-09-89	5.5
	4.8	39	08-04-79	10-30-89	3.8
	8.0 and 10.6	223	07-14-66	10-09-89	9.6
0420-014	14.5	125	08-19-77	11-29-89	10.2
	10.6	67	09-14-67	11-03-82	4.4
	8.0	144	06-09-77	10-09-89	11.5
	4.8	100	03-18-79	12-25-89	9.3
0422+004	14.5	87	09-03-79	12-19-89	8.4
	8.0	104	11-05-78	12-26-89	9.3
	4.8	53	02-16-80	12-24-89	5.4
0430+052	14.5	167	06-24-74	12-19-89	10.8
	10.6	153	11-01-66	02-12-83	9.4
	8.0	238	08-05-66	12-10-89	10.2
	4.8	101	04-19-78	12-24-89	8.6
0440-003	10.6	70	11-19-66	11-03-82	4.4
0723-008	14.5	45	08-10-82	04-30-89	6.7
	10.6	34	03-08-68	02-11-83	2.3
	8.0	77	04-19-78	12-08-89	6.6
	4.8	36	08-26-82	11-27-89	5.0
0735+178	14.5	108	08-19-77	12-18-89	8.8
	10.6	89	11-19-66	02-11-83	5.5
	8.0	122	03-11-77	12-08-89	9.6
	4.8	82	02-16-80	12-24-89	8.3

Table 2-4: (Continued)

1 Object	2 Frequency	3 N	4 Date of First	5 Date of Last	6 Average N per Year
0736+017	14.5	68	07-26-81	12-10-89	8.1
	10.6	84	11-01-66	02-11-83	5.2
	8.0	105	04-18-78	12-12-89	9.0
	4.8	52	02-17-82	11-26-89	6.7
	8.0 and 10.6	165	11-01-66	12-12-89	7.1
0754+100	14.5	85	11-18-78	12-21-89	7.7
	8.0	89	02-23-78	12-17-89	7.5
	4.8	41	02-16-80	12-24-89	4.2
0829+046	14.5	56	09-03-79	12-06-89	5.5
	8.0	62	03-28-78	12-23-89	5.3
	4.8	39	02-17-80	12-25-89	4.0
0851+202	14.5	162	05-08-74	12-17-89	10.4
	10.6	183	11-29-67	02-12-83	12.0
	8.0	184	01-27-71	12-08-89	9.8
	4.8	97	03-23-79	12-23-89	9.0
	10.6 and 14.5	278	11-29-67	12-17-89	12.6
0953+254	10.6	80	12-20-67	02-12-83	5.3
1101+384	14.5	64	04-20-79	12-19-89	6.0
	8.0	89	04-16-78	12-25-89	7.6
	4.8	62	02-16-80	12-24-89	6.3
1148-001	14.5	17	08-10-82	09-01-84	8.2
	10.6	31	08-18-70	02-12-83	2.5
	8.0	53	05-02-78	12-23-85	6.9

Table 2-4: (Continued)

1 Object	2 Frequency	3 N	4 Date of First	5 Date of Last	6 Average N per Year
	4.8	14	11-19-82	12-24-89	2.5
	8.0 and 10.6	71	08-18-70	12-23-85	4.6
1156+295	14.5	105	06-19-80	12-16-89	11.1
	8.0	113	05-29-77	12-12-89	9.0
	4.8	71	05-16-81	12-26-89	8.2
1219+285	14.5	63	11-19-78	12-19-89	5.7
	8.0	91	11-24-78	12-27-89	8.2
	4.8	61	06-20-79	12-25-89	5.8
1226+023	14.5	162	05-08-74	12-03-89	10.4
	10.6	148	07-14-66	02-12-83	8.9
	8.0	246	07-11-65	12-06-89	10.1
	4.8	97	04-18-78	11-28-89	8.4
1253-055	14.5	152	05-08-74	12-03-89	9.7
	10.6	145	07-14-66	02-12-83	8.7
	8.0	233	08-13-65	12-08-89	9.6
	4.8	109	12-24-77	12-24-89	9.1
1308+326	14.5	146	05-13-76	12-15-89	10.7
	10.6	34	12-10-77	02-12-83	6.6
	8.0	153	04-30-76	12-10-89	11.2
	4.8	104	09-01-78	12-24-89	9.2
1418+546	14.5	120	04-17-79	12-15-89	11.2
	8.0	127	08-05-78	12-21-89	11.2
	4.8	91	01-29-80	12-23-89	9.2

Table 2-4: (Continued)

1 Object	2 Frequency	3 N	4 Date of First	5 Date of Last	6 Average N per Year
1510-089	14.5	121	07-29-74	12-15-89	7.9
	10.6	143	02-17-67	02-12-83	8.9
	8.0	141	09-10-74	12-12-89	9.2
	4.8	93	04-18-78	12-26-89	8.0
	8.0 and 10.6	239	02-17-67	12-12-89	10.5
1514-241	14.5	55	07-29-79	09-28-89	5.4
	10.6	31	01-09-72	02-12-83	2.8
	8.0	60	04-19-78	12-15-89	5.2
	4.8	24	08-21-80	10-05-89	2.6
1611+343	14.5	56	05-14-82	12-19-89	7.4
	10.6	80	03-12-70	11-03-82	6.3
	8.0	99	06-15-79	12-09-89	9.4
	4.8	62	06-26-82	12-26-89	8.3
1641+399	14.5	159	05-08-74	12-19-89	10.2
	10.6	153	07-14-66	02-12-83	9.2
	8.0	242	08-14-65	12-13-89	9.9
	4.8	119	12-24-77	12-24-89	9.9
1652+398	14.5	61	04-15-79	09-28-89	5.8
	8.0	91	12-29-77	12-27-89	7.6
	4.8	49	08-21-80	12-24-89	5.2
1730-130	14.5	125	05-08-74	11-28-89	8.0
	10.6	114	07-14-66	11-03-82	7.0
	8.0	189	04-21-67	11-22-89	8.4
	4.8	60	10-26-77	08-18-89	5.1

Table 2-4: (Continued)

1 Object	2 Frequency	3 N	4 Date of First	5 Date of Last	6 Average N per Year
1749+701	14.5	69	03-18-80	09-29-89	7.2
	10.6	43	03-15-76	02-12-83	6.2
	8.0	83	02-03-80	12-27-89	8.4
	4.8	60	08-26-80	12-25-89	6.4
1749+096	14.5	122	11-20-78	12-12-89	11.0
	10.6	46	06-22-69	11-03-82	3.4
	8.0	126	04-28-78	12-13-89	10.8
	4.8	106	02-16-80	12-23-89	10.8
1807+698	14.5	71	09-03-79	12-17-89	6.9
	10.6	111	09-14-67	02-12-83	7.2
	8.0	122	06-12-79	12-20-89	11.6
	4.8	54	02-16-80	12-25-89	5.5
	10.6 and 14.5	166	09-14-67	12-17-89	7.4
1901+319	14.5	48	08-11-82	12-08-89	6.6
	8.0	99	07-23-74	12-08-89	6.4
	4.8	54	06-27-82	12-26-89	7.2
1921-293	14.5	143	08-26-74	11-29-89	9.4
	10.6	49	09-19-70	11-03-82	4.0
	8.0	140	09-13-74	12-14-89	9.2
	4.8	94	03-23-78	10-13-89	8.1
2134+004	14.5	122	06-13-74	12-18-89	7.9
	10.6	106	08-16-67	02-12-83	6.8
	8.0	162	08-11-67	11-20-89	7.3
	4.8	61	10-27-77	12-22-89	5.0

Table 2-4: (Continued)

1 Object	2 Frequency	3 N	4 Date of First	5 Date of Last	6 Average N per Year
2144+092	14.5	33	06-19-80	12-07-89	3.5
	8.0	78	04-22-78	12-07-89	6.7
	4.8	36	06-19-80	11-27-89	3.8
2145+067	14.5	114	07-13-74	12-17-89	7.4
	106	107	07-14-66	01-07-83	6.5
	8.0	147	11-09-67	12-09-89	6.7
	4.8	64	08-15-80	11-25-89	6.9
	8.0 and 10.6	222	07-14-66	12-09-89	9.5
2200+420	14.5	170	06-13-74	12-07-89	11.0
	10.6	511	11-26-67	01-07-83	33.8
	8.0	218	04-27-68	12-07-89	10.1
	4.8	118	10-27-77	12-22-89	9.7
	8.0 and 10.6	425	10-24-71	12-07-89	23.4
2201+315	14.5	59	12-08-81	12-10-89	7.4
	10.6	56	03-27-69	11-03-82	4.1
	8.0	110	04-22-78	12-08-89	9.5
	4.8	39	10-22-81	12-26-89	4.8
2223-052	14.5	110	08-25-74	12-10-89	7.2
	10.6	131	07-14-66	11-03-82	8.0
	8.0	153	04-20-67	12-13-89	6.8
	4.8	86	04-24-80	12-22-89	8.9
	10.6 and 14.5	218	07-14-66	12-10-89	9.3
2230+114	14.5	117	11-14-79	12-14-89	11.6
	10.6	127	07-14-66	11-03-82	7.8

Table 2-4: (Continued)

1	2	3	4	5	6
Object	Frequency	N	Date of First	Date of Last	Average N per Year
	8.0	125	07-26-74	12-08-89	8.1
	4.8	47	05-20-81	12-22-89	5.5
	8.0 and 10.6	228	07-14-66	12-08-89	9.7
2251+158	14.5	166	02-21-74	12-15-89	10.5
	10.6	149	06-15-66	01-07-83	9.0
	8.0	230	07-25-66	12-09-89	9.8
	4.8	110	10-27-77	12-26-89	9.0
2345-167	10.6	109	09-14-67	01-07-83	7.1

CHAPTER 3
CORRELATION ANALYSIS

Visual Inspection

Visual inspection, classical cross-correlation analysis and Discrete Correlation Function (DCF) analysis were used to search for correlated optical and radio events. Visual inspection is the simplest (and perhaps even the most reliable) method of searching for correlations between two data sets. For visual inspection, the optical and the radio flux densities curves are overlaid and shifted one with respect to the other until events overlap. An argument against visual inspection is that it is subjective. However, I would argue that even with other non-subjective techniques, you rely on results of visual inspection to decide if the results from those techniques are meaningful. In other words, I feel more confident in the results of visual inspection than I do in the analytical techniques used.

Classical Cross-Correlation Function Analysis

One of the nonsubjective methods of searching for correlations between optical and radio data is to use the classical cross-correlation function

$$R(\Delta\tau) = \frac{\sum(x(t_i) - \bar{x})(y(t_i + \Delta\tau) - \bar{y})}{\sqrt{\sum(x(t_i) - \bar{x})^2(y(t_i + \Delta\tau) - \bar{y})^2}} \tag{3-1}$$

where $x(t_i)$ = flux at frequency 1 at time t_i,

$y(t_i+\Delta\tau)$ = flux at frequency 2 at time $t_i+\Delta\tau$,

$\Delta\tau$ = offset or shift of y with respect to x,

$\overline{x} = \frac{1}{n}\sum x(t_i)$ and $\overline{y} = \frac{1}{n}\sum y(t_i)$.

One data set is shifted with respect to the other by an amount $\Delta\tau$ and R($\Delta\tau$) is computed from Equation 3-1. Using a range of offsets $\Delta\tau$, a family or set of R($\Delta\tau$) can be found. The value of $\Delta\tau$ for which R($\Delta\tau$) is a maximum is the lag time between the two data sets if there exists a correlation at all.

If the data is evenly sampled in time at intervals of Δt, all lag times from $\Delta\tau_{neg} = t_{x_1} - t_{y_m}$ to $\Delta\tau_{pos} = t_{x_n} - t_{y_1}$ can be examined. Here, t_{a_p} is the time of the pth observation of data set a. Data set x has n observations and y has m observations. However, unavoidable constraints on ground-based observations due to weather and constraints due to the position of an object with respect to the Sun and Moon make it impossible to obtain evenly sampled data. Long-term optical and radio monitoring observations made at the same times are non-existent. To work around this problem, one or both of the data sets is binned and/or interpolated to create evenly sampled data.

In this study, the data were binned into 30 day bins to create evenly sampled data. The 30 day binsize was chosen because the radio data from the UMRAO were given as averages in 30 day bins. Therefore, 30 days is the best resolution in the lag time that can be expected for the correlation analysis based on the radio data. Two variations of the classical cross-correlation technique were used, the interpolation method and the hole method. These are discussed in Pomphrey et al. (1976). Both methods were used in order to demonstrate the effects of "creating" data on the results. Comparison of the results from both of these methods to those of Discrete Correlation Function analysis (discussed in the next section), further demonstrates the effects of "creating" data on results. For the interpolation method, if there was a bin which did not contain any data, that bin was filled by interpolating the surrounding bins. With the hole method, if a bin did not contain any real data, that bin was not used in the calculation of R. For the classical cross-correlation function, R = +1 indicates perfect correlation, R = -1 indicates perfect anti-correlation, and R = 0 indicates that the data sets are uncorrelated.

Discrete Correlation Function Analysis

Edelson and Krolik (1988) point out some problems with the classical cross-correlation function as applied to astronomical data, the most important being that data is "invented" when interpolation is used. Another problem is that meaningful errors cannot be associated with the results. In fact, errors in the actual data are not even used in the equation for R. The Discrete Correlation Function (DCF) was developed by Edelson and Krolik to overcome these problems. The unbinned discrete correlation function is

$$UDCF_{ij} = \frac{\sum (x_i - \overline{x})(y_j - \overline{y})}{\sqrt{(\sigma_x^2 - e_x^2)(\sigma_y^2 - e_y^2)}} \qquad \text{(3-2)}$$

where σ_f is the standard deviation of the data set f and e_f is the measurement error associated with f. A $UDCF_{ij}$ is computed for each pair of points (x_i, y_j). A time difference $\Delta t_{ij} = t_j - t_i$ is associated with each pair. Every $UDCF_{ij}$ represents real information. There is no "invention" of data here as there is with classical correlation analysis. The $UDCF_{ij}$'s for the M pairs having $t - \frac{\Delta\tau}{2} \leq \Delta t_{ij} < t + \frac{\Delta\tau}{2}$ are binned where $\Delta\tau$ is the bin size. The DCF(Δt) is obtained from

$$DCF(\Delta t) = \frac{1}{M} \sum UDCF_{ij}. \qquad \text{(3-3)}$$

As Edelson and Krolik (1988, p. 647) point out, ". . . this binning implicitly means that one must accept a modest amount of interpolation in the correlation function (although not in the time series)." Also, an error can easily be associated with each lag time Δt from

$$\sigma_{DCF(\Delta t)} = \frac{1}{\sqrt{(M-1)(M'-1)}} \left(\sum [UDCF_{ij} - DCF(\Delta t)]^2 \right)^{1/2} \qquad \text{(3-4)}$$

where M′ is the number of bins used to calculate DCF(Δt).

Again, a binsize of 30 days was used, but on the $UDCF_{ij}$'s, not on the original data. As with the classical cross-correlation function, a value of $DCF(\Delta t) = 0$ indicates that the two data sets are uncorrelated for the lag time Δt. Also, the larger the value of the DCF, the stronger the correlation. If $DCF < 0$, the data sets are anti-correlated. Unlike the classical cross-correlation function, the DCF is not limited to values between ±1. This is because neither data set is a continuous time series. Instead, both are finite, and sampled at discrete times. For the majority of objects examined, $|DCF(\Delta t) \pm \sigma_{DCF(\Delta t)}|$ did not exceed 1.

Comparison of Classical Cross-Correlation Function and Discrete Correlation Function Analysis Results

In Figures 3-1 through 3-5, the DCF(dt) as a function of dt is shown in the top panel and the cross-correlation function R(dt) as a function of dt is shown in the bottom two panels. The results for the hole method are shown in the middle panel and those of the interpolation method are shown in the bottom panel. Figure 3-1 shows these functions for all lag times, dt. Figures 3-2 through 3-5 only show interesting portions of these curves.

The results of correlation analysis for III Zw 2 are shown in the left three panels of Figure 3-1. All three methods, the DCF, hole, and interpolation methods, are qualitatively similar. Note that the cross-correlation function R(dt) is bounded by ±1 for the hole and interpolation methods. This is not true of DCF(dt). The large scatter in the hole and DCF results as well as the large errorbars in the DCF for dt < -1500 days and dt > 4000 days is caused by too few data being correlated.

The right three panels of Figure 3-1 show DCF, hole, and interpolation method results for AO 0235+164. Again, all three methods give qualitatively similar results. Closely spaced peaks seen in the hole and DCF methods are merged in the interpolation method.

Figures 3-2, 3-3, 3-4, and 3-5 show interesting portions of the DCF, hole, and interpolation method results for III Zw 2, 0215+015, AO 0235+164, and OJ 287, respectively. In all figures, the DCF, hole, and interpolation results are qualitatively similar, with the results of the hole method being quite similar to the DCF results in most cases. The interpolation results show that individual peaks seen in the DCF and hole method results have been effectively smoothed out by the interpolation of the data. For OJ 287, even the results of the hole method appear to have had important features effectively smoothed out by binning the original data.

Because of the effects of binning and interpolating the original data in the cross-correlation analysis, and because the DCF method has an added advantage of errorbars to help in interpreting peaks in the DCF, only results of visual inspection and DCF analysis will be reported.

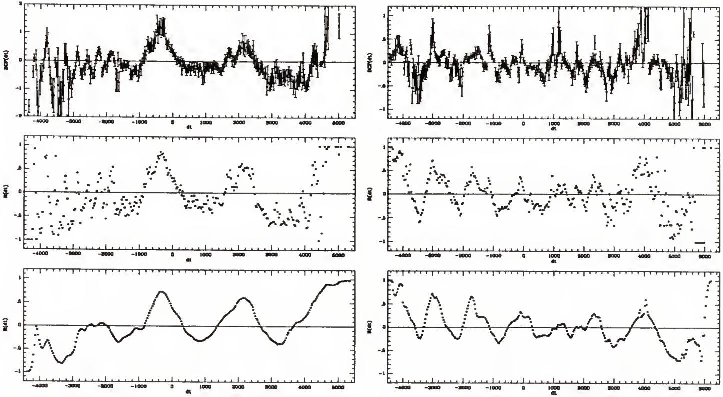

Figure 3-1: Comparison of Classical Cross-Correlation Function Analysis and Discrete Correlation Function Analysis on Optical and Radio Data
left) 0007+106 (III Zw 2)
right) AO 0235+164

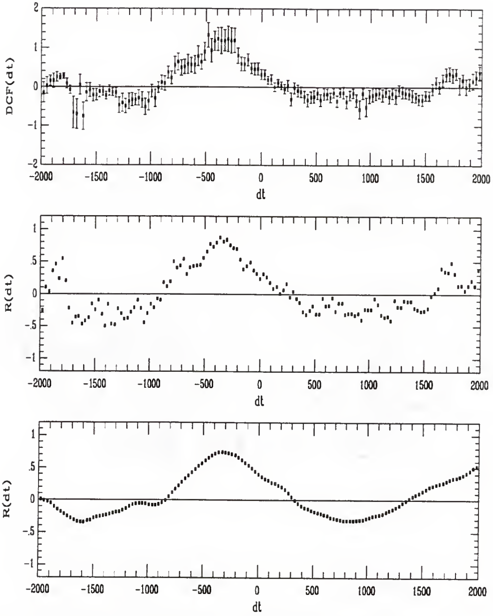

Figure 3-2: Comparison of DCF, Hole, and Interpolation Methods for III Zw 2

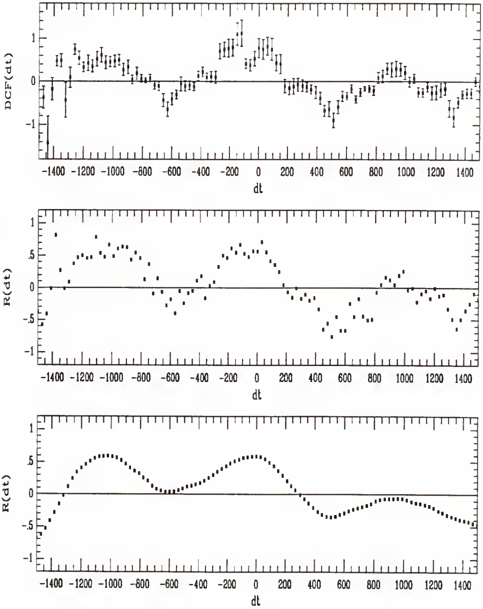

Figure 3-3: Comparison of DCF, Hole, and Interpolation Methods for 0215+015

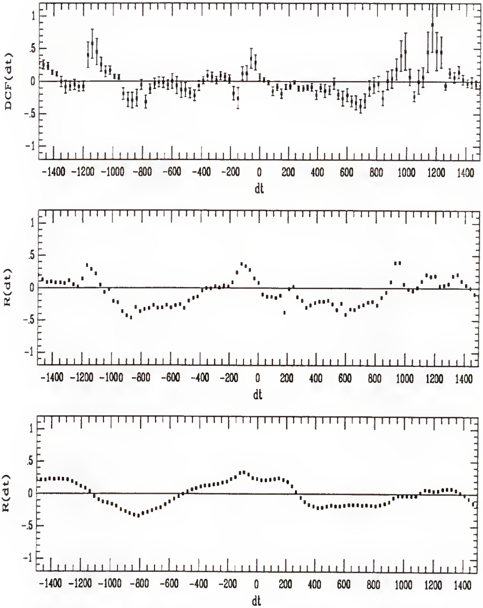

Figure 3-4: Comparison of DCF, Hole, and Interpolation Methods for AO 0235+164

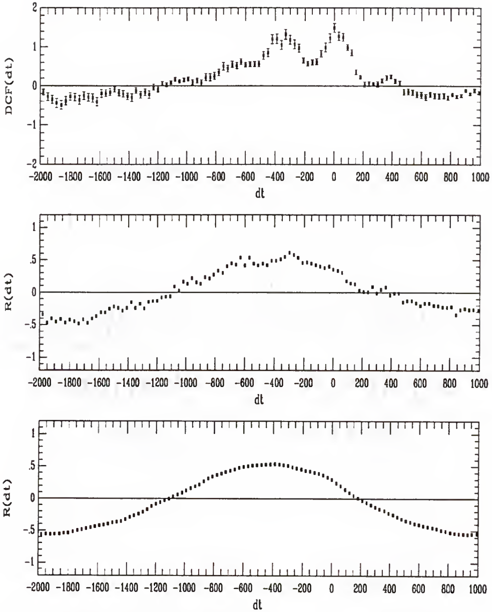

Figure 3-5: Comparison of DCF, Hole, and Interpolation Methods for OJ 287

CHAPTER 4
RESULTS

Optical-Radio Correlation Analysis Results

Results of the optical-radio correlation analysis are presented in this chapter. Figures 4-1 to 4-55 show the data and DCF results for all objects in the sample. In each figure, the top panel shows the optical flux (in mJy) versus time (in years), the middle panel shows the radio flux (in Jy) versus time (in years), and the bottom panel shows the DCF as a function of lag time (in days). Each figure caption provides the source and frequency of the radio fluxes. Some figures show results for analysis on subsets of the optical and/or radio data. Other figures show results for analysis using combinations of data sets. For example, an optical data set may consist of fluxes derived from B exposures as well as fluxes from m_{pg} exposures. A radio data set may consist of fluxes at both 14.5 GHz and 10.6 GHz or fluxes at both 10.6 GHz and 8.0 GHz. The figure caption will describe any combinations or subsets used. For some objects, the baseline was split into segments to allow for better resolution of activity in the light curves. Figures 4-56 to 4-71 show these segmented light curves. The top panel shows the optical data and the bottom panel shows the radio data.

Table 4-1 lists the results of the optical-radio correlation analysis for all objects having adequate optical and radio temporal coverage for reliable analysis. Column 1 gives the object designation by right ascension and declination. Column 2 gives the lag time found from visual inspection and Column 3 gives comments concerning the visual inspection. The lag times are given in months and are negative if the radio lags the optical and positive if the optical lags the radio. Results for the DCF analysis are given in Columns 4 - 7. Column 4 gives the lag time indicated by the DCF analysis, Column 5 gives the DCF for that lag time, Column 6 gives the σ_{DCF}, and Column 7 gives comments concerning the DCF analysis. Column 8 lists the optical color system used (B or m_{pg}). Column 9 lists the frequency of the radio observations. Any subsets used in the analysis are described in Columns 8 and 9. An entry of NC in Columns 2 or 4 indicates that no correlation is seen. A "?" in Columns 2 or 4 indicates that the results are uncertain or that the data are not adequate for reliable correlation analysis.

Results for individual objects are described below.

0007+103 (III Zw 2)

Optical observations began in late 1977. The baseline falls from 1978 to early 1981 and then remains approximately steady. Several events are superimposed on this baseline. Many events may be missing from the light curve due to the yearly gaps.

Radio observations at UMRAO began in earnest in 1978. This light curve is seen to have one long-term major event composed of 5 or 6 shorter-term events and 3 other large events which are somewhat isolated. The light curve rises and falls from 1978 to 1982 and then the baseline remains relatively flat if the 3 isolated events are ignored. The optical and radio light curves are therefore similarly shaped.

Visually, radio peaks appear to lag optical peaks by about 13 months. Also, with this 13 month lag, the 1989 8.0 GHz event falls in a period when no optical observations were made. The DCF is very strong and is flat for lag times of -8 to -16 months, consistent with a -13 month lag. DCF(-16 months) = 1.33 ± 0.31.

0048-097

Optical observations of this BL Lac object began in late 1970. The baseline declines steadily until 1980 or 1981. It then rises until 1985 or 1986 and then falls again by 1990. Many short-term events are seen to rise above this baseline.

The radio data used in the correlation analysis are a combination of ARO 10.6 GHz data from 1971 through 1980 and UMRAO 8.0 GHz data from 1981 through 1989. The baseline declines steadily from 1971 to mid-1979. After 1980, the baseline continues to decline, but more slowly, until 1987, although it may actually be flat from 1984 to 1987. Three large short-term events peak in early 1972, late 1972 and late 1974. Short-term events occur every 1 to 2 years.

Visual inspection shows that a lag of 0 months has the large optical peaks correlating with radio events in late 1972, late 1974 and late 1986. Some smaller optical events also correlate with radio events at zero lag. Longer lag times (up to -6 months) are necessary for correlating some optical and radio events (optical events in late 1980 and late 1981, for example). The zero lag seems most promising, although it appears that the lag time may vary from 0 to -6 months. The DCF does not show any correlation.

0215+015

Optical observations have been made since mid-1981 in B. Several flares are seen in the optical light curve, the strongest occurring toward the end of 1984.

Radio observations from UMRAO nicely overlap the optical baseline. Three long-term events (having durations of 2 or more years) are seen in the radio light curve with several short-term events superimposed. The overall shape is well sampled but some minor events may be missing.

The shapes of the optical and radio light curves are similar in that the optical flares coincide with the long-term radio events. Also, the largest event in the radio coincides with the largest event in the optical. If the optical event of late 1984 is made to coincide with the radio peak in early 1985, the lag time between optical and radio is about -3.3 months. The DCF shows a maximum at -4 to -5 months, consistent with the visual inspection. DCF(-4 months) = 1.12 ± 0.30. A smaller peak in the DCF occurs at 0 to +3 months. DCF(+2 months) = 0.82 ± 0.20. Visual inspection does not eliminate zero lag as a possibility. The optical appears to lead the radio by 0 to 5 months.

0229+131

Optical observations have been made since late 1969. This object has been fairly inactive. The baseline is rather constant, though it may rise slowly from 1971 to 1980 or 1981 and then decline slowly thereafter.

The radio data are 10.6 GHz observations from ARO. The baseline rose steadily from 1969 to 1975. It then rose more quickly until mid-1976. Since then, it has remained fairly constant. Only a few small events are seen on this baseline. Of course, the higher, fairly constant baseline since 1976 may be due to the superposition of several large short-term events.

No correlation is seen visually or in the DCF. Comparing the behavior of the baseline suggests that the optical and radio are uncorrelated.

AO 0235+164

Optical observations in B have been made since 1977. Two major events and several minor events are seen in the light curve. One major event occurred in early 1979 and the other in early 1987. Most of the minor events occurred prior to 1985. This object has been very faint since 1985 and therefore has been observed less frequently since then.

The radio data from UMRAO overlap the optical nicely. Radio data start in 1974 and go through 1989. Ignoring radio data prior to 1977, there are 2 major events and several minor events in the radio light curve. Events occur every 1 to 1.5 years. Four major events occur in late 1974, early 1975, early 1982 and in early 1987.

With a 0 to -1 month lag, the large optical event in early 1979 coincides with the radio event in early 1979. However, the large optical peak in early 1987 leads the large radio peak in 1987 by a little over 2 months. Overall, radio events lag optical events with lag times varying from 0 to 2 months. The DCF shows a small peak at -1 to -2 months, consistent with the visual inspection. DCF(-2 months) = 0.35 ± 0.15. This is also consistent with the 0 month lag found by Balonek (1982) for 0235+164.

0333+321 (NRAO 140)

From mid-1971, when observations were first made, until 1988, the baseline remained fairly constant. The last four data points in the light curve appear to be samples of a long-term event, although more than one event may be sampled.

The radio data are 8.0 GHz flux densities from UMRAO. When observations began in early 1978, the object appears to have been undergoing a long-term major event which lasted until 1985. Since 1985, the baseline has been relatively flat. The long-term event may be due to the superposition of several short-term events which are seen superimposed on the long-term event.

The optical light curve is not sampled well enough to determine for certain if the short-term events seen in the radio light curve have optical counterparts. Based on their overall shapes, the light curves do not appear correlated. The DCF also shows no correlation.

0336-019 (CTA 26)

Optical observations began in late 1969. Six major events, each consisting of one observation well above the base level, occur in the light curve. These events are certainly not resolved. The baseline is flat from 1973 through 1986. After 1986, the baseline increases.

The radio data are a combination of ARO 10.6 GHz observations prior to 1979.0 and UMRAO 8.0 GHz observations after 1979.0. The 8.0 GHz data were chosen because they more closely follow the 10.6 GHz data than did the 14.5 GHz data. Ignoring radio data prior to 1970, five long-term events are seen in the radio light curve. The largest event peaks in early 1972.

A one year lag between optical and radio events is suggested visually. This is based on the single point optical events correlating with radio events. The DCF shows a broad peak from -5 to -23 months, with DCF(-10 months) = 0.42 ± 0.16. This is consistent with the results suggested by the visual inspection. More confidence in this result would have been possible if the optical events had been resolved.

0420-014

Optical and 8.0 GHz

In late 1969, optical observations of this object were first taken. Several outbursts (at least 6) stand out above the very slowly rising baseline.

Radio observations at 8.0 GHz began at UMRAO in mid-1977. Four large peaks, with several minor peaks superimposed, are seen in the radio.

Visually, zero lag gives coincidence between the optical and radio events in late 1979. A lag of -20.5 months has optical events in late 1977, late 1978, and late 1979 coincident with radio events in late 1979, mid-1980, and mid-1981. In this case, the optical event in early 1982 does not coincide with any radio event. A lag of -43 months has more of the optical events coincident with radio events. Also, with the -43 month lag, the low, inactive state in the optical prior to 1975 coincides with the low state in the radio prior to 1978. (Admittedly, there are few radio points prior to 1978.) The DCF shows a small peak at -20 to -21 months, DCF(-20 months) = 0.28 ± 0.10, and at -51 months, DCF(-51 months) = 0.48 ± 0.14. The DCF shows nothing at -43 months, which is visually the most compelling lag time. The number and spacing of events in both light curves make positive identification of correlated optical and radio events impossible.

Optical and 14.5 GHz

The radio events in 1981 and 1983 are better resolved with the 14.5 GHz data. Using the 14.5 GHz data in the correlation analysis gives identical results with visual inspection as did analysis with 8.0 GHz data. The DCF is a bit different than for analysis of optical and 8.0 GHz data. The peaks in the DCF are also stronger. There is a peak at -20 to -24 months with DCF(-20 months) = 0.35 ±0.17. Also, a peak occurs at -44 to -45 months with DCF(-45 months) = 0.38 ± 0.14. Both of these are consistent with the possible results found with visual inspection. Again, the number and spacing of events in the two light curves make positive identification of correlated optical and radio events impossible.

0422+004

Optical observations began in 1976. The baseline falls from mid-1976 to 1979. It then remains flat, perhaps rising a bit through 1985 and falling again from 1985 to 1990. Three large short-term events (unresolved) are seen, one in late 1977, one in late 1982, and one in late 1987. These events are seen as single points well above the baseline.

The 8.0 GHz radio data start in late 1978. The baseline falls through late 1983 and remains fairly steady thereafter. Events occur roughly every 1 to 2 years.

The optical data are too sparse to reliably search for correlated optical and radio events. The DCF shows nothing.

0430+052 (3C 120)

Optical observations of this Seyfert galaxy began in late 1971. Long-term meandering of the baseline occurs with several short-term outbursts superimposed.

Radio observations from UMRAO began in 1966. Events occur superimposed on the baseline about once every 1 to 1.5 years.

Prior to 1978, the drop in the radio baseline is accompanied by a drop in the optical baseline. After 1978, the baselines for the two light curves diverge with the optical rising and the radio approximately constant or falling. Radio events prior to 1978 appear to lag optical events with the lag seemingly varying from 0 to -4 months. The DCF shows nothing. After 1980, the optical no longer appears to be correlated with the radio. For this reason, subsets of the optical and radio data were analyzed with the DCF method. Optical and radio data obtained between 1971.0 and 1980.0 were analyzed. The DCF shows a stong peak using the subsets. The DCF is flat from 0 to -5 months. DCF(-2 months) = 1.05 ± 0.08. Optical and radio data after 1980.0 were analyzed as well. There are too few events in the optical to search for correlated optical and radio events. The DCF for this subset shows nothing.

The visual correlation for a lag varying from 0 to -4 months is fair for pre-1980 optical and radio data. The positive results from DCF analysis on the pre-1980 subsets for 0 to -5 months corroborate this result. This is in agreement with the lag time found by Balonek (1982) of -3 to -5 months.

0440-003 (NRAO 190)

Optical data were first obtained in late 1969. The baseline is fairly flat, falling a bit until 1980 or 1981 and rising a bit until 1988. Several short-term events are seen.

The 10.6 GHz observations from ARO began in late 1966 and ended in late 1982. The baseline falls throughout. There is a gap in the data from 1974 to 1978.

The optical events do not fall at times when there are radio observations. There is no correlation evident.

0723-008

The optical baseline has been fairly constant since observations began in 1980. Many single point events stand out above the baseline.

Radio observations from UMRAO began in 1978. There is an overall decline in the baseline from 1978 until 1990. A long-term event occurs from mid-1980 to mid-1982. Several short-term events are seen in the light curve.

The object was not sampled frequently enough in the optical to resolve events. The optical data are relatively sparse, as are the radio data after mid-1984. Correlation analysis is not reliable with this quality of data. The DCF shows one point well above its neighbors at -5 months. The error bars are rather large though. This lag is not seen visually.

0735+178

Optical observations began in earnest in 1977 although there are some observations as far back as early 1974. The baseline slowly undulates, falling from 1977 through late 1978, rising until 1982, and falling again by late 1984. The baseline seems fairly flat thereafter.

The 8.0 GHz data begin in early 1977. From 1978, the baseline rises slightly until 1982 and falls again by late 1985. The baseline then rises into a large event, which peaks in mid-1989.

The large optical event in 1977 does not coincide with any radio events. The large radio event in 1989 does not coincide with any optical event. The baselines do look somewhat similar between these events. On the whole, the optical and radio do not appear to be correlated. The DCF also shows no correlation.

Because the optical and radio baselines outside the large events look somewhat similar, subsets excluding the large events were analyzed. Optical and radio data between 1978.0 and 1988.0 were analyzed. Visually, there are a few small optical and radio events that coincide with zero lag. These events peak in early 1979, late 1980, late 1981, and late 1983. However, for each optical-radio pair of events that correlate, either the optical or the radio event is a very small glitch on its baseline. For this reason, the zero lag found visually is doubtful. The DCF is positive and flat for the most part from -27 to +24 months.

0736+017

Optical observations began in late 1969. The baseline falls from 1971 through 1980 or 1981. It then rises until about 1987 and falls again through 1991. Several short-term events are seen superimposed on this baseline. The number of observations per year falls off after 1981.

Combined 8.0 GHz data and 10.6 GHz data were used in the correlation analysis. The 8.0 GHz data began in early 1978 but not in earnest until 1980. A deep minimum is seen in early 1981 and many short-term events are seen after 1981. The baseline seems to fall from 1982 to 1990. The ARO 10.6 GHz data began in 1966 and, except for one point in 1977, ended in 1973. Therefore, there is effectively a gap in the radio light curve from 1974 to 1980. The 10.6 GHz baseline fell until 1974 when the gap began. The point in 1976 is at a much higher level than the last point in 1974, so the baseline obviously rose from 1974 to 1976. It then fell again to the minimum in early 1981.

Both the large gap in the radio data from 1974 to 1980 and the low density of optical observations since 1982, make correlation analysis difficult and unreliable. The DCF does show a tiny peak at -3 months. DCF(-3 months) = 0.32 ± 0.22.

0754+100 (OI 090.4)

Optical observations began in early 1979. Many events are seen but are poorly resolved.

Radio observations at UMRAO began in early 1978. The baseline rises steadily from 1978 to 1984. A large event then occurs. The flux density falls off in 1986. Three to four events are seen from 1982 to 1986.

With a zero lag, some optical events coincide with some radio events. Specifically, optical and radio peaks coincide with zero lag in late 1982, early 1985, and late 1985. With a -27 month lag, the optical peaks in early 1982, late 1982, and early 1987 coincide with radio peaks in mid-1984, early 1985 and early 1989 respectively. The DCF shows a peak at -29 months. DCF(-29 months) = 0.96 ± 0.39.

There are too few optical data to feel confident in any correlation found with either visual inspection or with DCF analysis.

0829+049

Optical data begin in late 1980. The baseline is fairly constant. Large scale flickering is seen in early 1981 and in early 1983.

The 8.0 GHz data begin in 1978 but not in earnest until early 1981. The baseline rises from 1978 to mid-1986. There is a major event which begins in mid-1986 and peaks in early 1987, ending in the latter half of 1988. Another smaller event then begins, perhaps peaking in late 1989. The entire event is not seen.

There appears to be no correlation between optical and radio events for this object. The DCF also shows nothing.

0851+202 (OJ 287)

Optical and 8.0 GHz

Optical observations began in early 1970. A long-term event occurred from 1970 to 1974. From 1974 to 1983 the baseline was constant or rising. From 1983 to 1984, several outbursts occurred. Since mid-1984, OJ 287's baseline has been constant or falling and lower than the 1974 to 1983 base level.

Radio observations at UMRAO began in early 1971. Long-term meandering of the base occurs with short-term bursts superimposed.

The overall shape of the optical and radio light curves is somewhat similar. Many radio peaks show no optical counterpart. A short lag varying from 0 to -2 months has optical and radio events in the early 1970s and from late 1982 to early 1984 correlating. However, the largest optical event does not correspond to the largest radio event. The overall shapes match better with a -14 month lag. A -14 month lag correlates the largest optical event with the largest radio event and would allow for the minimum in the optical in early 1970 to correlate with the apparent radio minimum in early 1971. The DCF shows peaks at both -1 month, DCF(-1 month) = 0.53 ± 0.08, and -9 months, DCF(-9 months) = 0.81 ± 0.12. The peak at -9 months is rather flat from -9 to -15 months, consistent with the -14 month lag found from visual inspection. This is in good agreement with the -10 to -11 months lag found by Pomphrey et al. (1976).

Optical and Combined 14.5 GHz and 10.6 GHz

Data from ARO were used to extend the radio baseline to earlier times. The ARO 10.6 GHz data and the UMRAO 14.5 GHz data were combined and used in correlation analysis with the optical data. The 14.5 GHz data were used because they more closely followed the 10.6 GHz data than did the 8.0 GHz data.

With the additional data, it is evident that the radio minimum is closer to 1970.0 than 1971.5. This nicely matches the apparent minimum in the optical data. Also, an event is seen in early 1971 in the radio which would lag an optical event by -1 to -2 months. The DCF again shows two peaks, one at a lag of 0 months and one at a lag of -10 to -14 months. This time, the DCF peak at zero lag is the larger of the two. DCF(0 months) = 1.49 ± 0.12 and DCF(-11 months) = 1.32 ± 0.12. The -1 to -2 months lag is in good agreement with the Balonek (1983) result of 0 to -1 month and the Valtaoja et al. (1987) result of -2 to -3 months. Balonek also points out work by Usher (1979) which shows that at frequencies greater than 15 GHz, the 1972 radio event is stronger than the 1973 event. This lends support to the shorter -1 to -2 month lag time.

0953+254 (OK 290)

Optical observations have been made since early 1970. The overall light curve falls off until 1982 and then rises. Several short-term bursts are seen above this baseline.

Radio observations from ARO began in earnest in early 1970 and ended in early 1983. The overall baseline drops throughout this period with short-term bursts superimposed. Three "double peaked" events are seen to occur approximately every 3.5 years. The first peak in each event is stronger than the second although this is likely due to the overall decline in the light curve.

The overall shapes of the optical and radio light curves do seem to match. Visual inspection shows that some optical and radio events peak nearly simultaneously, for example, the events in early 1975 and early 1976. Visual inspection also shows that a lag of about -1 year is a possibility. The DCF shows a strong peak at -1 year. DCF(-12 months) = 1.32 ± 0.36. This correlation is questionable however, because the rapid flickering in the optical data confuses the analysis.

1101+384 (Mkn 421)

The optical observations began in early 1977. The data are very sparse. From 2 to 4 short-term events are seen prior to 1980. Only 4 observations were made between 1982 and 1985. One of these shows Mrk 421 to be at a very high state. Observations were made more frequently from 1985 to mid-1987. In late 1987 and early 1988, two short-term events are seen. The 3 data points made after 1989 are all high relative to the baseline between 1985 and 1987.

The 8.0 GHz radio data began in early 1978. The frequency of observations falls off after mid-1984. A large short-term event is unresolved in late 1979. The object undergoes a long-term event between 1980 and 1984 and perhaps again after 1987.

Although the optical data are extremely sparse and the radio data are not much better, the overall shapes of the optical and radio light curves suggests a short lag time between the two. Both light curves are at a minimum near early 1980 and again near early 1984 with a maximum in between somewhere. Both baselines seem fairly flat between 1984 and 1987. There also appears to be a long-term event in both, beginning in early 1987.

The DCF shows a peak at -1 month. DCF(-1 month) = 0.86 ± 0.25. The optical data are so sparse, however, that the reality of this correlation is dubious.

1148-001

Optical observations are extremely sparse. The baseline remains fairly constant from 1969 to 1980. After 1980, the object exhibits some variability.

The radio data are from ARO and are also extremely sparse. The data begin in early 1970 and end in mid-1982. There is a large gap in the observations from 1974 to 1980 with only two observations in that gap. An overall upward trend in the baseline is seen from 1970 to 1980, when it appears to level off.

Both optical and radio data sets are too poor for reliable correlation analysis. The DCF does not show any correlation.

1156+295

Optical observations began in mid-1980. The overall light curve has a fairly flat baseline with very active short-term flickering prior to 1986. After 1986, the object has been fairly constant with only one small event observed. The events are not resolved.

Radio observations from UMRAO began in earnest in early 1980. There is one isolated long-term event which lasts from 1982 to mid-1983. There are a succession of events thereafter.

The DCF analysis shows a peak at -20 months. DCF(-20 months) = 0.44 ± 0.09. This correlation cannot be confirmed with visual inspection. The overall shapes of the optical and radio light curves are not similar except that they both show a lot of activity. The extremely rapid flickering in the optical makes correlating specific optical events with specific radio events impossible. Based on the overall shapes of their light curves, the optical and radio data do not appear to be correlated.

1219+285 (W Com)

Optical observations began in 1972. The baseline increases slightly from 1972 to 1990. This object displays flickering behavior, with several short-term outbursts seen.

The radio data begin in late 1978. The baseline declines steadily from 1978 to 1990. Short-term events occur approximately every year.

No correlation is seen with DCF analysis. If events in the optical were better resolved, perhaps short-term events in the optical could be correlated with those in the radio.

1226+023 (3CR 273)

Optical observations began in 1974. The frequency of observations drops in 1981. It appears that this object may undergo flickering behavior. With the sparse coverage and the yearly gaps in observations, events are not well resolved. The baseline appears fairly constant.

Radio observations began in 1965. Two major long-term events are seen, one which began prior to the first observation in 1965 and ended in 1980, and the other beginning in 1980 and ending in 1988. Short-term events are superimposed on these long-term events, occurring every 1 to 2 years.

The optical and radio baselines do not correlate. The DCF also shows nothing.

1253-055 (3C 279)

Though initially made in 1971, optical observations did not begin in earnest until 1977. Prior to 1988, 3C 279 did very little in the optical. In 1988, it underwent a major outburst which petered out in early 1990, although it showed signs of flaring again in 1991.

Radio observations from UMRAO began in late 1965. Four major events and part of another are seen with many minor events superimposed. The major events each span roughly 4 to 6 years.

There are no optical events corresponding to the four radio events prior to 1986. The 1988 to 1989 optical event may be correlated with the radio event which began in 1986 but which had not petered out by the end of 1989. The DCF shows nothing.

Optical and radio observations between 1985.0 and 1990.0 were analyzed. Visually, a lag of about -1/2 year is a possibility. The DCF is scattered, indicating that not enough data are being used in the analysis. There is a broad maximum from -5 to -13 months. DCF(-13 months) = 1.39 ± 0.44. Too few events are used in the correlation analysis and therefore the -13 month result is questionable at best.

1308+326

The optical baseline has remained fairly constant, perhaps declining slowly, since observations began in 1976. Prior to 1984, several short-term outbursts are seen. Little activity has been exhibited since 1984.

The radio baseline was fairly constant, undulating only slightly, from 1976, when observations began, to 1987. From 1987 to 1988, the baseline drops to less than half its previous value. Many short-term events are seen in the light curve.

It might be argued that optical and radio events in 1977, 1978, and 1983 correlate with a lag of less than half a year. The DCF analysis does not really show this and the visual correlation is not compelling.

1418+546

The optical observations are extremely rare. Despite this, the baseline is seen to be approximately constant. There do appear to be a few events captured in the act, but none resolved. Radio data from UMRAO show a light curve characterized by 4 or 5 long-term events.

The optical observations were made too infrequently for reliable correlation analysis with radio data. The DCF shows a peak at -4 months, but with very large error bars due to the sparse optical data. DCF(-4 months) = 0.49 ± 0.34.

1510-089

Optical data begin in mid-1969. The baseline meanders up and down. Three to four short-term bursts are seen.

The radio light curve is a combination of ARO 10.6 GHz data from 1967.0 to 1978.5 and UMRAO 8.0 GHz data thereafter. This object is extremely variable in the radio, especially after 1979 when outbursts occur approximately once per year.

Visually, a -1 month lag shows the optical peak in mid-1988 correlating with the radio event of mid-1988. A -6 month lag has the optical peak in early 1987 coinciding with the radio peak in 1987. Also, the minimum from 1977 to 1978 in the optical coincides with the minimum in the radio in 1978. The optical data are not good enough to tell if the minimum corresponds with a -1 month or a -6 month lag. The DCF shows strong peaks at -4 months and at -15 months. The -4 month peak is stronger with a smaller error bar than the -15 month peak. DCF(-4 months) = 0.44 ± 0.16 and DCF(-15 months) = 0.41 ± 0.29. The -15 month peak results from the optical peak in early 1987 correlating with the radio peak in mid-1988. For this -15 month lag, the optical event in mid-1988 does not correlate with any radio event. The -15 month lag cannot be ruled out though.

The correlations found at -4 and at -15 months are based on so few events that the reality of the correlations is questionable.

1514-241 (AP Lib)

Optical observations began in 1972. A number of short-term outbursts are seen on a relatively constant baseline. One very large outburst occurred in mid-1977.

Radio observations began in 1978 and are fairly sparse. At least two, and perhaps three, long-term events are seen. There is an overall decline in the flux density.

Neither the optical nor the radio observations were made frequently enough for reliable correlation analysis. The DCF(dt) curve for dt greater than -1200 days has a scattered appearance, indicative of too little data being analyzed.

1611+343

The optical data are very sparse. Since 1980, when observations began, the baseline seems to have slowly increased. A few events are seen in the light curve, although they are not resolved.

The radio light curve, like the optical light curve, has a baseline which increases slowly and steadily after 1982.

Analysis with the DCF shows a broad maximum from -7 to -34 months. The maximum is at -29 months where DCF(-29 months) = 1.10 ± 0.54. The positive DCF values here are due to the fact that both optical and radio baselines increase. The optical data, however, are too rare to feel confident in any correlation found.

1641+399 (3CR 345)

In mid-1970, optical observations of 3CR 345 began. The baseline undulates quite a bit. At least two major long-term events are seen. Several smaller events are also seen.

Radio observations from UMRAO began in mid-1965. Two broad events are evident and appear to be the result of the superposition of several shorter events.

A -2 year lag between optical and radio events would have the large optical peaks in mid-1971 and mid-1972 correlating with the large radio peaks in mid-1973 and mid-1974 respectively. The optical peak in mid-1977 would correlate with a small radio peak in mid-1979. Also, the large optical peak in late 1982 would correlate with a small radio event in early 1984 which is superimposed on the large long-term radio event of 1980-1990. The DCF shows a very broad maximum which peaks at -28 months. DCF(-28 months) = 0.53 ± 0.07. The DCF is quite flat from -17 to -30 months, and is therefore consistent with the -2 year lag found from visual inspection.

Because the overall shapes of the two light curves are so different and since relatively few events in the optical and radio correlate, the reality of any correlation found is doubtful.

1652+398 (Mkn 501)

The optical baseline is quite constant as is the radio baseline. Few, if any, outbursts are seen in either light curve. Both light curves have fairly sparse coverage. This is true for the entire optical data set and the radio data set after mid-1982.

There are really no events positively seen in either light curve which could be visually correlated. The DCF has the scattered appearance of too little data being correlated. No peaks stand out in the DCF.

1730-130 (NRAO 530)

There are very few optical observations. A flat baseline and two outbursts characterize the light curve.

The radio baseline increases steadily from 1967, when observations began, through 1989. Several events are seen, especially after 1982.

The optical data are too infrequent for reliable correlation analysis. Based on their different baseline behaviors, the optical and radio do not appear to be correlated. The DCF shows nothing.

1749+701

Optical observations began in early 1979. The data are relatively sparse. The radio data from UMRAO began in early 1980.

The overall shapes of the optical and radio light curves are somewhat similar if a -16 to -21 month lag between optical and radio events exists. The DCF shows a correlation for a lag of -21 months, DCF(-21 months) = 0.65 ± 0.20. The optical data are really too sparse to reliably determine if the optical and radio light curves are correlated.

1749+096

Optical observations began in 1979. The data are very sparse but many outbursts are evident and follow the radio well. Many events may have been missed.

Radio observations from UMRAO began in early 1978. Events occur about every 1/2 to 1 year.

A -3 to 0 month lag is suggested from visual inspection. The DCF shows a -2 month lag, DCF(-2 months) = 0.63 ± 0.22.

Although the optical data are very sparse, the major optical outbursts do nicely coincide with the major radio outbursts with a -2 month lag. Because of this, and the strong peak at -2 months found with the DCF, this correlation is pretty good.

1807+698 (3CR 371)

Optical observations began in late 1969. The baseline meanders up and down slightly a few times. Outbursts are not resolved and many events may be missing.

The ARO 10.6 GHz data prior to 1981.5 were combined with UMRAO 14.5 GHz data after 1981.5. The 10.6 GHz data were used to extend the baseline to earlier times. The 14.5 GHz data were used instead of the 8.0 GHz data since it more closely matched the 10.6 GHz data. Since 1972, the radio baseline has slowly and steadily decreased. Prior to 1972, the baseline was at a much lower level although the error bars on the ARO flux densities at that time were extremely large. Many small events are seen on this baseline.

Because of the rapid flickering in the optical, it is very difficult to decide which optical and radio events, if any, are correlated with each other. The DCF does not really show anything, although the DCF value at -17 months lag stands out a bit above the rest. DCF(-17 months) = 0.50 ± 0.14.

1901+319

Optical observations show a slowly declining baseline. A short-term event is definitely seen in 1980 with others perhaps seen in 1981, 1983, and 1985.

The radio observations show a steadily increasing baseline with a couple of short-term events in 1979-1980 and in 1982. One long-term event is seen from 1984 to 1987 and part of another is seen, beginning in 1988.

The DCF is negative for lag times from -42 to +25 months because of the opposite trends in the optical and radio baselines. No correlation is seen visually. Events are too rare in both data sets and observations too infrequent in the optical to search for correlated events. However, based on the opposite slopes of their baselines, the optical and radio do not appear to be correlated.

1921-293 (OV-236)

Optical observations began in mid-1971, but began in "earnest" in mid-1976. The data are very sparse with no observations between 1972 and 1976 and less than 3 per year after 1982. Four or five sharp peaks are seen in the light curve. Many, many events may be missing. Most events are not resolved.

Radio observations at UMRAO began in mid-1974. One major event and the start of another are seen along with many smaller events superimposed on the baseline.

Visually, a lag of -5 to -6 months shows the largest optical event in mid-1979 coinciding with the largest radio event in late 1979. However, other events do not coincide. A lag of -10 to -11 months has more optical events coincident with radio events. Also, with this lag, the optical and radio light curves are similar in that both curves are low initially (e.g., the optical light curve in 1976), are low again about 5 years later (e.g., the optical light curve in 1981), and again are low toward the end of the data set (e.g., the optical light curve in 1988). The DCF shows a peak at a lag of -7 to -11 months, DCF(-9 months) = 0.67 ± 0.18. This is a strong peak in the DCF curve. This result is also in relatively good agreement with the result found by Balonek (1983) that optical leads radio by -6 to -8 months.

2134+004

The optical observations, which began in 1971, show a baseline that wanders slowly up and down. Two short-term events are seen as single points well above this baseline.

The radio observations began in 1967, but not frequently until 1974. The radio data also show a wandering baseline with an overall downward trend. Only very tiny short-term events are seen.

The baselines for the two data sets are similar in character and, for this reason, they may be correlated with an optical to radio lag of -2 to -4 years. The minimum in the optical near 1978-1979 correlates with the minimum in the radio in 1981-1982. The optical minimum in 1986 correlates with the radio minimum in 1989. Because the data ends so soon after the "minimum" in 1989, it is uncertain if it is a minimum and not just a glitch in a still declining baseline. The DCF shows a broad maximum from -51 to -19 months with a maximum at -33 months, consistent with the results from visual inspection. Because this is only a two-event (or even one-event) correlation, its reality is dubious.

2144+092

The frequency of optical observations is relatively high until 1982. The optical baseline slowly declines from 1970 to 1979 and then remains fairly constant. Many short-term outbursts are seen, especially prior to 1980.

Radio observations began in 1978, but not consistently until late 1979. The radio is characterized by short-term events lasting 1 to 1.5 years in the pre-1985 data. There is a gap in the observations from mid-1984 until early 1986.

Unfortunately, the radio data overlap the poorly sampled part of the optical light curve and there are no radio data prior to 1978 when the optical was most active. Based solely on the behavior of their baselines, the optical and radio do not appear to be correlated. No optical events are seen which would correspond to radio events between 1980 and 1984. The DCF shows a peak at +7 months. This can be attributed to the optical event in late 1987 correlating with the radio event in 1987. This is a one event correlation and should not be given much credence.

2145+067

The optical baseline meanders up and down. Since 1970, the baseline steadily increased until 1981. The baseline has since remained fairly constant. A couple of short-term events may be seen, but these are within the noise of the baseline.

The radio light curve is a combination of ARO 10.6 GHz observations made prior to 1979.0 and UMRAO 8.0 GHz observations made after 1979.0. The baseline declines from 1966 through 1976 and then steadily increases again until 1988. No short-term events are seen which really stand out above this baseline.

There are no short-term events in either data set to use to search for correlations between optical and radio short-term events. Based on the baselines, the optical and radio do not appear correlated. No positive correlation is seen in the DCF either.

2200+420 (BL Lac)

Optical observations began in mid-1971. From then until 1982, the light curve showed rapid flickering. In 1982, it appears to have changed its behavior, flickering less. (This may be due to reduced frequency of observations.) It also appears to be at a low in 1982.

The ARO 10.6 GHz data have better temporal coverage than the 8.0 GHz data prior to 1979. For this reason, ARO 10.6 GHz data prior to 1979.0 were combined with UMRAO 8.0 GHz data after 1979.0. The combined radio data were used in the correlation analysis with the optical data. Prior to 1976, very rapid flickering is seen in the radio with several short-term events occurring per year. After 1976, the flickering slows a bit, but events still occur about once per year.

With the better temporal coverage of these combined data, many optical and radio events prior to 1977.5 are seen to correlate with short lag times of -2 to 0 months. After 1977.5, many optical events show no radio counterpart. The DCF shows a strong peak at a lag of -2 months. DCF(-2 months) = 0.62 ± 0.12.

The optical and radio data sets were split into subsets and those subsets analyzed. Data prior to 1977.0 were analyzed giving a peak in the DCF at -2 months again. The DCF as a function of lag time is very similar to that for analysis on the entire data sets. In this case, DCF(-2 months) = 0.58 ± 0.16. Data after 1977.0 were analyzed giving a very different DCF as a function of time. In this case, there is a very broad maximum in the DCF from -33 months to -13 months. The maximum is at -21 months with DCF(-21 months) = 0.55 ± 0.14.

Based on this analysis, it appears that the optical and radio data prior to 1977 are correlated with a lag time of -2 months. The optical and radio do not really appear to be correlated after 1977.

2201+315

From sparse optical observations, it appears that the optical baseline is fairly constant. No short-term events are positively seen above the noise of the baseline, although there may be a couple in 1980 and 1981.

The radio baseline shows an overall upward trend. One large, long-term event is seen to last from 1983 to late 1986.

The optical and radio baselines do not appear correlated. No events are seen in the optical to correlate with the large radio event. The DCF also shows nothing.

2223-052 (3C 446)

Optical observations began in late 1971. Several large outbursts are seen in the light curve. After 1984, the object becomes less variable.

The ARO 10.6 GHz data prior to 1980.0 were combined with UMRAO 14.5 GHz data after 1980.0. The 14.5 GHz data more closely followed the 10.6 GHz data and were therefore used instead of the 8.0 GHz data. One major event is seen in the light curve along with a few minor ones. The beginning of another major event is seen at the end of the radio data set.

Optical events in mid-1980, mid-1981, mid-1984, late 1983, and late 1988 occur almost simultaneously with radio events, leading radio events by 0 to 4 months. Other optical events do not have radio counterparts at a 0 to -4 month lag. A lag of -11 to -8 months is also a possibility. This would have the optical events in late 1974 and early 1976 correlating with the small peaks in the long-term radio event of 1974-1977. The optical events in mid-1979 and mid-1983 would correlate with the radio peaks in mid-1980 and late 1984 respectively. The DCF shows a fairly broad peak from -2 to -6 months. DCF(-5 months) = 0.72 ± 0.24.

2230+114 (CTA 102)

Optical observations began in mid-1973. The baseline undulates slightly. Superimposed on that undulation are a few events.

The ARO 10.6 GHz radio data prior to 1980.0 were combined with 8.0 GHz data after 1980.0 to extend the baseline to earlier times. The baseline declined slowly until mid-1978. From mid-1978 to early 1980, the flux density doubled. Since then, the baseline has been steadily declining. A few outbursts are seen superimposed on this baseline, two strong ones in 1975 and in 1981.

The shapes of the optical and radio light curves are not similar. The two do not appear to be correlated visually. The DCF does not show any correlation either.

2251+158 (3CR 454.3)

A few short-term events are seen on this object's flat baseline. One large event is unresolved in late 1988.

Radio observations began in 1966. Six long-term events are clearly seen, the largest lasting from before 1966 to 1970.

The DCF is very flat except for a small bump between -42 and -2 months. The peak is very flat from -13 to -28 months, with a maximum at -16 months. DCF(-16 months) = 0.28 ± 0.05. This bump is due to the optical activity from late 1979 to late 1981 correlating with the large radio event which lasts from 1980 to 1984. No correlation is seen visually.

2345-167

Four short-term events are seen on the flat optical baseline. The largest is in early 1970, with smaller ones in mid-1970, late 1973, and late 1979. The data are very sparse from 1974 to 1979 and also after 1982.

The ARO 10.6 GHz data show a relatively flat baseline from 1968 to 1972. A short-term event occurs during this time, peaking in 1971. Another event is seen to peak in 1973. After this peak, the baseline steadily declines until 1978 and remains low. Two other events are seen to occur, one lasting from mid-1978 to mid-1980, and the other beginning in 1981.

If the large optical event of early 1970 is made to correlate with the radio event which peaks in early 1971, a lag of approximately -1 year is indicated. This is seen in the DCF as an ill-defined peak from -7 to -11 months. DCF(-11 months) = 0.78 + 0.39. This is a one event correlation, however, and should not be given a lot of credence. Based on the different characteristics of their baselines, the optical and radio do not appear to be correlated.

A Plug for Visual Inspection

In order to determine what causes the various bumps and wiggles in a plot of DCF as a function of lag time, the light curves for the two frequencies being analyzed must be visually inspected and compared. For example, the DCF as a function of lag time for the optical-radio correlation analysis of 0235+164 (top, right panel of Figure 3-1) shows peaks at -100, -38, -2, +33, and +39 months. Visual inspection shows that the true lag time is probably -2 months even though it is the peak with the smallest DCF. The other peaks are caused by the large optical peak in early 1979 being correlated with various large radio peaks. Specifically, the -100 month lag arises when the large optical event in early 1979 is correlated with the large radio event in 1987. The -38 month lag is caused by this optical event correlating with the radio peak in early 1982. The +33 month lag comes from this optical event correlating with the radio peak in mid-1976 and the +39 month lag is caused by the optical peak of early 1979 correlating with the radio peak of late 1978 to early 1979.

Also, visual inspection is used to determine the reliability of results from DCF analysis. To illustrate this, consider Figure 4-54 for 3CR 454.3. DCF analysis shows a small peak at a lag of -16 months. DCF(-16 months) = 0.28 ± 0.05. However, a correlation is not clearly seen with a visual inspection of the optical and radio light curves. For another illustration, consider 0235+164 again, Figure 3-1 or Figure 4-5. The DCF at the lag time between optical and radio data is fairly small with DCF(-2 months) = 0.35 ± 0.15. Yet visual inspection shows that the correlation for 0235+164 is strong, with many optical and radio events correlating.

The point being made in this section is that visual inspection is the technique ultimately used in searching for correlations. Even if a purely analytical technique is used, visual inspection is relied upon to decipher and judge the results of that analytical method.

Comparison of Results on Real Data with Results on Simulated Data

In this section, a much less subjective method of appraising the reliability of the correlation analysis results is described. This method involves comparing the results of the DCF analysis on real data with the results of the DCF analysis on "perfectly correlated" data having the same temporal sampling as the real data and having the same lag time as was found for the real data. "Perfectly correlated" optical data were created by shifting the radio data in time by -dt, where dt is the lag time previously found for the real optical and radio data, and interpolating to the times of the optical data. DCF analysis was performed on this "perfectly correlated" optical data and the real radio data.

These results can be compared to results for "perfectly *un*correlated" data. "Perfectly uncorrelated" optical data for each object were created by interpolating the 8.0 GHz radio data for 3C 120 to the times of that object's real optical data. For 3C 120, the 8.0 GHz data of object 1921-293 were used to create "perfectly uncorrelated" optical data. The results for "perfectly correlated" and "perfectly uncorrelated" DCF analysis are shown in Figures 4-72 to 4-99. The top panel of each figure shows the simulated optical data, the middle panel shows the real radio data, and the bottom panel shows the results of the DCF analysis on these two data sets. The figure captions describe the radio observations and the time shift (-dt) used to generate the "perfectly correlated" or "perfectly uncorrelated" optical data.

For almost every object examined in this way, the "perfectly correlated" DCF results nicely resemble the real DCF results, whereas the "perfectly uncorrelated" DCF results do not. Results of this analysis for individual objects are described below.

0007+106 (III Zw 2)

The "perfectly correlated" (or PC, for short) DCF results using a -13 month offset between the simulated optical data and the radio data are very similar to those of the real DCF results, with even the broad peak from -16 to -8 months matching. The "perfectly uncorrelated" (or PUC, for short) DCF results do not resemble the real DCF results.

0048-097

The PC DCF results using no offset between simulated optical data and real radio data only vaguely resemble the real DCF results. This may be due to the different behaviors of the simulated optical and real optical baselines. The PUC DCF results do not resemble the real DCF results at all.

0215+015

The three PC DCF results for offsets of 0, -3.3, and -5 months are all similar in shape to the real DCF results. The PC DCF results for the case where an offset of -3.3 months was used to generate the simulated optical data are most similar to the real results. The PUC DCF results are not similar to the real DCF results.

AO 0235+164

The overall shapes of the PC DCF results, with no lag used to generate the simulated optical data, more closely resemble the PC results when a lag of -2 months is used in that more of the peaks seen in the real DCF results are seen in the PC DCF results. However, the main peak is at the wrong lag (-1 instead of -2 months) with the no lag PC DCF results. The PC DCF results for a lag of -2 months show a peak at the proper lag. The PUC DCF results are not similar to the real DCF results.

0430+052 (3C 120)

Offsets of 0 and -4 months were used to generate simulated optical data. For both offsets, the PC DCF results on pre-1980.0 data resemble the real DCF results fairly well. The results for both offsets are quite similar. However, the results for a -4 month offset are slightly more similar to the real results than are the results for the 0 month offset. The PUC DCF results do not resemble the real results.

0851+202 (OJ 287)

Offsets of 0 and -14 months were used to generate the simulated optical data. The overall shape of the PC DCF results for the 0 month offset more closely resemble that of the real DCF results than does the shape of the PC DCF results for a -14 month offset. The PC results for the 0 month offset also peak at the proper lag whereas the PC results for a -14 month lag do not. The PUC DCF results do not really resemble the real DCF results.

1749+096

Both the PC DCF results for no lag and for a -3 month lag are equally good, nicely resembling the real DCF results and having their peaks at the correct lag. The PUC DCF results do not resemble the real DCF results.

1921-293 (OV-236)

The PC DCF results using a -10 month lag to generate the simulated optical data nicely resemble the real DCF results whereas the PUC DCF results do not.

2200+420 (BL Lac)

Offsets of 0 and -2 months were used to generate "perfectly correlated" optical data. The PC DCF results using the 0 month offset do not resemble the real DCF results as nicely as the PC DCF results using a -2 month offset. The main peak is at the correct lag for the 0 month offset PC results, but not the -2 month offset PC results. The PUC DCF results do somewhat resemble the real DCF results, probably because the overall shape of the simulated optical data is similar in overall shape to the real optical data.

When subsets of the simulated optical data and the radio data between 1971.5 and 1981.0 were used, the PC DCF results for a 0 month offset more closely resemble the real DCF results than do PC DCF results for an offset of -2 months. In this case, the PUC DCF results do not resemble the real DCF results.

Results of Correlation Analysis on Data at Two Radio Frequencies

This section deals with results of correlation analysis between two radio frequencies. Results of some are shown graphically in Figures 4-100 to 4-103. The top panel in these figures shows the 14.5 GHz flux density (in Jy) as a function of time (in years). The 8.0 GHz flux density as a function of time is shown in the middle panel. The DCF as a function of lag time (in days) is shown in the bottom panel.

Results of the DCF analysis are tabulated in Table 4-2 for 14.5 GHz - 8.0 GHz and in Table 4-3 for 8.0 GHz - 4.8 GHz. In each table, Column 1 gives the coordinate name, Column 2 gives the lag times found with visual inspection and Column 3 gives comments on the visual inspection. Column 4 gives the lag time between the two frequencies found from the DCF analysis. Column 5 and 6 give the DCF and the σ_{DCF}, respectively, for the lag time listed in Column 4. Column 7 gives comments on the DCF analysis.

Table 4-1: Optical-Radio Correlation Analysis Results

1	2	3	4	5	6	7	8	9
	Visual Inspection		DCF Analysis					
Object	lag (mo)	comments	lag (mo)	DCF	σ_{DCF}	comments	optical color	radio frequency
0007+106	-13		-16	1.33	0.31	-16 to -8	B	8.0
0048-097	-6 to 0	mostly 0	NC				m_{pg}	10.6 and 8.0
0215+015	-5 to 0		-4	1.12	0.30	-5 to -4	B	8.0
"	"		+2	0.82	0.20	0 to +3	"	"
0229+131	NC		NC				m_{pg}	10.6
0235+164	-2 to 0		-2	0.35	0.15	-2 to -1	B	8.0
0333+321	NC		NC				m_{pg}	8.0
0336-021	?	-1 year ?	-10	0.42	0.16	-23 to -5	m_{pg}	10.6 and 8.0
0420-014	?	-43 mo ?	-20	0.28	0.10		m_{pg}	8.0
"	"	"	-51	0.48	0.14	nothing at -43	"	"
"	?	-43 mo ?	-20	0.35	0.17	-24 to -20	m_{pg}	14.5
"	"	"	-45	0.38	0.14	-45 to -44	"	"
0422+004	?		NC				B	8.0
0430+052	-4 to 0		-2	1.05	0.18	-5 to 0	B	8.0
0440-003	?		NC				1971.0 to 1980.0 m_{pg}	10.6

Table 4-1: (Continued)

1	2	3	4	5	6	7	8	9
	Visual Inspection		DCF Analysis					
Object	lag (mo)	comments	lag (mo)	DCF	σ_{DCF}	comments	optical color	radio frequency
0723-008	?		-5	0.45	0.37	dubious	B	8.0
0735+178	NC		NC				B	8.0
0736+017	?		-3	0.32	0.22	blip	m_{pg}	10.6 and 8.0
0754+100	?		-29	0.96	0.39	-36 to -26	B	8.0
0829+046	NC		NC				B	8.0
0851+202	-2 to 0		-1	0.53	0.08	-3 to -1	B	8.0
"	-14		-9	0.81	0.12	-15 to -9	B	8.0
"	-2 to 0		0	1.49	0.12		B	14.5 and 10.6
"	-14		-11	1.32	0.12	-14 to -10	B	14.5 and 10.6
0953+254	?	-12 to 0 possible	-4	0.92	0.28	dubious	m_{pg}	10.6
"	"	"	-12	1.32	0.36	"	"	"
1101+384	?	perhaps -12 to 0	-1	0.86	0.25		B	8.0
"	"	"	+9	1.21	0.42	+9 to +14	"	"
1148-001	?		NC			redo	m_{pg}	8.0
1156+295	NC		-20	0.44	0.09	-20 to -17	B	8.0
1219+285	?		NC				B	8.0

Table 4-1: (Continued)

1	2	3	4	5	6	7	8	9
	Visual Inspection		DCF Analysis					
Object	lag (mo)	comments	lag (mo)	DCF	σ_{DCF}	comments	optical color	radio frequency
1226+023	NC		NC				B	8.0
1253-055	?	perhaps -6 to 0, post-1986	NC				m_{pg}	8.0
"	"		-13	1.39	0.44	-13 to -10	post-1986.0	
"	0		-10	0.54	0.19		m_{pg}	14.5
"	"		-10	1.38	0.39	-10 to -5	post-1986.0	
1308+326	?	perhaps -6 to 0	-23	0.41	0.06	-28 to -21	B	8.0
1418+546	?		NC				B	8.0
1510-089	?	-6 to 0 possible	-4	0.44	0.16	-5 to -1	m_{pg}	10.6 and 8.0
1514-241	?		-3	0.97	0.36	dubious	m_{pg}	8.0
"	"		-12	1.10	0.35	"	"	"
1611+343	?		-16	0.95	0.23	-23 to -15	B	8.0
1641+399	?	-2 years possible	-28	0.53	0.07	-33 to -17	B and m_{pg}	8.0
"	"	"	-28	0.50	0.06	-30 to -17	post-1970.5	
1652+398	?		NC				B	8.0
1730-130	?	baselines NC	-6	0.10	0.10	blip	m_{pg}	8.0

Table 4-1: (Continued)

1	2	3	4	5	6	7	8	9
	Visual Inspection		DCF Analysis					
Object	lag (mo)	comments	lag (mo)	DCF	σ_{DCF}	comments	optical color	radio frequency
1749+701	?	perhaps -21 to -16	-21	0.65	0.20		B	8.0
1749+096	-3 to 0		-2	0.63	0.22		B	8.0
1807+698	?		-17	0.50	0.14		m_{pg}	14.5 and 10.6
1901+319	?	baselines NC	NC				B	8.0
1921-293	-11 to -10		-9	0.67	0.18	-11 to -7	m_{pg}	8.0
2134+004	?	-4 to -2 yrs possible	-33	0.67	0.19	-51 to -19	B	8.0
2144+092	?	baselines NC	NC				m_{pg}	8.0
2145+067	?	baselines NC	NC				m_{pg}	10.6 and 8.0
2200+420	-2 to 0		-2	0.62	0.12	sharp peak	B	10.6 and 8.0
"	-2 to 0		-2	0.58	0.16	sharp peak	pre-1977.0	
"	NC		-21	0.55	0.14	-33 to -13	post-1977.0	
2201+315	NC		NC				B	8.0
2223-052	?	-11 to 0 possible	-5	0.72	0.24	-6 to -2	B	14.5 and 10.6
2230+114	NC		NC				B	10.6 and 8.0

Table 4-1: (Continued)

1	2	3	4	5	6	7	8	9
	Visual Inspection		DCF Analysis					
Object	lag (mo)	comments	lag (mo)	DCF	σ_{DCF}	comments	optical color	radio frequency
2251+158	NC		-16	0.28	0.05		B	8.0
2345-167	NC	-12 possible	-11	0.78	0.39	-11 to -7	m_{pg}	10.6

Table 4-2: Results of 14.5 GHz - 8.0 GHz Correlation Analysis

1	2	3	4	5	6	7
	Visual Inspection		DCF Analysis			
Object	Lag (mo)	Comments	Lag (mo)	DCF	σ_{DCF}	Comments
0007+106	-3 to 0	0 prior to 1985 -2 to -3 post-1985	-4	0.82	0.19	-8 to -3
0048-097	0		0	0.86	0.31	-2 to +2
0215+015	0	14.5 GHz not well resolved	-1	1.01	0.19	-1 to +4
0235+164	0		0	1.15	0.23	very sharp peak
0333+321	-13 to -11		-10	0.90	0.13	-12 to +3
0336-019	-2 to 0		-2	0.83	0.09	-5 to +1
0420-014	-1 to 0		-1	0.82	0.09	-6 to -1
0422+004	0		0	0.78	0.14	
0430+052	0		+27	0.92	0.18	flat from -2 to +36
"	"		-2	0.72	0.09	"
0723-008	?	difficult to tell	+22	1.05	0.41	+22 to +27
"	"	"	0	0.44	0.20	tiny peak
0735+178	0		0	1.22	0.29	-2 to +2
0736+017	-2 to 0		-1	0.79	0.17	
0754+100	-2 to 0	mostly 0	-2	1.08	0.17	-3 to -2

Table 4-2: (Continued)

1	2	3	4	5	6	7
	Visual Inspection		DCF Analysis			
Object	Lag (mo)	Comments	Lag (mo)	DCF	σ_{DCF}	Comments
0829+046	?	coverage poor	-6	1.12	0.43	-9 to +3 lots of scatter
0851+202	0		-1	0.81	0.10	-1 to 0
1101+384	?	coverage lousy shapes, not peaks, suggest -6 to 0	0	1.32	0.22	-2 to +2
1148-001	?	not enough data	NC			scatter diagram
1156+295	-1 to 0	perhaps -4.5 for late 1986 event	-2	0.90	0.12	-2 to 0
1219+285	-1 to 0	events not resolved at 14.5 GHz	+6	1.04	0.15	-6 to +9
1226+023	-7 to -3		-6	0.81	0.08	-12 to -2
1253-055	0		-2	0.53	0.06	-3 to -1
1308+326	-4 to 0		-2	1.00	0.11	-3 to +1
1418+546	0		+1	0.92	0.15	-1 to +1
1510-089	-1 to 0		-1	0.98	0.16	sharp peak
1514-241	?	resolution poor -1 to 0 possible	0	0.73	0.19	-7 to +3
1611+343	0	difficult to tell 0 based on one opt.-rad. pair	-7	0.91	0.35	-7 to +8

Table 4-2: (Continued)

1	2	3	4	5	6	7
	Visual Inspection		DCF Analysis			
Object	Lag (mo)	Comments	Lag (mo)	DCF	σ_{DCF}	Comments
1641+399	0		-7	1.04	0.08	-14 to +1
1652+398	?		NC			no real peak
1730-130	-4 to 0	0 most likely, 1986 -1989.5 esp.	-2	0.90	0.10	-2 to 0
1749+701	?	around 0, but resolution poor	0	0.86	0.10	-4 to +1
1749+096	-1 to 0		-1	1.02	0.22	sharp peak
1807+698	?	scatter too great coverage too poor	-1	0.48	0.21	-1 to +2
1901+319	?	shapes ok for 0 lag	-2	0.79	0.14	-8 to 0
1921-293	-1 to 0		-2	0.92	0.12	-2 to 0
2134+004	-12 to 0	tough to tell, closer to 0 though	0	0.63	0.09	0 to +5
2144+092	?	very little data, overall shapes suggest lag near 0	-1	0.97	0.28	-1 to 0
2145+067	-5 to +1	8.0 GHz too smooth to tell	-6	0.91	0.05	-12 to +5
2200+420	0		-1	0.78	0.13	-1 to +1
2201+315	?	-6 to 0 based on overall shapes	-3	0.74	0.15	-7 to -1

Table 4-2: (Continued)

1	2	3	4	5	6	7
	Visual Inspection		DCF Analysis			
Object	Lag (mo)	Comments	Lag (mo)	DCF	σ_{DCF}	Comments
2223-052	-1 to 0	0 best	-3	1.02	0.16	-3 to -1
2230+114	-2 to 0		-1	0.83	0.16	-3 to 0
2251+158	-3 to 0		-3	0.63	0.07	-7 to -1

Table 4-3: Results of 8.0 GHz - 4.8 GHz Correlation Analysis

1	2	3	4	5	6	7
	Visual Inspection		Discrete Correlation Function Analysis			
Object	Lag (mo)	Comments	Lag (mo)	DCF	σ_{DCF}	Comments
0007+106	-4 to 0	0 pre-1984 -4 to -2 post-1984	-11	1.66	0.26	-13 to -10
0048-097	0	4.8 GHz coverage not so good	-2	0.52	0.16	-2 to +1
0215+015	0	4.8 GHz coverage not so good	+4	0.98	0.28	-2 to +4
0235+164	0		-1	0.79	0.13	
0333+321	-5 to -4		-14	0.96	0.10	-25 to 0
0336-019	-1 to 0	4.8 GHz no good really	-9	0.92	0.21	-24 to +20
0420-014	-4 to 0		-4	0.94	0.13	-6 to -1
0422+004	0	4.8 GHz coverage poor	-1	1.01	0.27	
0430+052	0		-9	0.25	0.09	-9 to 0
0723-008	?	perhaps -1 month	-20	1.93	0.44	-25 to -15
0735+178	0		0	0.99	0.31	
0736+017	-2 to 0		-2	1.07	0.20	-2 to 0
0754+100	-2 to 0		-6	1.21	0.20	-9 to +3
0829+046	?	coverage of peaks too sparse	-3	1.37	0.54	lots of scatter -6 to +9
0851+202	0		0	0.78	0.10	0 to +2

Table 4-3: (Continued)

1	2	3	4	5	6	7
	Visual Inspection		Discrete Correlation Function Analysis			
Object	Lag (mo)	Comments	Lag (mo)	DCF	σ_{DCF}	Comments
1101+384	?	coverage lousy -6 to 0 based on shapes, not peaks	+2	1.58	0.41	lots of scatter -4 to +2
1148-001	?	very little data	NG			
1156+295	-3 to 0	-3 for one event	-2	0.98	0.13	-4 to 0
1219+285	?	events not resolved at 4.8 GHz	-9	1.07	0.12	-15 tp +2
1226+023	-5 to 0		-13	0.68	0.09	-25 to -8
1253-055	0		-4	0.56	0.06	-10 to -1
1308+326	-3 to 0		-1	1.07	0.13	-5 to +1
1418+546	0		0	0.89	0.16	
1510-089	-2 to 0		-1	0.91	0.18	-1 to 0
1514-241	?	resolution lousy	-13	1.52	0.53	no good lots of scatter
1611+343	-3 to 0	tough to tell, probably closer to 0	-1	0.97	0.32	-3 to -1
1641+399	0		-8	0.93	0.07	-12 to -2
1652+398	?		NC			no real peak
1730-130	-3 to 0	resolution in 4.8 pretty poor	-4	0.78	0.18	-4 to +1

Table 4-3: (Continued)

1	2	3	4	5	6	7
	Visual Inspection		Discrete Correlation Function Analysis			
Object	Lag (mo)	Comments	Lag (mo)	DCF	σ_{DCF}	Comments
1749+701	?	near 0, but resolution poor lots of scatter	0	1.12	0.14	-5 to 0
1749+096	0		-1	0.97	0.17	-3 to -1
1807+698	?	scatter too great, coverage too poor	-8	1.25	0.69	lots of scatter perhaps -3 better
1901+319	?	shapes ok for 0 lag	-1	0.86	0.17	
1921-293	-1 to 0		-1	0.78	0.09	
2134+004	?	very tough to tell				no real max very broad, flat 'peak'
2144+092	?	near 0, but 4.8 GHz data very sparse	-1	1.30	0.39	-3 to -1
2145+067	?		-6	0.99	0.10	-15 to +1
2200+420	0		0	0.85	0.13	
2201+315	?	not really enough 4.8 GHz data to tell	-8	0.82	0.25	-8 to -1
2223-052	-4 to 0	0 best	-2	1.05	0.18	-5 to -2
2230+114	?	not really enough 4.8 GHz to tell	-2	1.40	0.30	-4 to -2
2251+158	-3 to 0	possibly up to -7	-6	0.62	0.08	-8 to -5

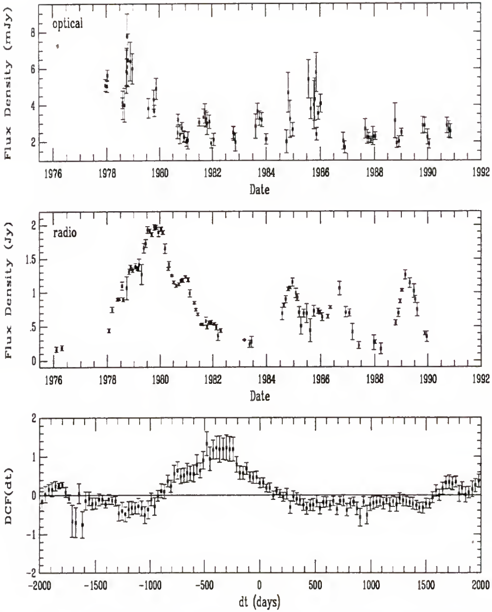

Figure 4-1: 0007+106 (III Zw 2) — DCF Analysis on Optical and Radio Light Curves
top) Optical color system: B
middle) Radio frequency: 8.0 GHz
bottom) DCF analysis results

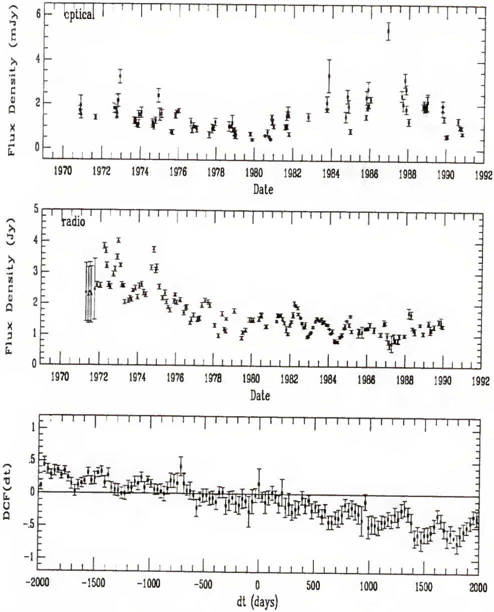

Figure 4-2: 0048-097 — DCF Analysis on Optical and Radio Light Curves
top) Optical color system: m_{pg}
middle) Radio frequency: 10.6 GHz prior to 1981.0 and 8.0 GHz after 1981.0
bottom) DCF analysis results

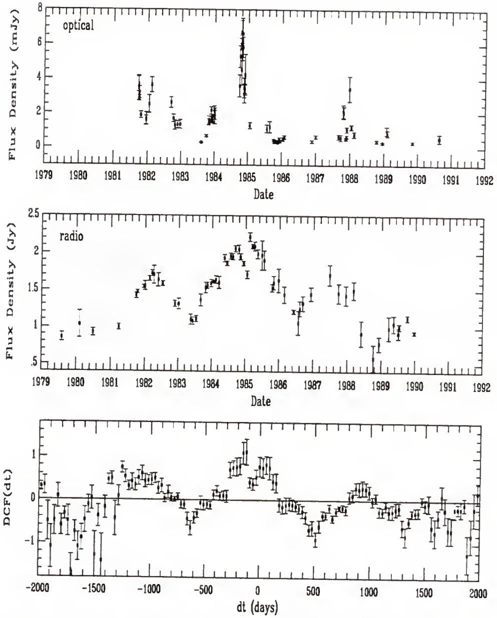

Figure 4-3: 0215+015 — DCF Analysis on Optical and Radio Light Curves
top) Optical color system: B
middle) Radio frequency: 8.0 GHz
bottom) DCF analysis results

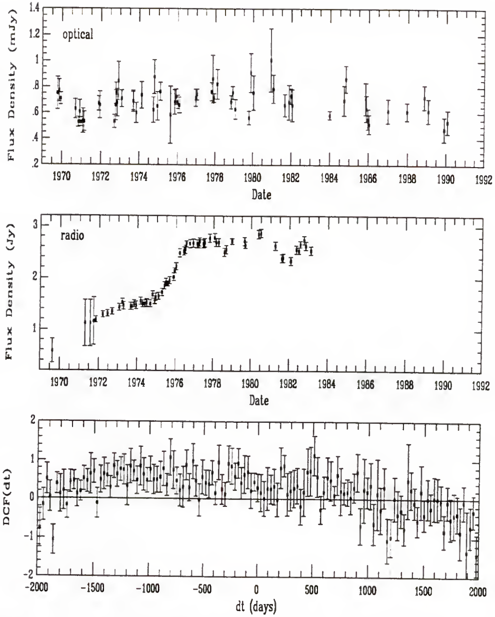

Figure 4-4: 0229+131 — DCF Analysis on Optical and Radio Light Curves
top) Optical color system: m_{pg}
middle) Radio frequency: 10.6 GHz
bottom) DCF analysis results

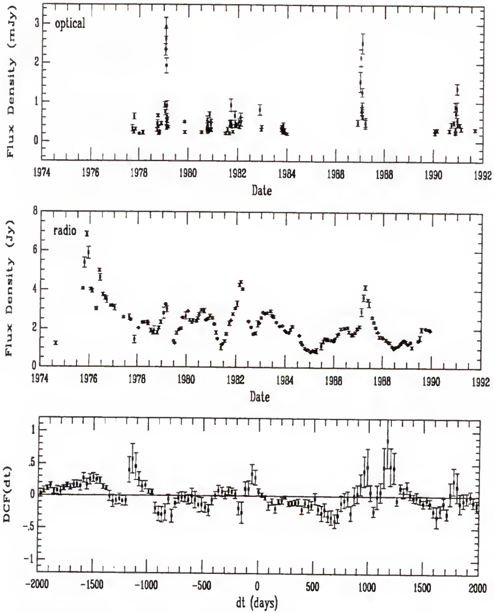

Figure 4-5: AO 0235+164 — DCF Analysis on Optical and Radio Light Curves
top) Optical color system: B
middle) Radio frequency: 8.0 GHz
bottom) DCF analysis results

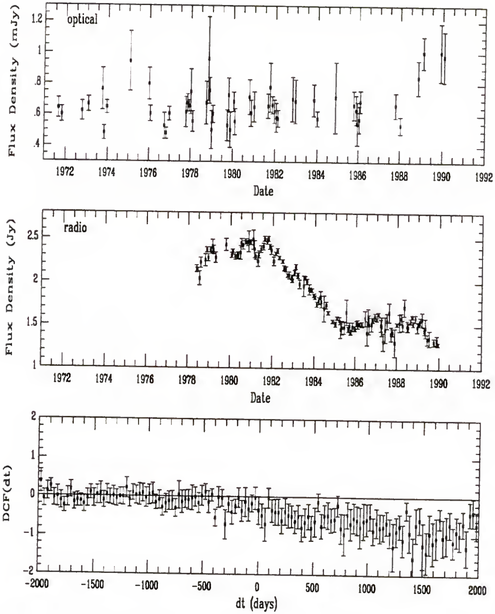

Figure 4-6: 0333+321 (NRAO 140) — DCF Analysis on Optical and Radio Light Curves
top) Optical color system: m_{pg}
middle) Radio frequency: 8.0 GHz
bottom) DCF analysis results

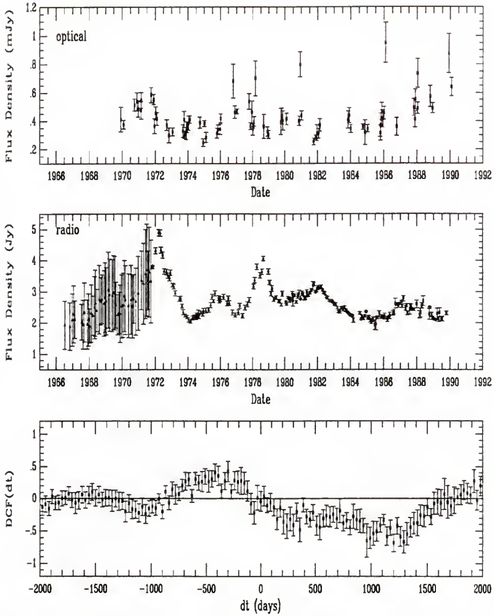

Figure 4-7: 0336-019 (CTA 26) — DCF Analysis on Optical and Radio Light Curves
top) Optical color system: m_{pg}
middle) Radio frequency: 10.6 GHz prior to 1979.0 and 8.0 GHz after 1978.0
bottom) DCF analysis results

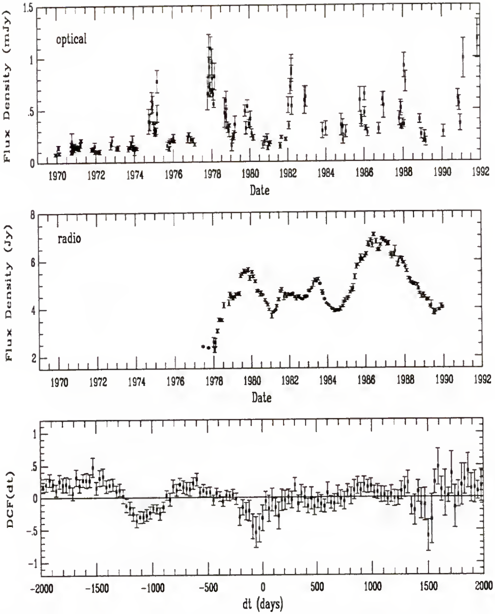

Figure 4-8: 0420-014 — DCF Analysis on Optical and Radio Light Curves
top) Optical color system: m_{pg}
middle) Radio frequency: 8.0 GHz
bottom) DCF analysis results

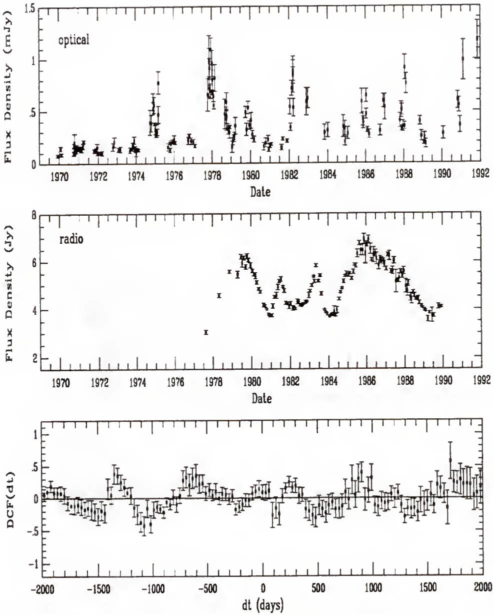

Figure 4-9: 0420-014 — DCF Analysis on Optical and Radio Light Curves
top) Optical color system: m_{pg}
middle) Radio frequency: 14.5 GHz
bottom) DCF analysis results

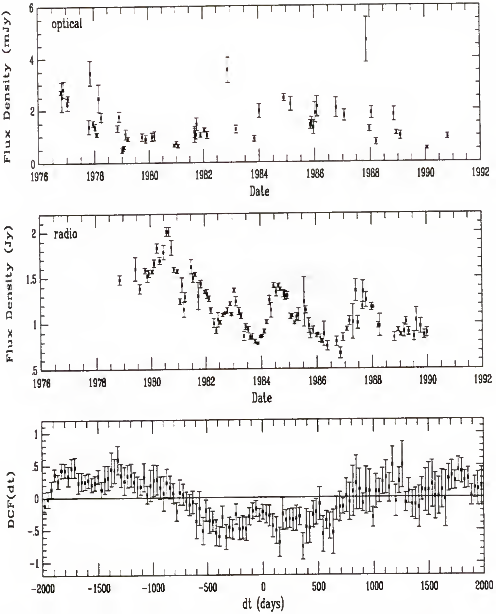

Figure 4-10: 0422+004 — DCF Analysis on Optical and Radio Light Curves
top) Optical color system: B
middle) Radio frequency: 8.0 GHz
bottom) DCF analysis results

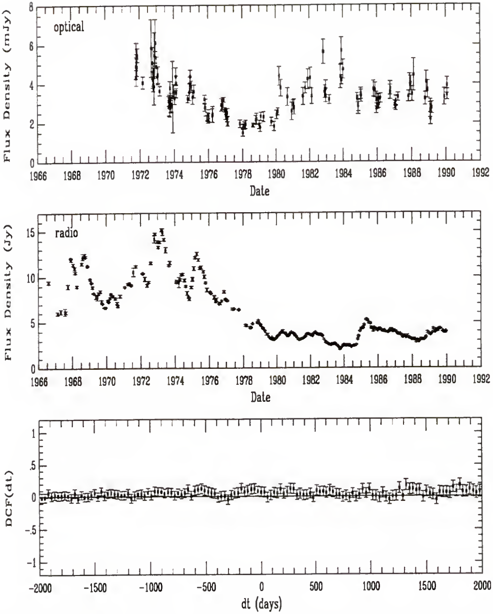

Figure 4-11: 0430+052 (3C 120) — DCF Analysis on Optical and Radio Light Curves
top) Optical color system: B
middle) Radio frequency: 8.0 GHz
bottom) DCF analysis results

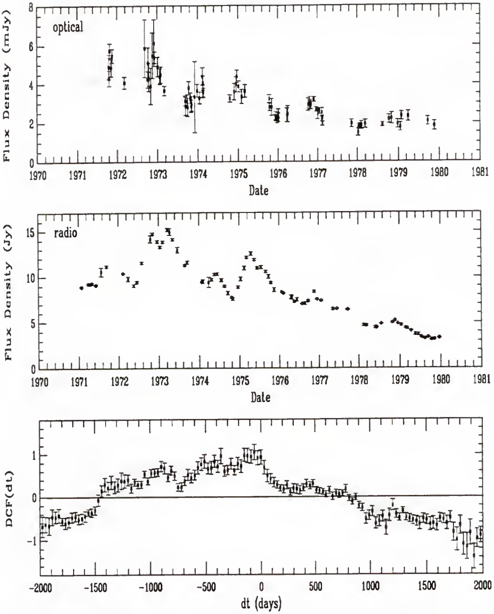

Figure 4-12: 0430+052 (3C 120) — DCF Analysis on Optical and Radio Light Curves — Subsets: 1971.0 to 1980.0
top) Optical color system: B
middle) Radio frequency: 8.0 GHz
bottom) DCF analysis results

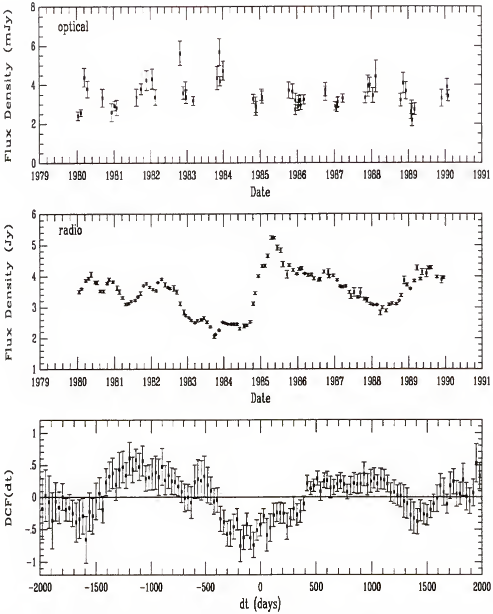

Figure 4-13: 0430+052 (3C 120) — DCF Analysis on Optical and Radio Light Curves — Subsets: post-1980.0
top) Optical color system: B
middle) Radio frequency: 8.0 GHz
bottom) DCF analysis results

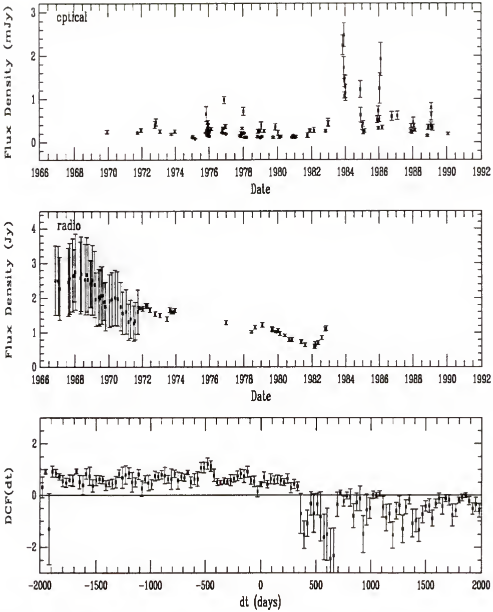

Figure 4-14: 0440-003 (NRAO 190) — DCF Analysis on Optical and Radio Light Curves
top) Optical color system: m_{pg}
middle) Radio frequency: 10.6 GHz
bottom) DCF analysis results

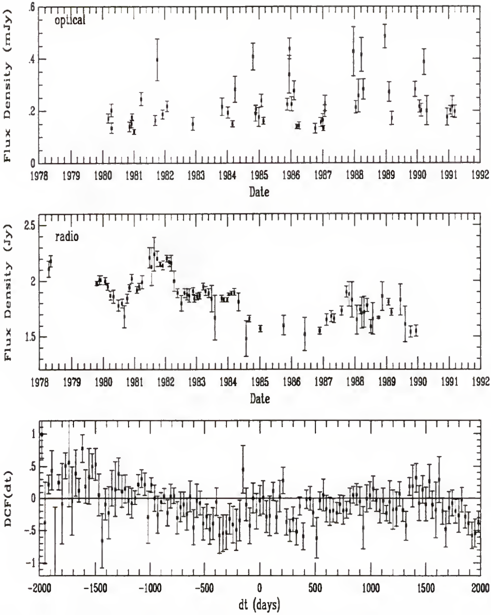

Figure 4-15: 0723-008 — DCF Analysis on Optical and Radio Light Curves
top) Optical color system: B
middle) Radio frequency: 8.0 GHz
bottom) DCF analysis results

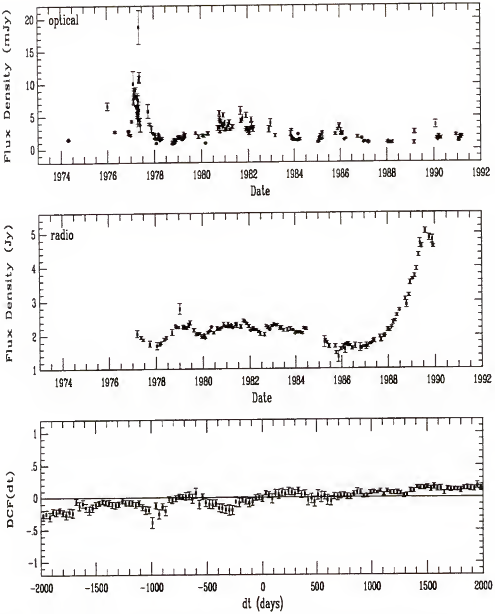

Figure 4-16: 0735+178 — DCF Analysis on Optical and Radio Light Curves
top) Optical color system: B
middle) Radio frequency: 8.0 GHz
bottom) DCF analysis results

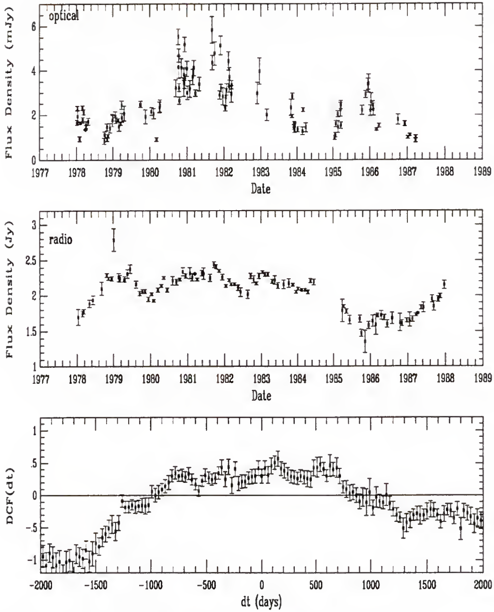

Figure 4-17: 0735+178 — DCF Analysis on Optical and Radio Light Curves — Subsets: 1978.0 to 1988.0
top) Optical color system: B
middle) Radio frequency: 8.0 GHz
bottom) DCF analysis results

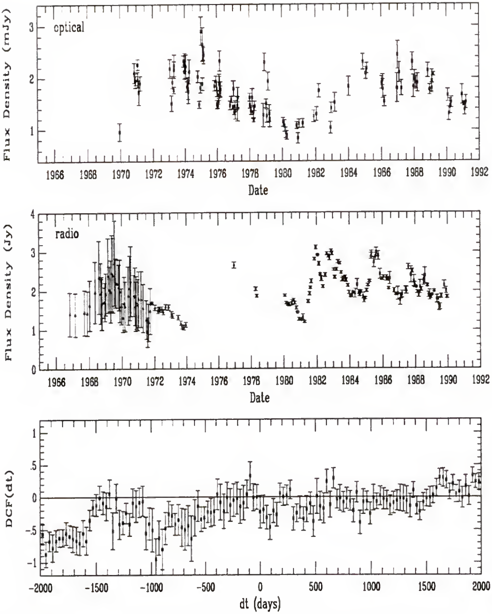

Figure 4-18: 0736+017 — DCF Analysis on Optical and Radio Light Curves
top) Optical color system: m_{pg}
middle) Radio frequency: 10.6 GHz prior to 1978.0 and 8.0 GHz after 1978.0
bottom) DCF analysis results

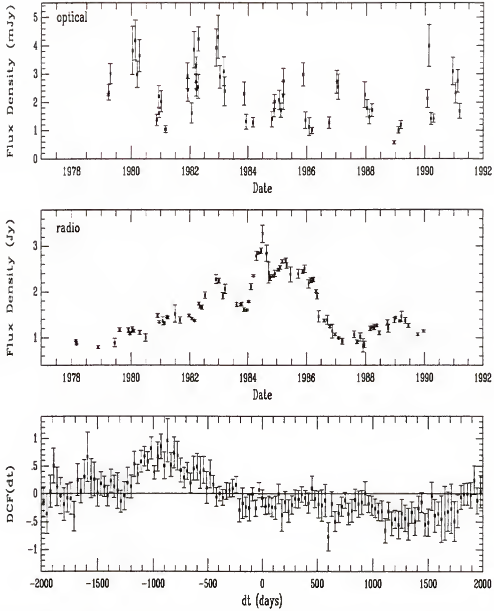

Figure 4-19: 0754+100 (OI 090.4) — DCF Analysis on Optical and Radio Light Curves
top) Optical color system: B
middle) Radio frequency: 8.0 GHz
bottom) DCF analysis results

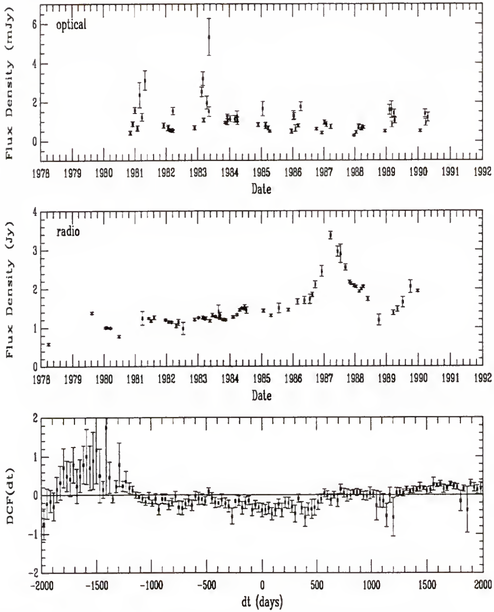

Figure 4-20: 0829+046 — DCF Analysis on Optical and Radio Light Curves
top) Optical color system: B
middle) Radio frequency: 8.0 GHz
bottom) DCF analysis results

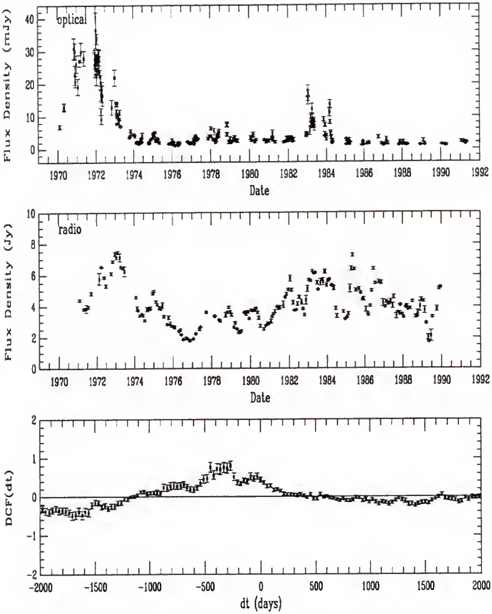

Figure 4-21: 0851+202 (OJ 287) — DCF Analysis on Optical and Radio Light Curves
top) Optical color system: B
middle) Radio frequency: 8.0 GHz
bottom) DCF analysis results

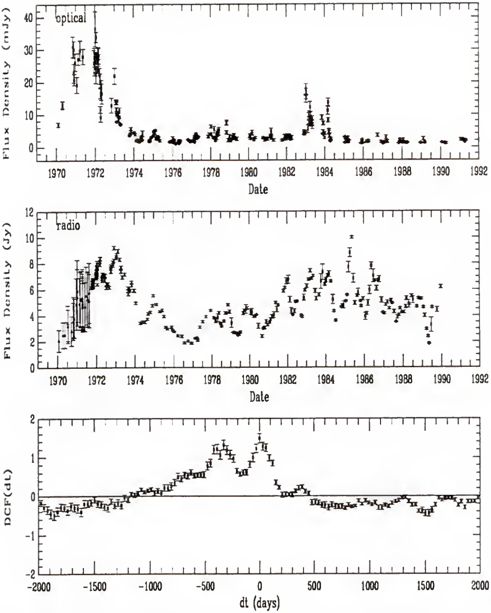

Figure 4-22: 0851+202 (OJ 287) — DCF Analysis on Optical and Radio Light Curves
top) Optical color system: B
middle) Radio frequency: 10.6 GHz prior to 1978.0 and 14.5 GHz after 1978.0
bottom) DCF analysis results

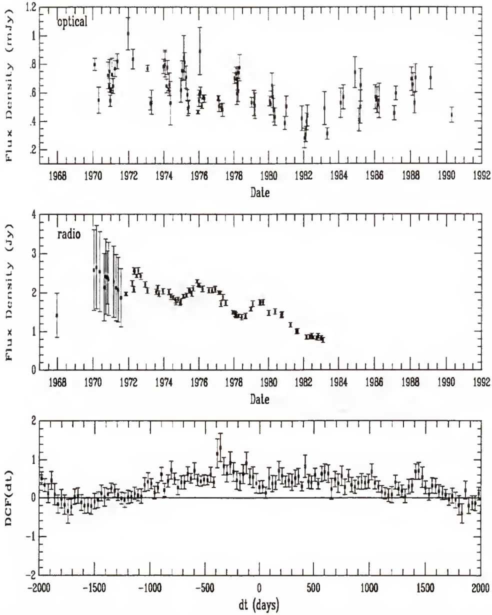

Figure 4-23: 0953+254 (OK 290) — DCF Analysis on Optical and Radio Light Curves
top) Optical color system: m_{pg}
middle) Radio frequency: 10.6 GHz
bottom) DCF analysis results

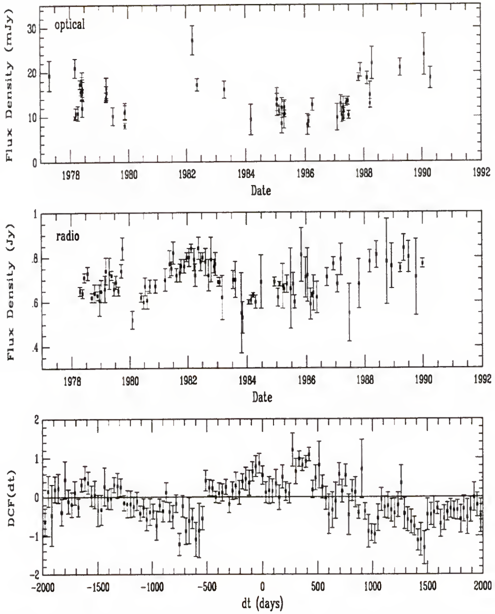

Figure 4-24: 1101+384 (Mkn 421) — DCF Analysis on Optical and Radio Light Curves
top) Optical color system: B
middle) Radio frequency: 8.0 GHz
bottom) DCF analysis results

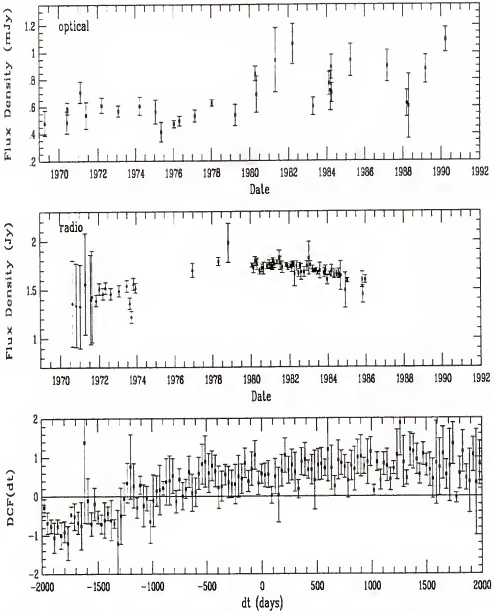

Figure 4-25: 1148-001 — DCF Analysis on Optical and Radio Light Curves
top) Optical color system: m_{pg}
middle) Radio frequency: 8.0 GHz
bottom) DCF analysis results

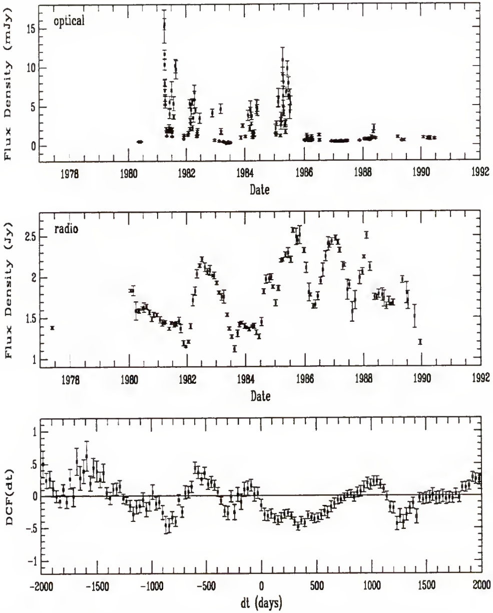

Figure 4-26: 1156+295 — DCF Analysis on Optical and Radio Light Curves
top) Optical color system: B
middle) Radio frequency: 8.0 GHz
bottom) DCF analysis results

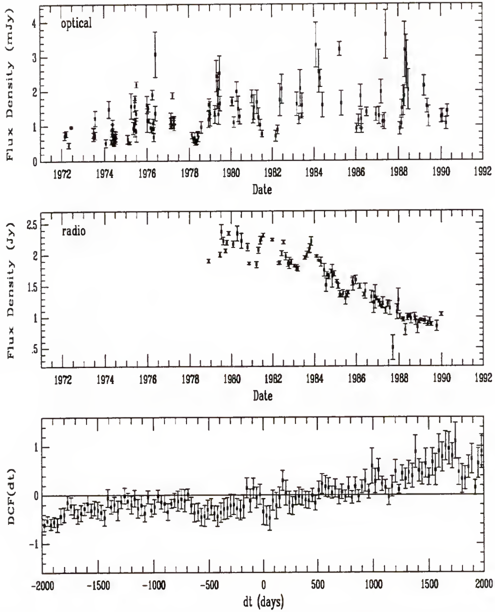

Figure 4-27: 1219+285 (W Com) — DCF Analysis on Optical and Radio Light Curves
top) Optical color system: B
middle) Radio frequency: 8.0 GHz
bottom) DCF analysis results

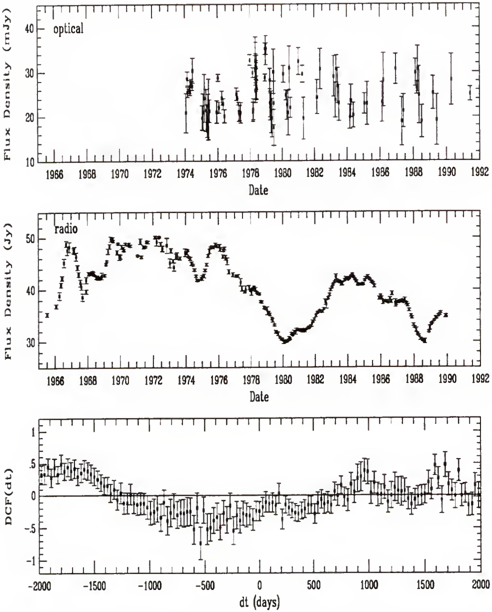

Figure 4-28: 1226+023 (3CR 273) — DCF Analysis on Optical and Radio Light Curves
top) Optical color system: B
middle) Radio frequency: 8.0 GHz
bottom) DCF analysis results

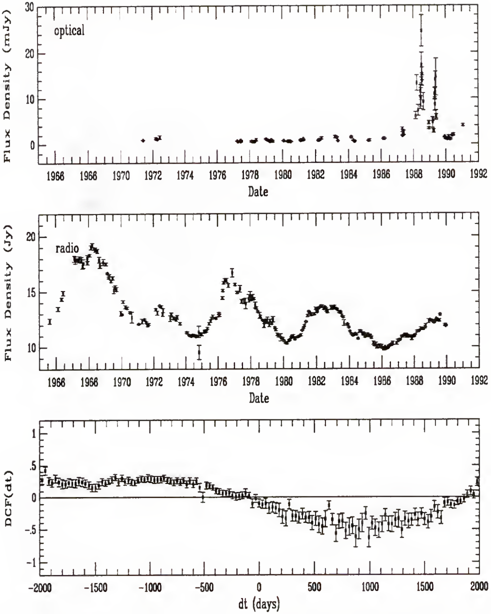

Figure 4-29: 1253-055 (3C 279) — DCF Analysis on Optical and Radio Light Curves
top) Optical color system: m_{pg}
middle) Radio frequency: 8.0 GHz
bottom) DCF analysis results

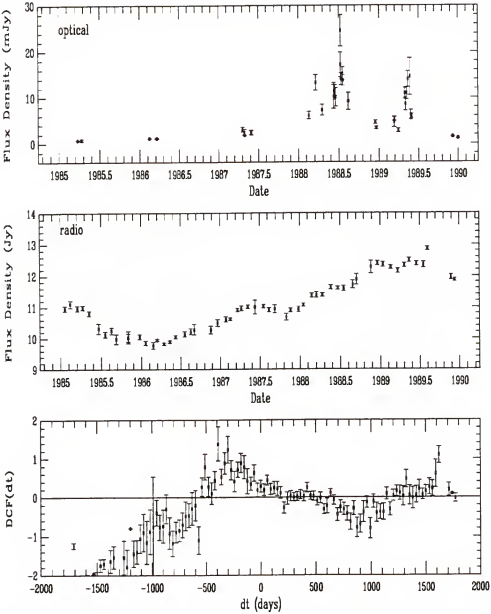

Figure 4-30: 1253-055 (3C 279) — DCF Analysis on Optical and Radio Light Curves — Subsets: 1985.0 to 1990.0
top) Optical color system: m_{pg}
middle) Radio frequency: 8.0 GHz
bottom) DCF analysis results

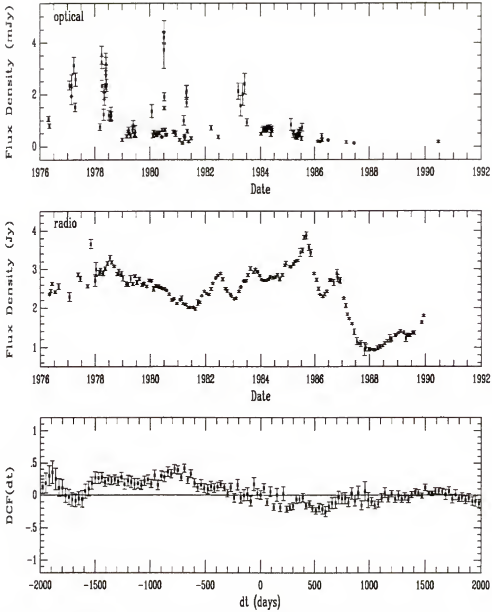

Figure 4-31: 1308+326 — DCF Analysis on Optical and Radio Light Curves
top) Optical color system: B
middle) Radio frequency: 8.0 GHz
bottom) DCF analysis results

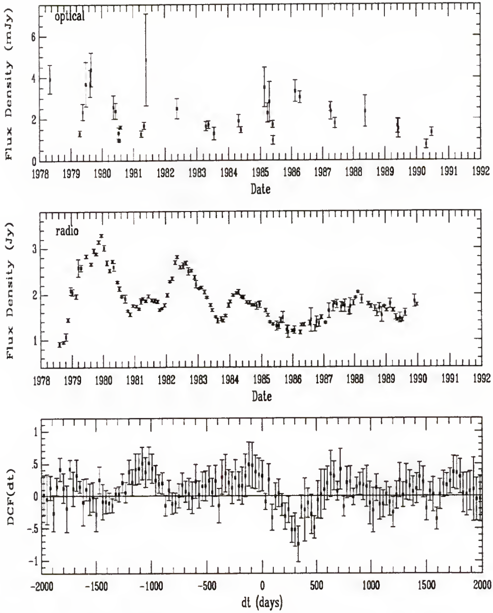

Figure 4-32: 1418+546 — DCF Analysis on Optical and Radio Light Curves
top) Optical color system: B
middle) Radio frequency: 8.0 GHz
bottom) DCF analysis results

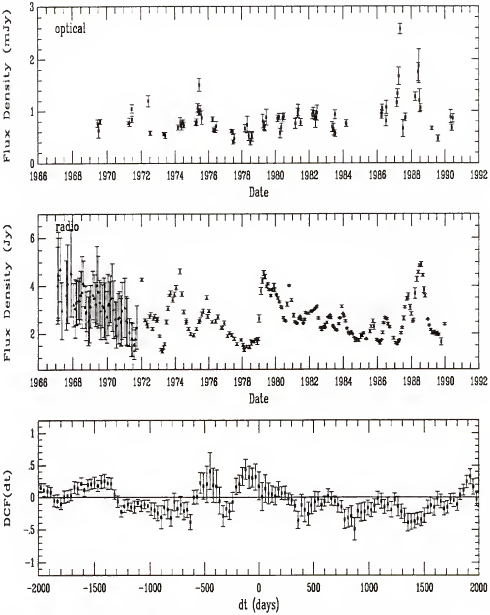

Figure 4-33: 1510-089 — DCF Analysis on Optical and Radio Light Curves
top) Optical color system: m_{pg}
middle) Radio frequency: 10.6 GHz prior to 1978.0 and 8.0 GHz after 1978.0
bottom) DCF analysis results

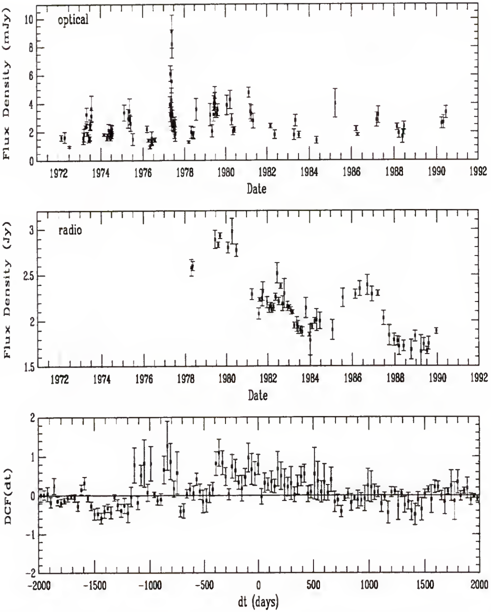

Figure 4-34: 1514-241 (AP Lib) — DCF Analysis on Optical and Radio Light Curves
top) Optical color system: m_{pg}
middle) Radio frequency: 8.0 GHz
bottom) DCF analysis results

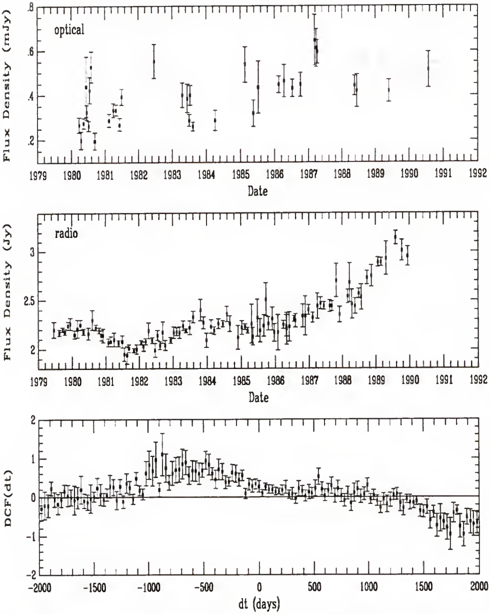

Figure 4-35: 1611+343 — DCF Analysis on Optical and Radio Light Curves
top) Optical color system: B
middle) Radio frequency: 8.0 GHz
bottom) DCF analysis results

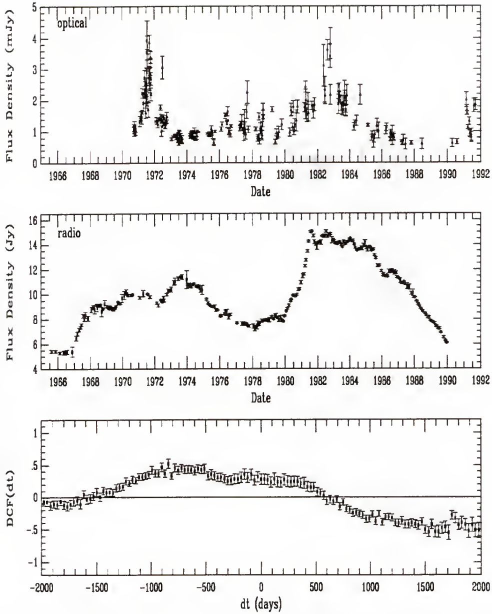

Figure 4-36: 1641+399 (3CR 345) — DCF Analysis on Optical and Radio Light Curves
top) Optical color system: B and m_{pg}
middle) Radio frequency: 8.0 GHz
bottom) DCF analysis results

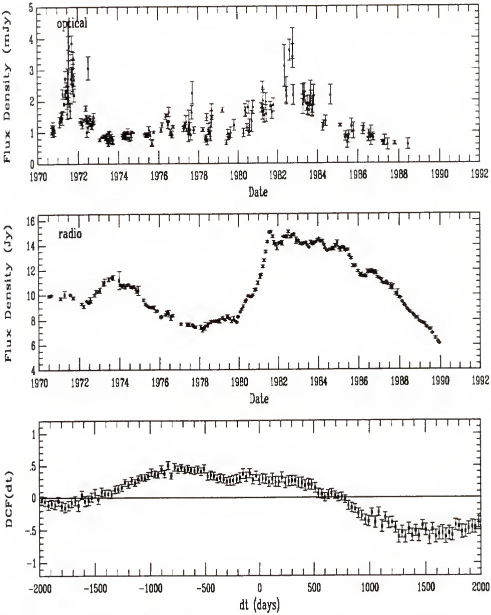

Figure 4-37: 1641+399 (3CR 345) — DCF Analysis on Optical and Radio Light Curves — Subsets: post-1970.5
top) Optical color system: B and m_{pg}
middle) Radio frequency: 8.0 GHz
bottom) DCF analysis results

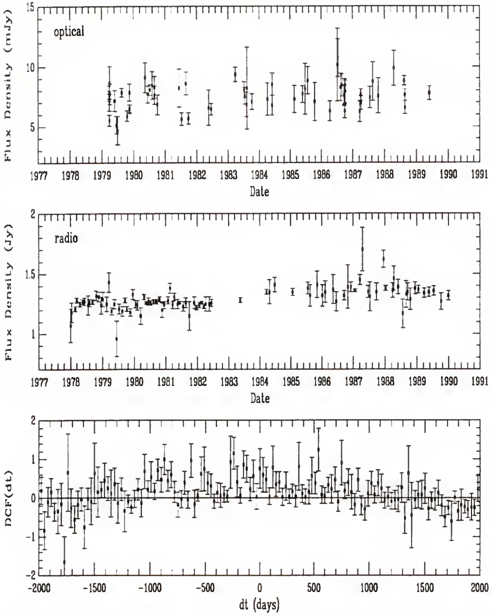

Figure 4-38: 1652+398 (Mkn 501) — DCF Analysis on Optical and Radio Light Curves
top) Optical color system: B
middle) Radio frequency: 8.0 GHz
bottom) DCF analysis results

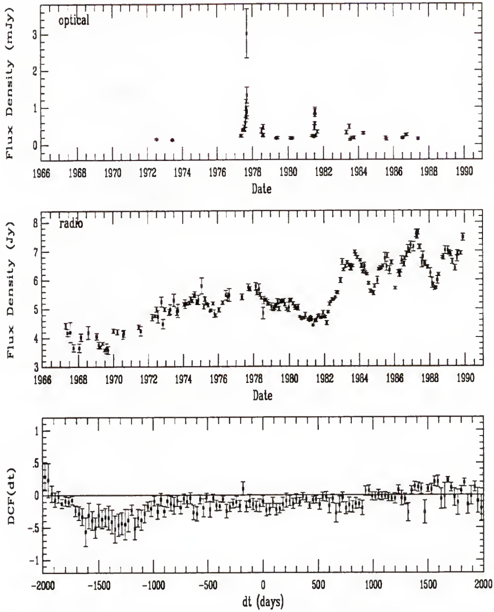

Figure 4-39: 1730-130 (NRAO 530) — DCF Analysis on Optical and Radio Light Curves
top) Optical color system: m_{pg}
middle) Radio frequency: 8.0 GHz
bottom) DCF analysis results

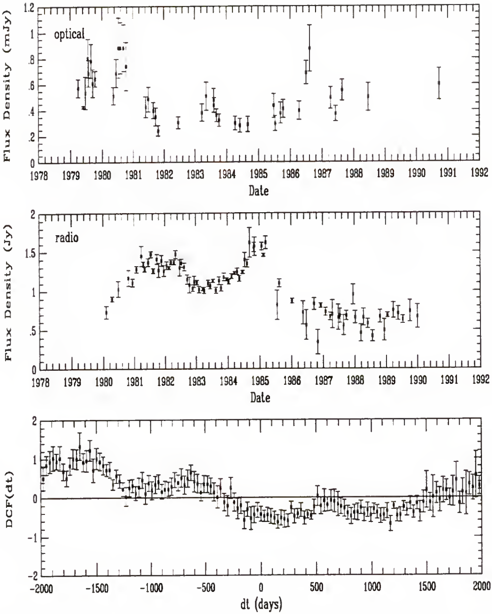

Figure 4-40: 1749+701 — DCF Analysis on Optical and Radio Light Curves
top) Optical color system: B
middle) Radio frequency: 8.0 GHz
bottom) DCF analysis results

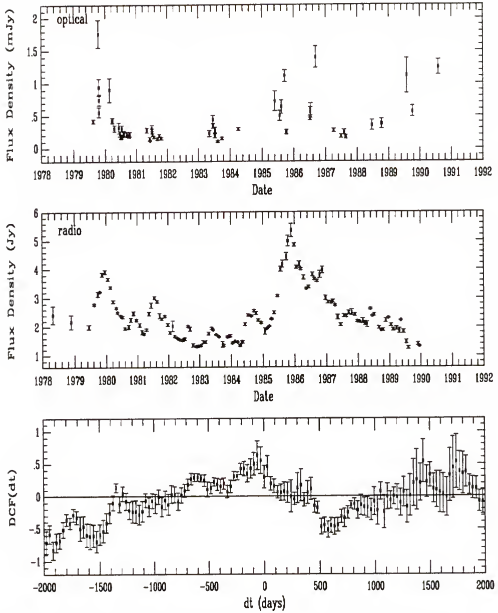

Figure 4-41: 1749+096 — DCF Analysis on Optical and Radio Light Curves
top) Optical color system: B
middle) Radio frequency: 8.0 GHz
bottom) DCF analysis results

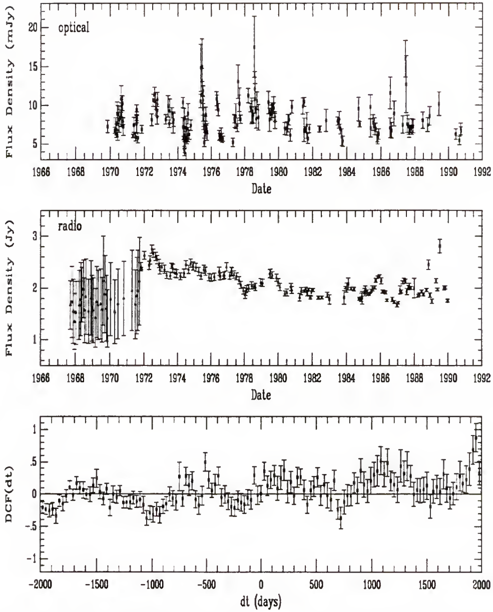

Figure 4-42: 1807+698 (3CR 371) — DCF Analysis on Optical and Radio Light Curves
top) Optical color system: m_{pg}
middle) Radio frequency: 10.6 GHz prior to 1981.5 and 8.0 GHz after 1981.5
bottom) DCF analysis results

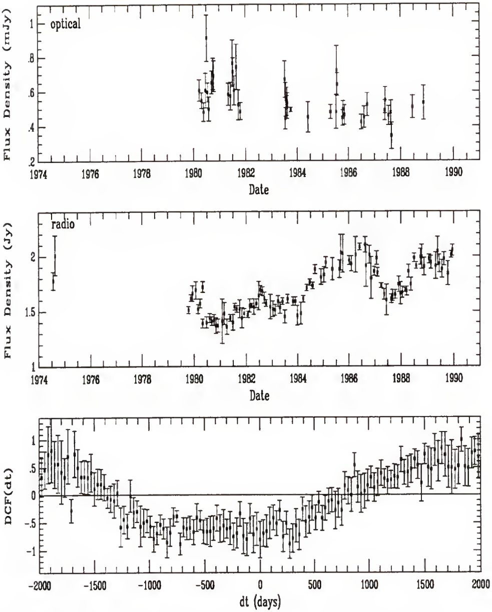

Figure 4-43: 1901+319 — DCF Analysis on Optical and Radio Light Curves
top) Optical color system: B
middle) Radio frequency: 8.0 GHz
bottom) DCF analysis results

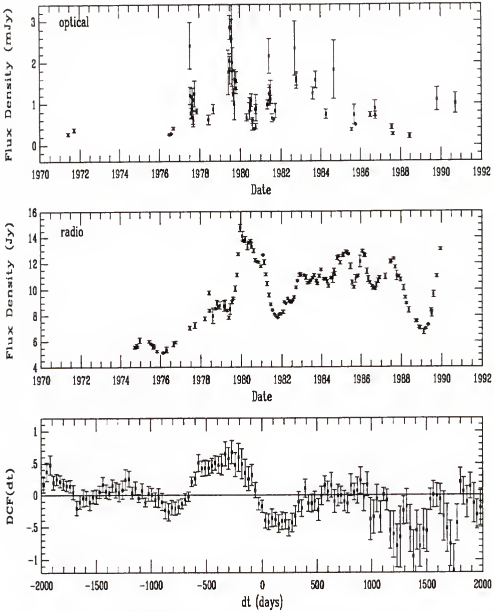

Figure 4-44: 1921-293 (OV-236) — DCF Analysis on Optical and Radio Light Curves
top) Optical color system: m_{pg}
middle) Radio frequency: 8.0 GHz
bottom) DCF analysis results

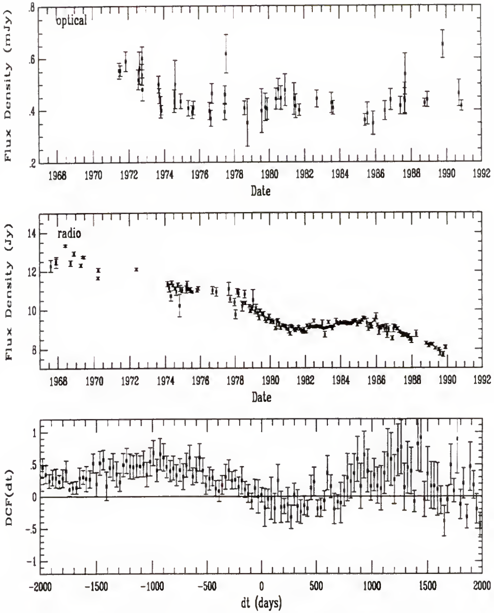

Figure 4-45: 2134+004 — DCF Analysis on Optical and Radio Light Curves
top) Optical color system: B
middle) Radio frequency: 8.0 GHz
bottom) DCF analysis results

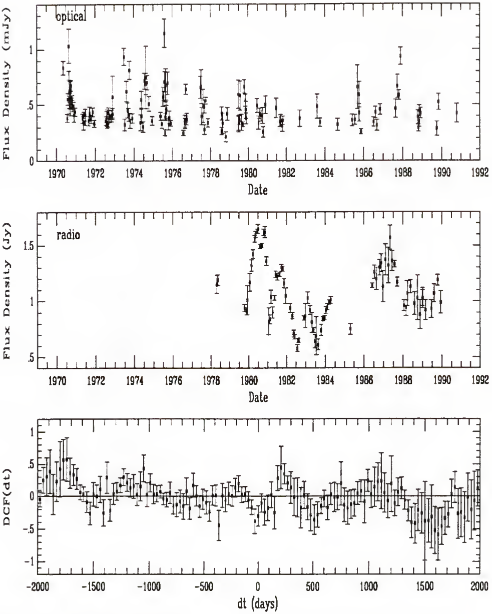

Figure 4-46: 2144+092 — DCF Analysis on Optical and Radio Light Curves
top) Optical color system: m_{pg}
middle) Radio frequency: 8.0 GHz
bottom) DCF analysis results

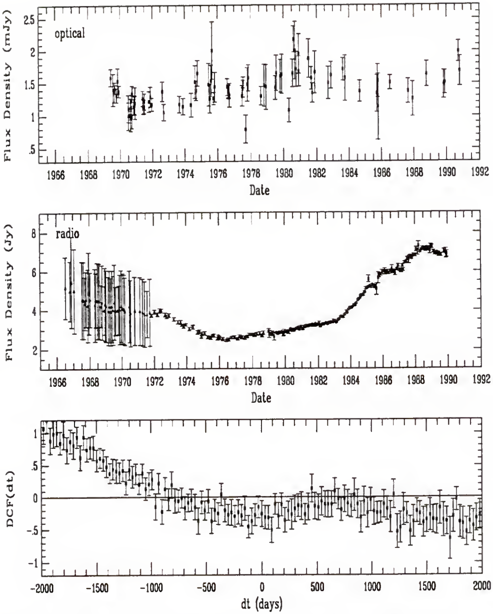

Figure 4-47: 2145+067 — DCF Analysis on Optical and Radio Light Curves
top) Optical color system: m_{pg}
middle) Radio frequency: 10.6 GHz prior to 1979.0 and 8.0 GHz after 1979.0
bottom) DCF analysis results

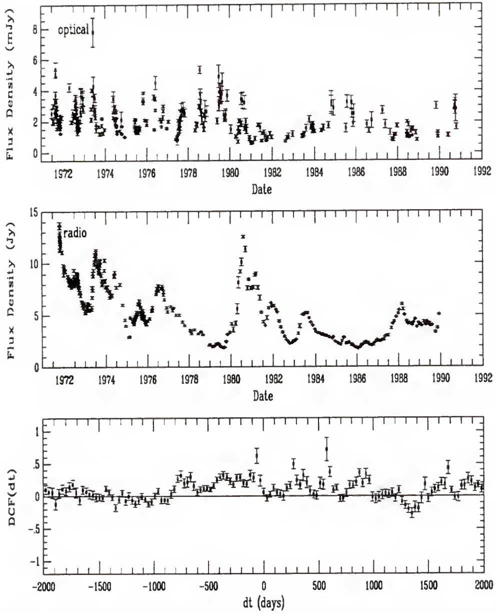

Figure 4-48: 2200+420 (BL Lac) — DCF Analysis on Optical and Radio Light Curves
top) Optical color system: B
middle) Radio frequency: 10.6 prior to 1979.0 and 8.0 GHz after 1979.0
bottom) DCF analysis results

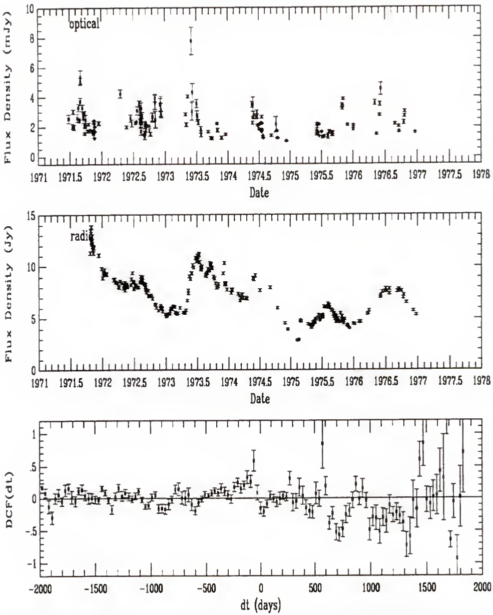

Figure 4-49: 2200+420 (BL Lac) — DCF Analysis on Optical and Radio Light Curves — Subsets: 1971.5 to 1977.0
top) Optical color system: B
middle) Radio frequency: 10.6 GHz prior to 1979.0 and 8.0 GHz after 1979.0
bottom) DCF analysis results

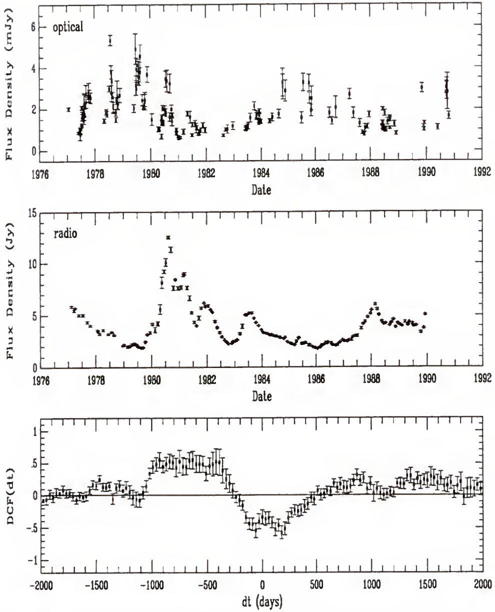

Figure 4-50: 2200+420 (BL Lac) — DCF Analysis on Optical and Radio Light Curves — Subsets: post-1977.0
top) Optical color system: B
middle) Radio frequency: 10.6 GHz prior to 1979.0 and 8.0 GHz after 1979.0
bottom) DCF analysis results

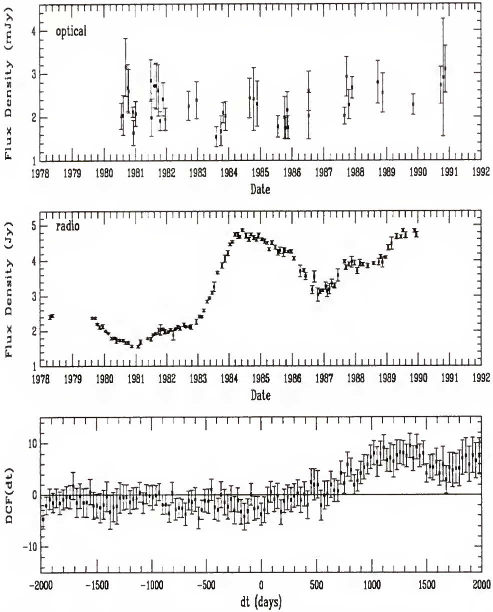

Figure 4-51: 2201+315 — DCF Analysis on Optical and Radio Light Curves
top) Optical color system: B
middle) Radio frequency: 8.0 GHz
bottom) DCF analysis results

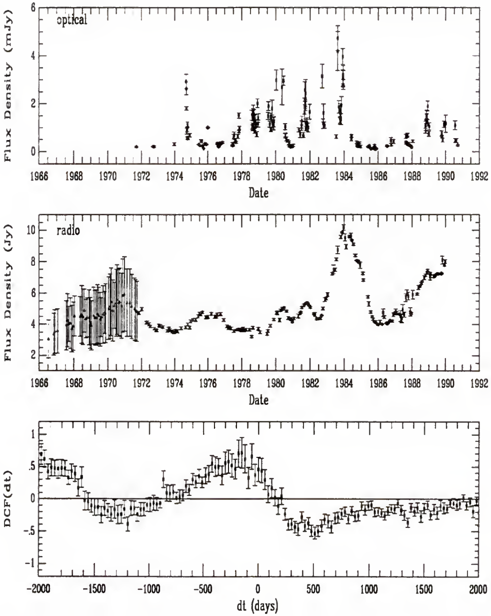

Figure 4-52: 2223-052 (3C 446) — DCF Analysis on Optical and Radio Light Curves
top) Optical color system: B
middle) Radio frequency: 10.6 GHz prior to 1980.0 and 14.5 GHz after 1980.0
bottom) DCF analysis results

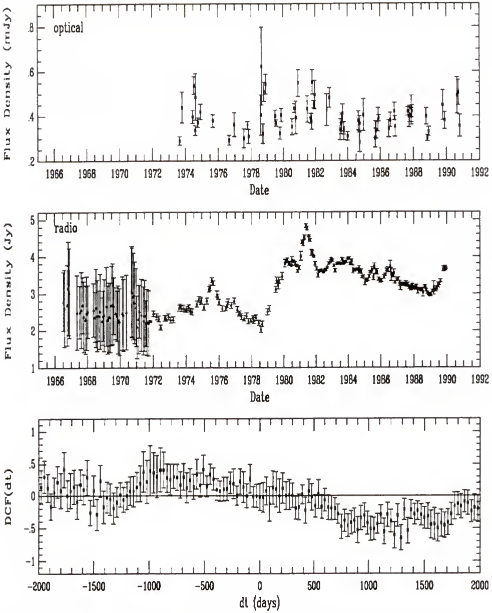

Figure 4-53: 2230+114 (CTA 102) — DCF Analysis on Optical and Radio Light Curves
top) Optical color system: B
middle) Radio frequency: 10.6 GHz prior to 1980.0 and 8.0 GHz after 1980.0
bottom) DCF analysis results

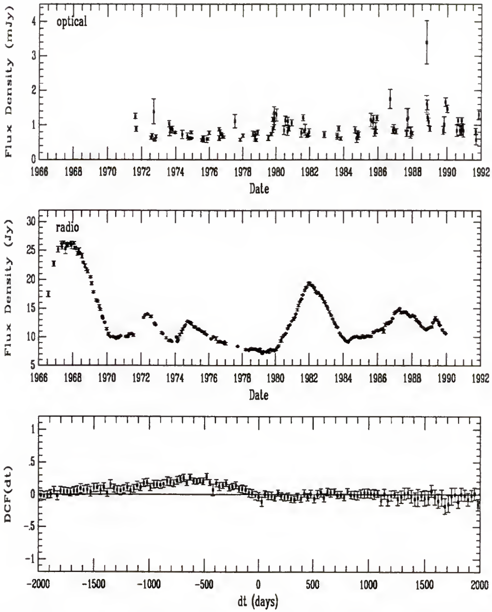

Figure 4-54: 2251+158 (3C 454.3) — DCF Analysis on Optical and Radio Light Curves
top) Optical color system: B
middle) Radio frequency: 8.0 GHz
bottom) DCF analysis results

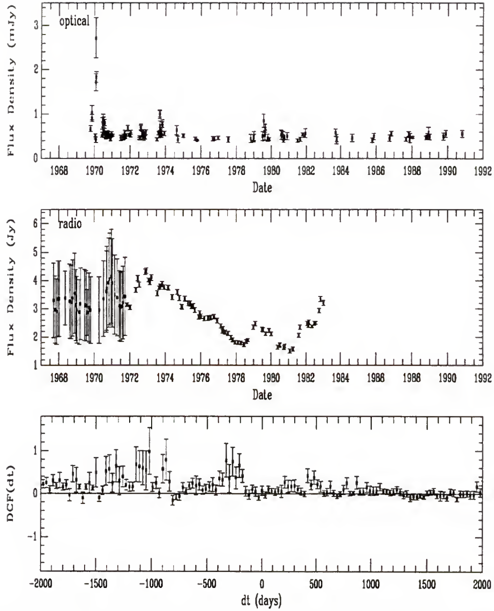

Figure 4-55: 2345-167 — DCF Analysis on Optical and Radio Light Curves
top) Optical color system: m_{pg}
middle) Radio frequency: 8.0 GHz
bottom) DCF analysis results

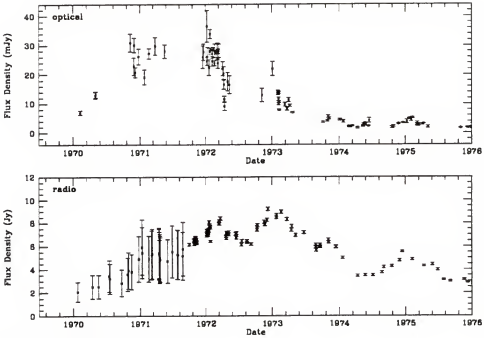

Figure 4-56: 0851+202 (OJ 287)

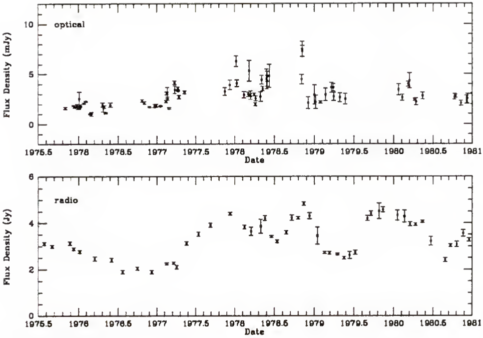

Figure 4-57: 0851+202 (OJ 287)

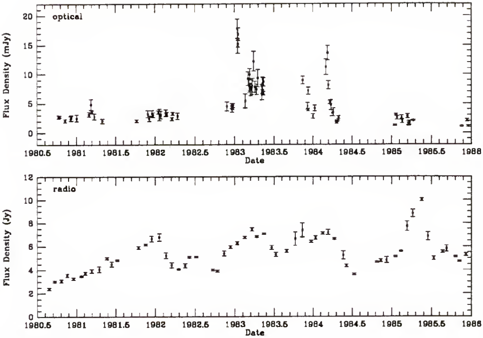

Figure 4-58: 0851+202 (OJ 287)

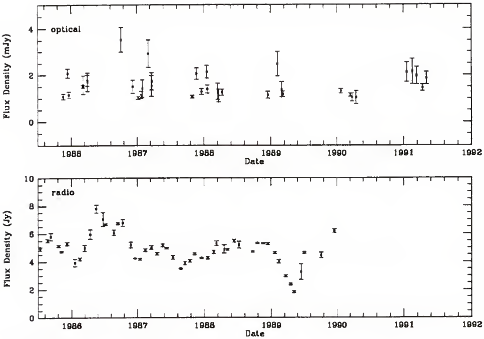

Figure 4-59: 0851+202 (OJ 287)

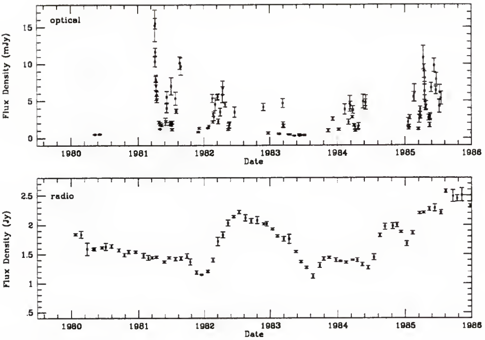

Figure 4-60: 1156+295

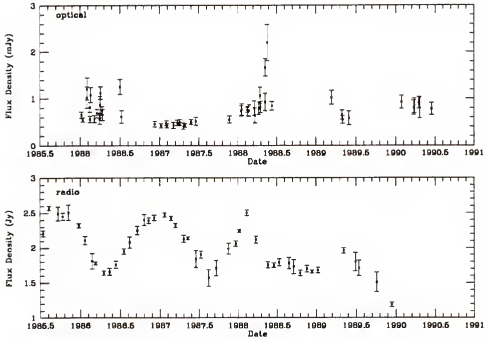

Figure 4-61: 1156+295

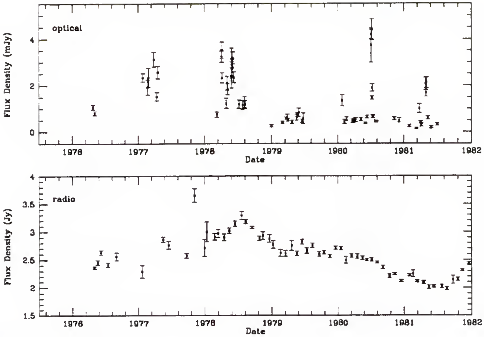

Figure 4-62: 1308+326

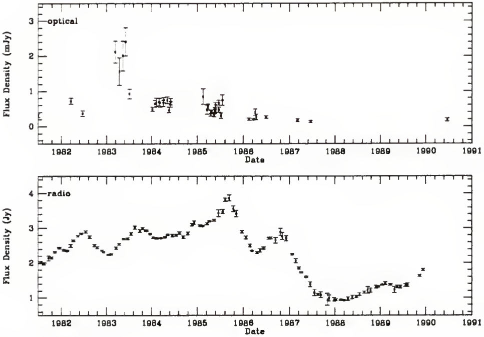

Figure 4-63: 1308+326

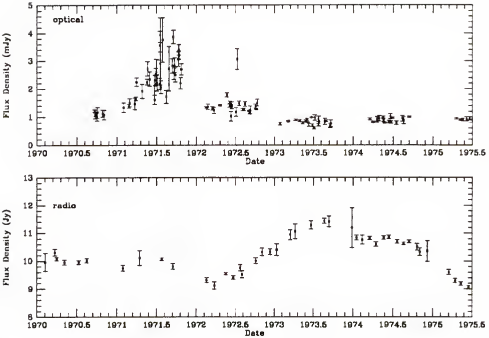

Figure 4-64: 1641+399 (3CR 345)

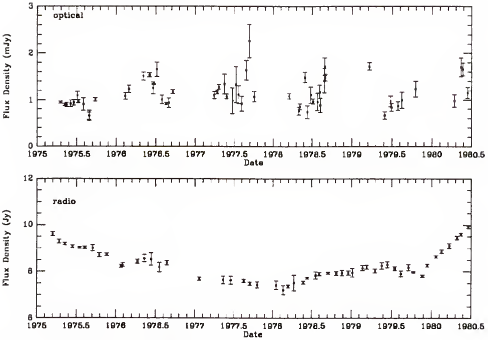

Figure 4-65: 1641+399 (3CR 345)

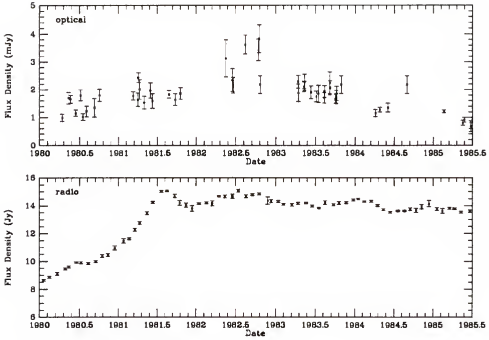

Figure 4-66: 1641+399 (3CR 345)

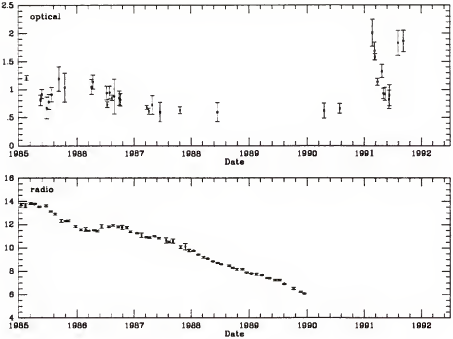

Figure 4-67: 1641+399 (3CR 345)

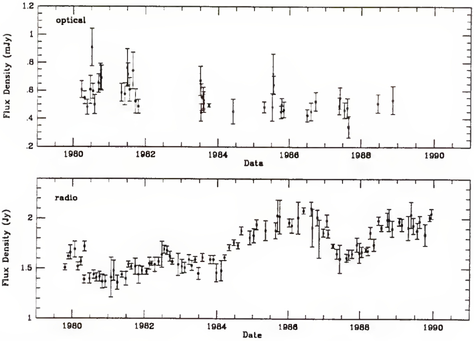

Figure 4-68: 1901+319

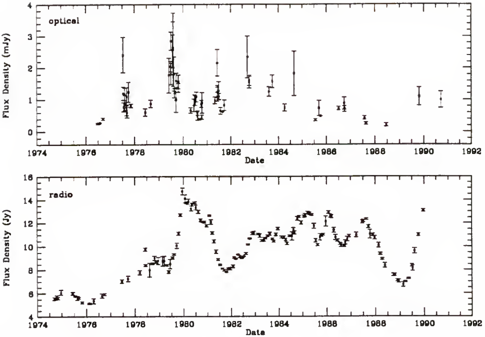

Figure 4-69: 1921-293 (OV-236)

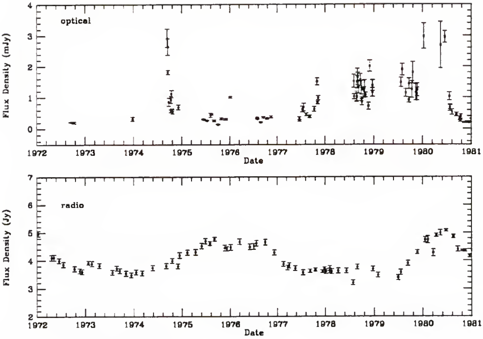

Figure 4-70: 2223-052 (3C 446)

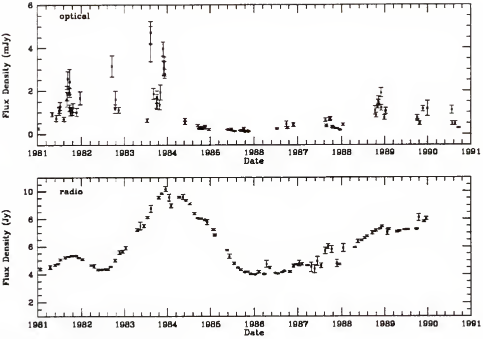

Figure 4-71: 2223-052 (3C 446)

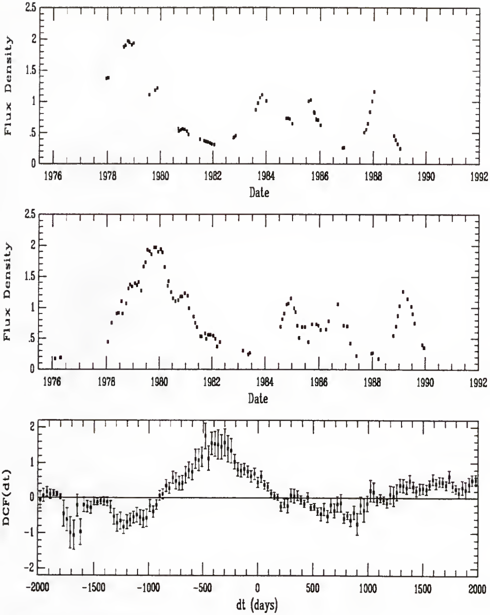

Figure 4-72: 0007+106 (III Zw 2) — "Perfectly correlated" — Offset: -13 months

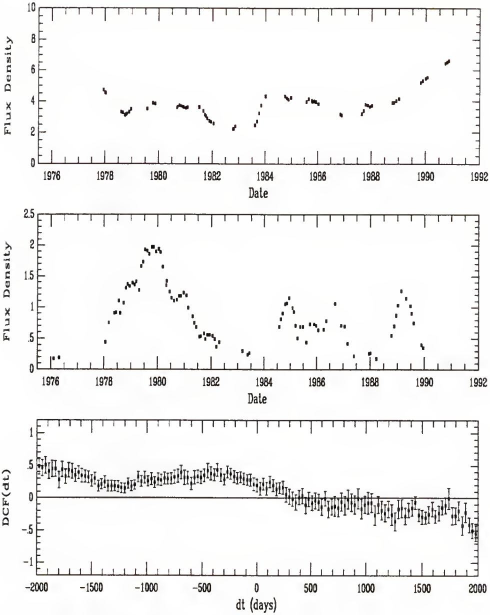

Figure 4-73: 0007+106 (III Zw 2) — "Perfectly uncorrelated"

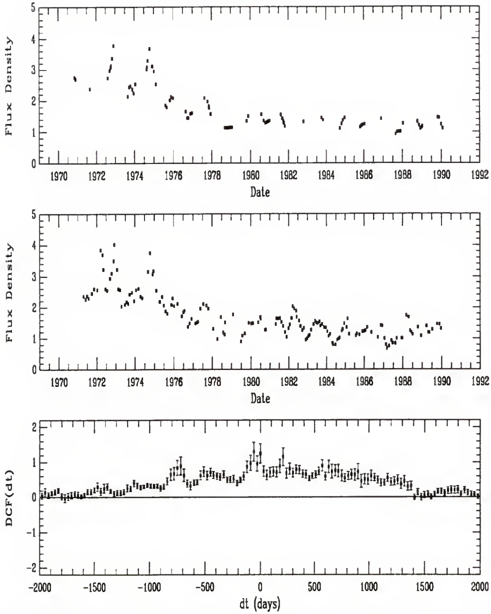

Figure 4-74: 0048-097 — "Perfectly correlated" — Offset: 0 months

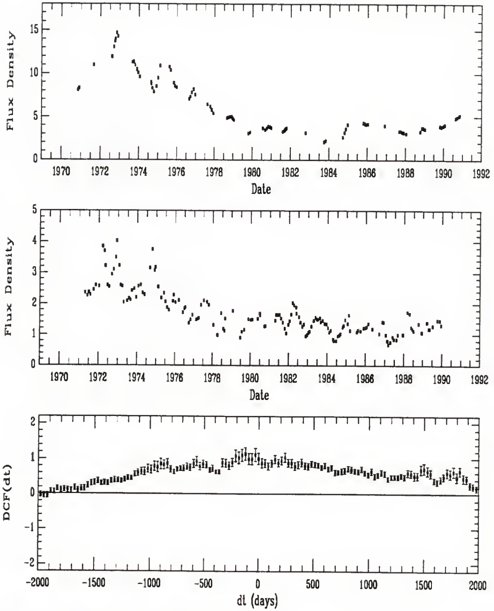

Figure 4-75: 0048-097 — "Perfectly uncorrelated"

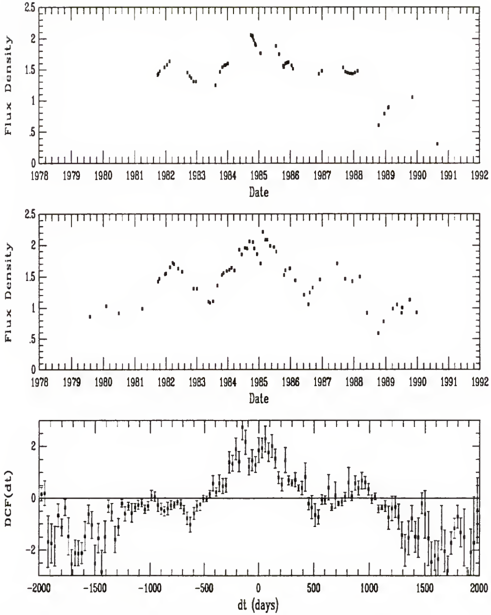

Figure 4-76: 0215+015 — "Perfectly correlated" — Offset: 0 months

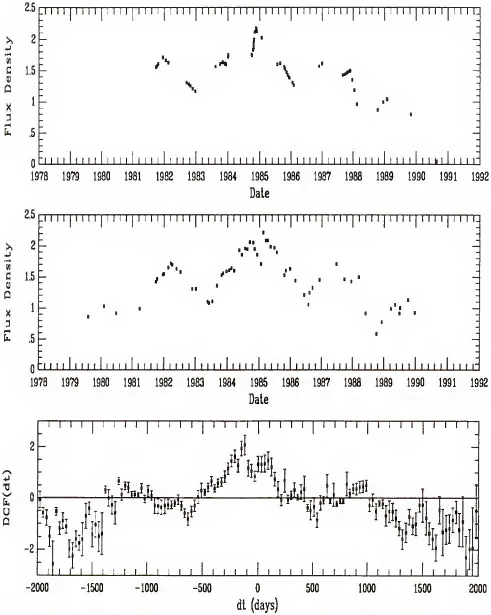

Figure 4-77: 0215+015 — "Perfectly correlated" — Offset: -3.3 months

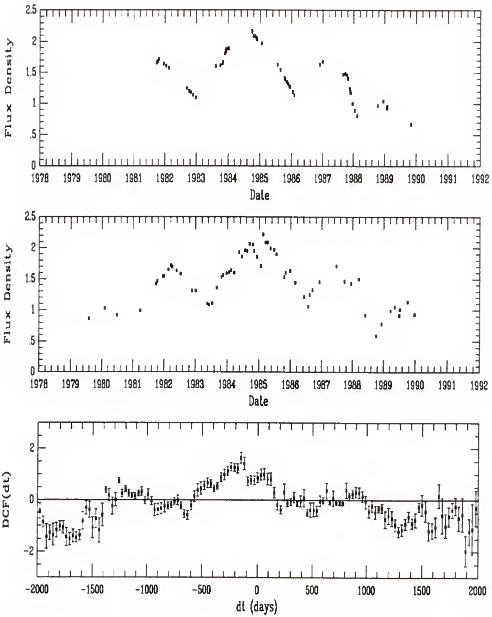

Figure 4-78: 0215+015 — "Perfectly correlated" — Offset: -5 months

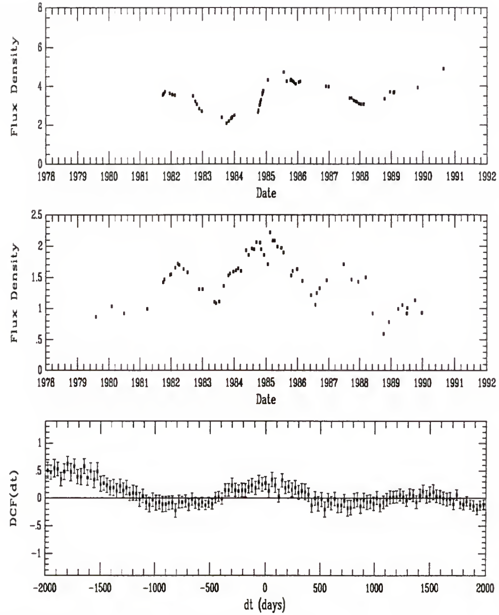

Figure 4-79: 0215+015 — "Perfectly uncorrelated"

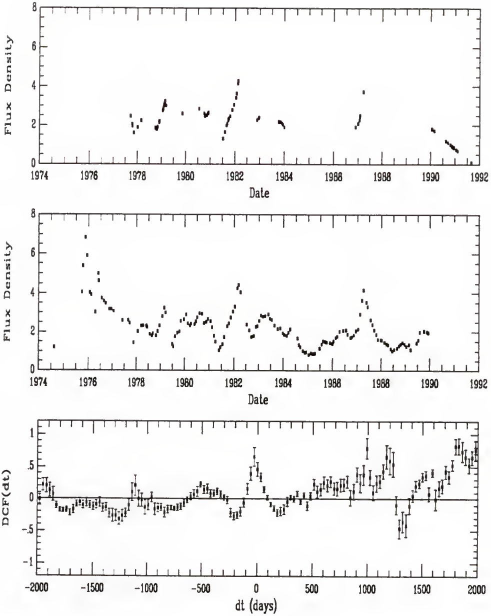

Figure 4-80: AO 0235+164 — "Perfectly correlated" — Offset: 0 months

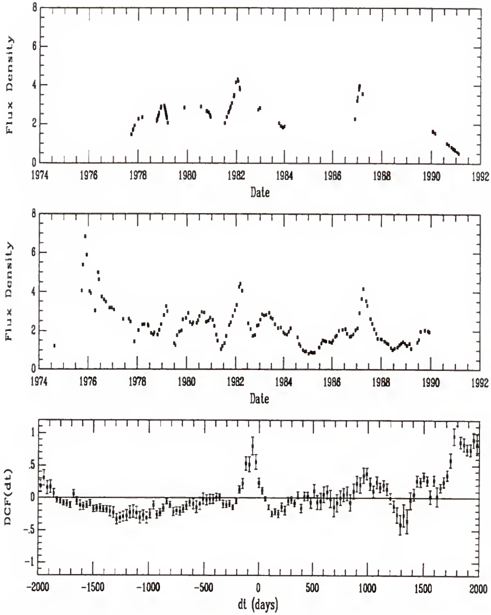

Figure 4-81: AO 0235+164 — "Perfectly correlated" — Offset: -2 months

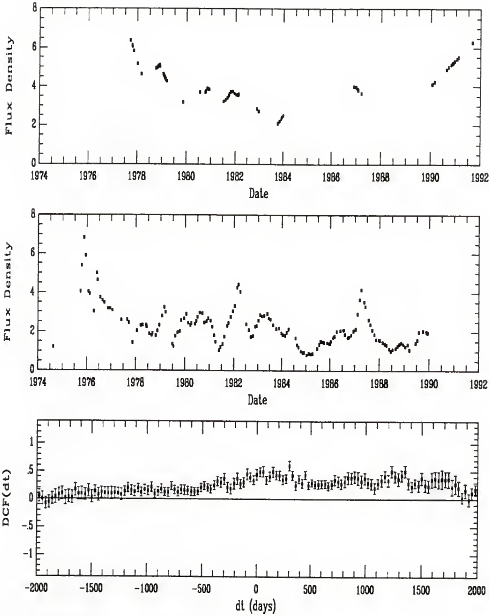

Figure 4-82: AO 0235+164 — "Perfectly uncorrelated"

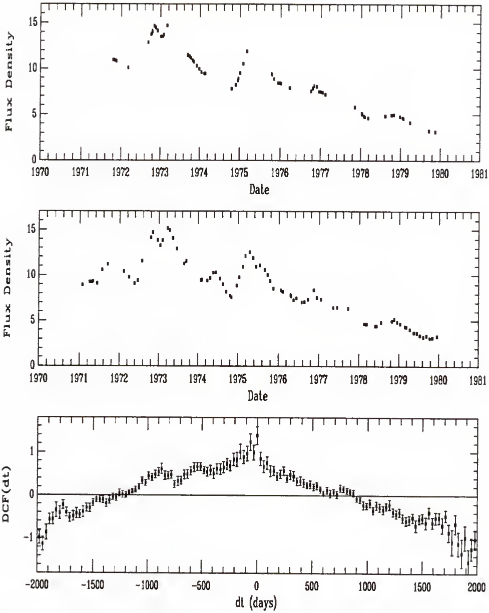

Figure 4-83: 0430+052 (3C 120) — "Perfectly correlated" — Offset: 0 months

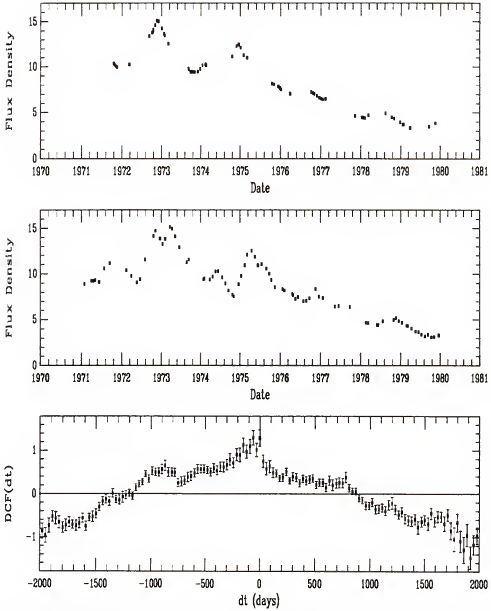

Figure 4-84: 0430+052 (3C 120) — "Perfectly correlated" — Offset: -4 months

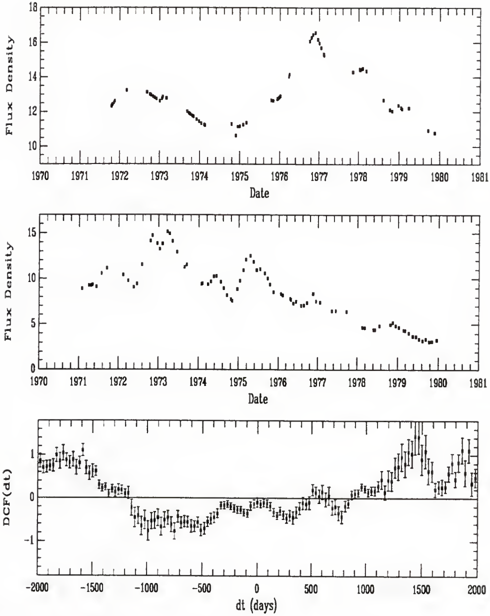

Figure 4-85: 0430+052 (3C 120) — "Perfectly uncorrelated"

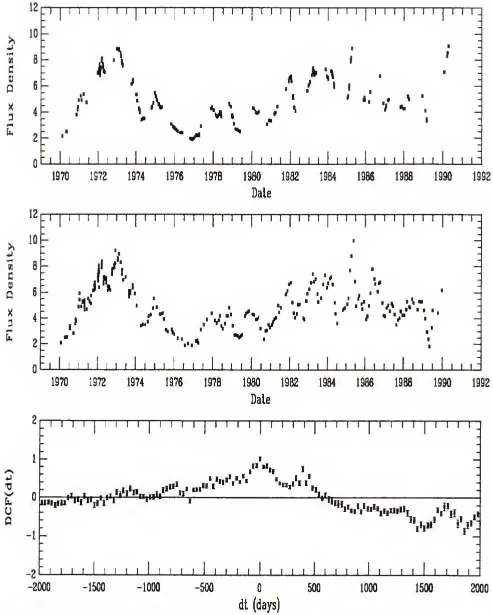

Figure 4-86: 0851+202 (OJ 287) — "Perfectly correlated" — Offset: 0 months

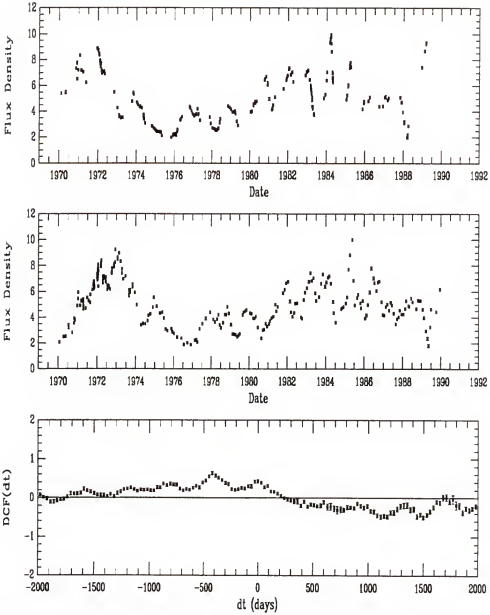

Figure 4-87: 0851+202 (OJ 287) — "Perfectly correlated" — Offset: -14 months

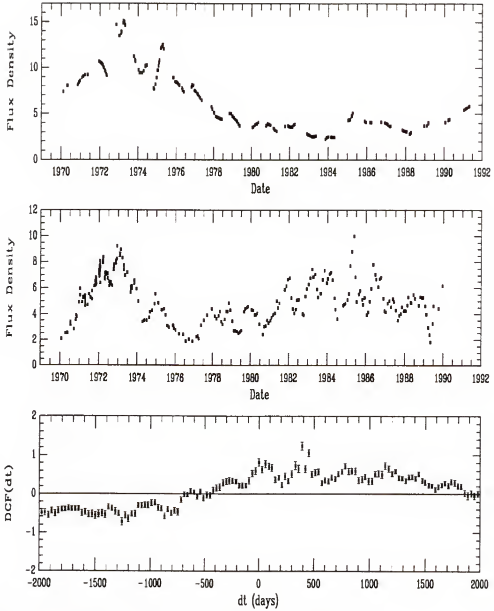

Figure 4-88: 0851+202 (OJ 287) — “Perfectly uncorrelated”

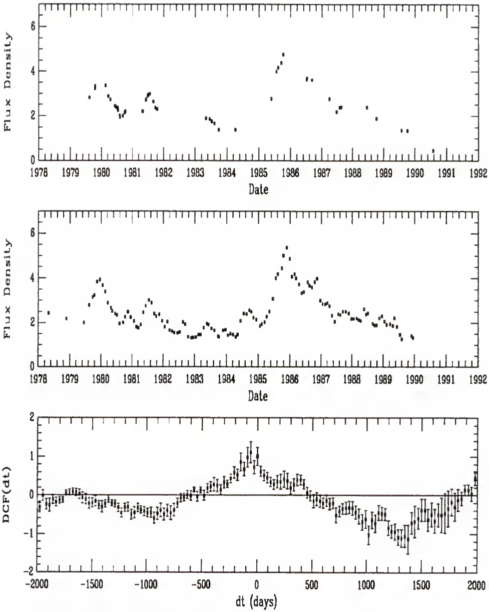

Figure 4-89: 1749+096 — "Perfectly correlated" — Offset: 0 months

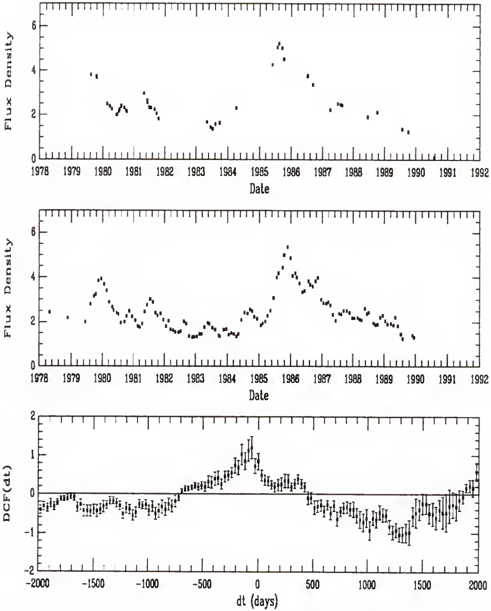

Figure 4-90: 1749+096 — "Perfectly correlated" — Offset: -3 months

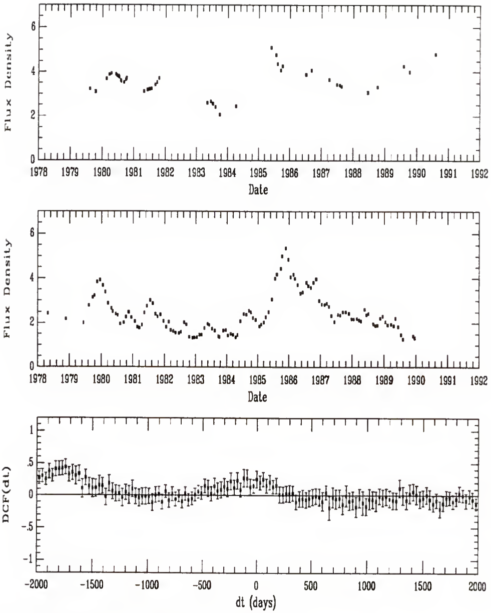

Figure 4-91: 1749+096 — "Perfectly uncorrelated"

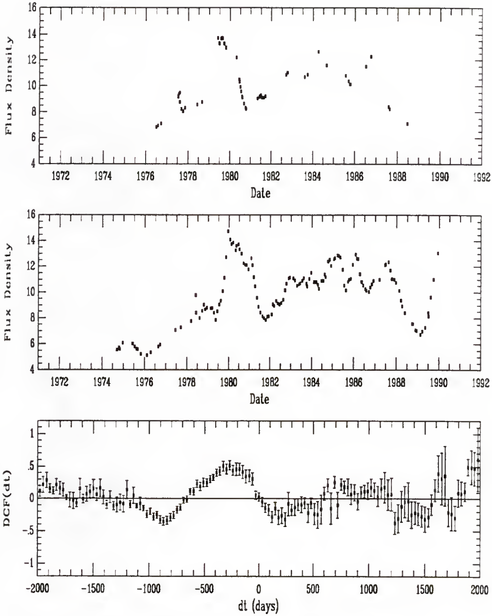

Figure 4-92: 1921-293 (OV-236) — "Perfectly correlated" — Offset: -10 months

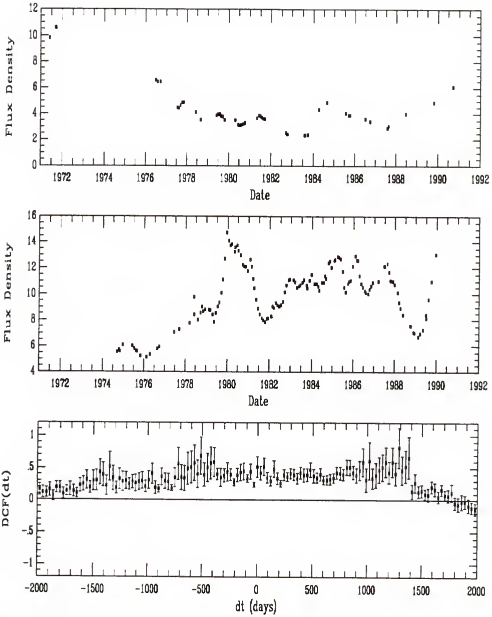

Figure 4-93: 1921-293 (OV-296) — "Perfectly uncorrelated"

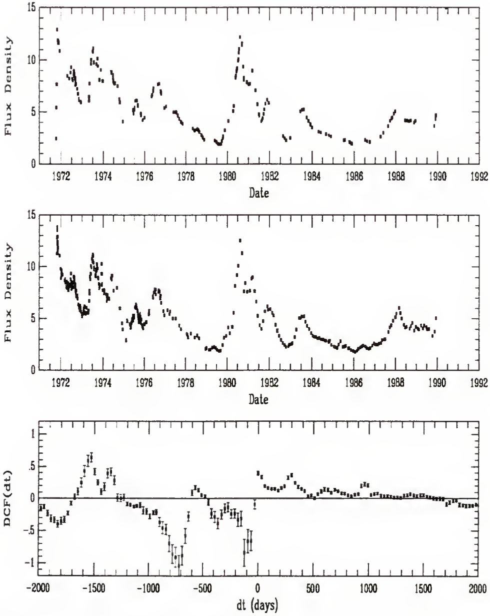

Figure 4-94: 2200+420 (BL Lac) — "Perfectly correlated" — Offset: 0 months

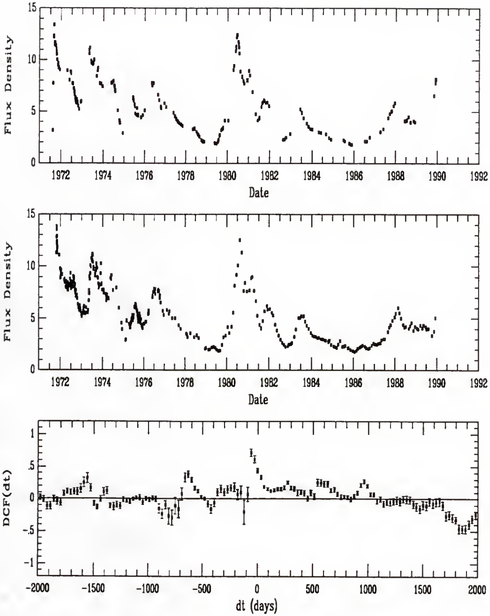

Figure 4-95: 2200+420 (BL Lac) — "Perfectly correlated" — Offset: -2 months

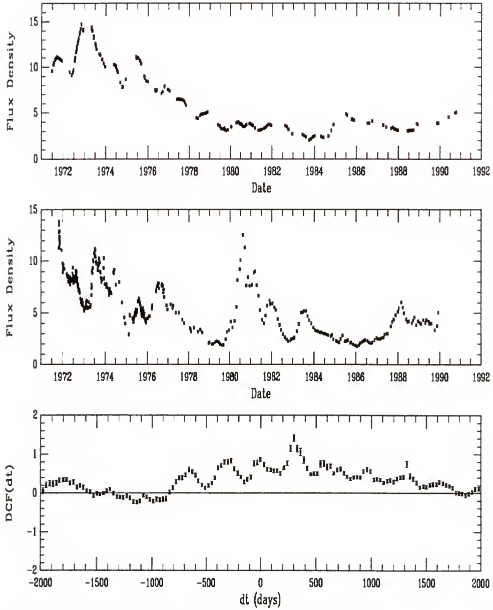

Figure 4-96: 2200+420 (BL Lac) — "Perfectly uncorrelated"

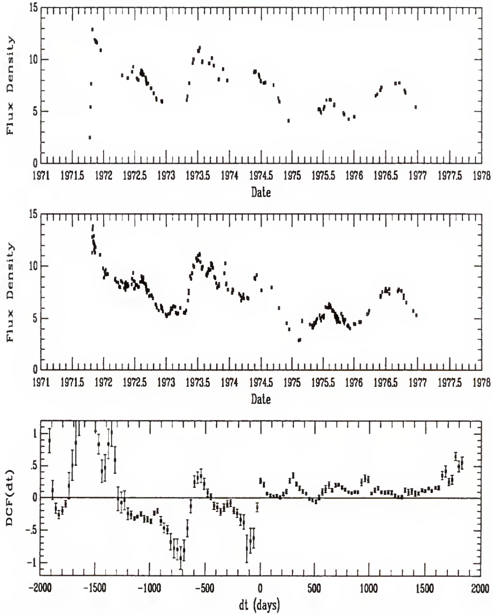

Figure 4-97: 2200+420 (BL Lac) — "Perfectly correlated" — Subsets: 1971.5 to 1977.0 — Offset: 0 months

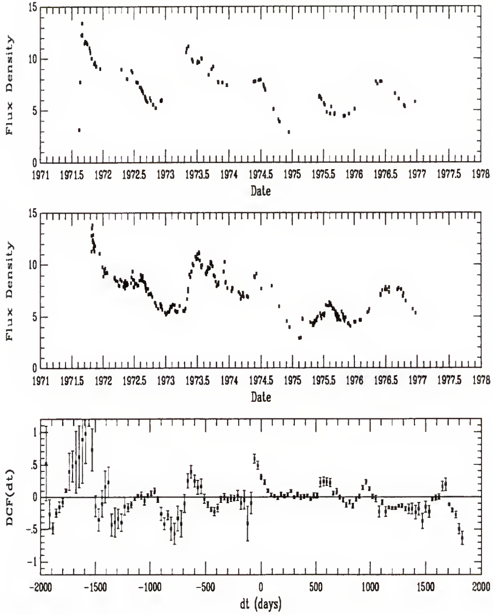

Figure 4-98: 2200+420 (BL Lac) — "Perfectly correlated" — Subsets: 1971.5 to 1977.0 — Offset: -2 months

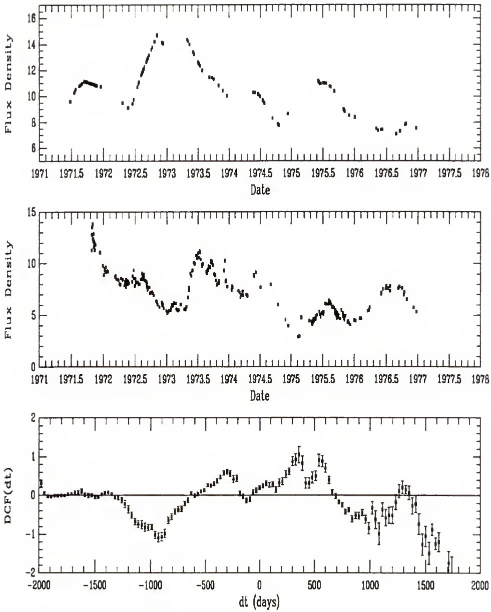

Figure 4-99: 2200+420 (BL Lac) — "Perfectly uncorrelated" — Subsets: 1971.5 to 1977.0

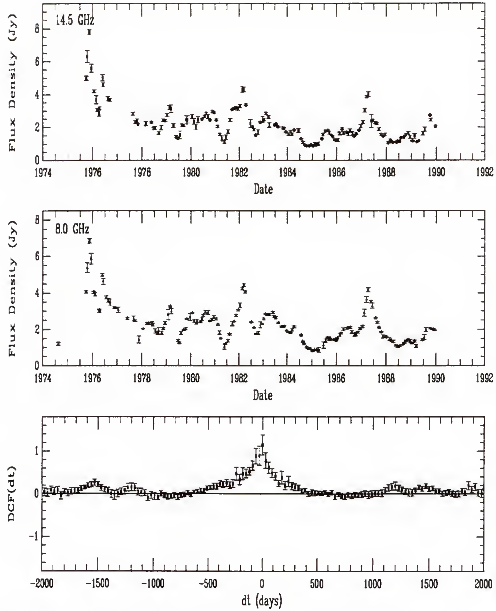

Figure 4-100: AO 0235+164 — DCF Analysis on 14.5 GHz and 8.0 GHz Radio Light Curves

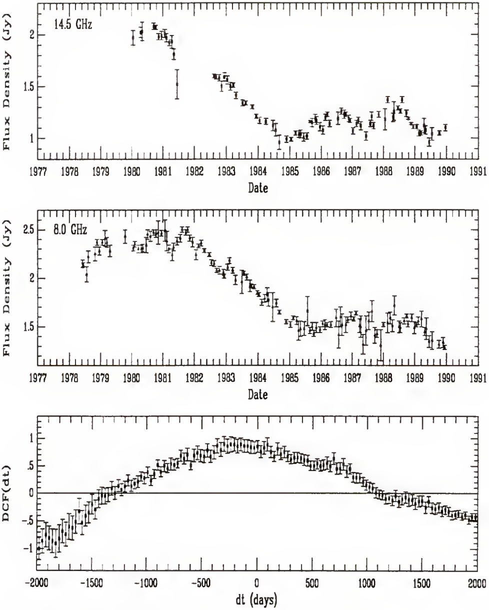

Figure 4-101: 0333+321 (NRAO 140) — DCF Analysis on 14.5 GHz and 8.0 GHz Radio Light Curves

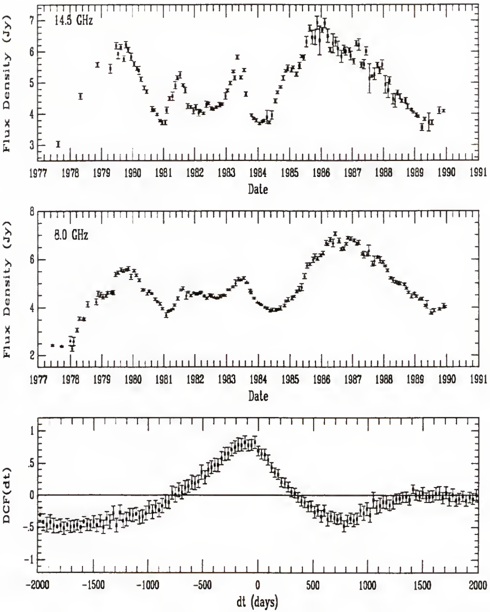

Figure 4-102: 0420-014 — DCF Analysis on 14.5 GHz and 8.0 GHz Radio Light Curves

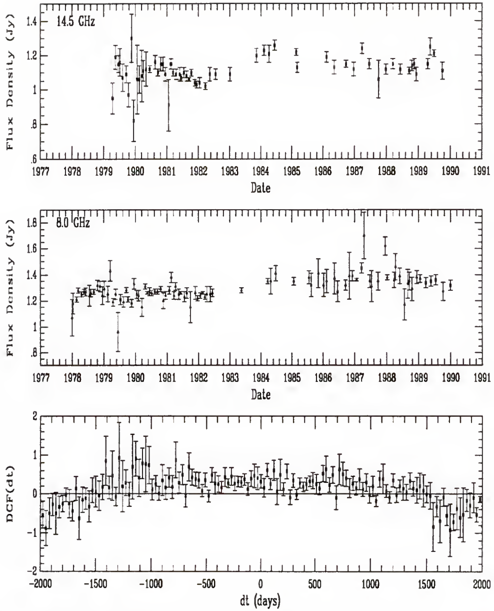

Figure 4-103: 1652+398 (Mkn 501) — DCF Analysis on 14.5 GHz and 8.0 GHz Radio Light Curves

CHAPTER 5
DISCUSSION OF RESULTS

BL Lacs and QSOs in Light of the Results

There are nine objects which I feel fairly confident have correlated optical and radio events. These objects are listed in Table 5-1. In this table, Column 1 gives the coordinate designation. Column 2 lists the optical-radio lag time. Column 3 lists the 14.5 GHz - 8.0 GHz lag time and Column 4 lists the 8.0 GHz - 4.8 GHz lag time. All lag times are given in units of months where a month is defined here to be 30 days. Negative lag times indicate that the frequency listed first leads. For example, a negative lag time in Column 2 indicates that optical events lead radio events. Column 5 gives the type of object (BL Lac, QSO, Seyfert, or NSO). Column 6 gives other descriptions for the object (BZR for blazar, HPQ for high polarization quasar, and OVV for optically violent variable). Column 7 indicates if the object has been detected in X-rays (XD) or if it is a superluminal radio source (SLS). Column 8 lists the average number of optical data points per year and Column 9 lists the average number of radio data points per year.

There are also nine objects which I feel fairly confident do not have correlated optical and radio events. These objects are listed in Table 5-2. The column headings are the same as for Table 5-1. Of course, all entries in Column 2 (optical-radio lag time) of Table 5-2 are NC for "not correlated".

The remaining 28 objects either did not have adequate temporal coverage in one or both data sets for reliable optical-radio correlation analysis (as was the case for 1148-001), or identifying possible correlated optical and radio events was confused by the number and spacing of events in one or both data sets (as was the case for 0420-014). These 28 objects are listed in Table 5-3. The column headings are the same as for Table 5-1, with all of the entries for Column 2 (optical-radio lag time) being "?", representing "unable to tell". Note that there are no entries in Tables 5-1, 5-2, or 5-3 which have not been given in other tables elsewhere in this work. The tables in this chapter are merely reorganizations of what has been previously reported. This reorganization was done so that comparisons could more easily be made between objects exhibiting correlated optical and radio events, those not exhibiting correlated optical and radio events, and those which had insufficient data to determine the optical-radio relationship. References for Tables 5-1, 5-2, and 5-3 are the same as references found for other tables in this work.

Of the 18 objects which had adequate temporal coverage for reliable analysis, 8 are BL Lacs, 8 are QSOs, and 2 are Seyfert galaxies. There is no significant difference between Table 5-1 (correlated optical and radio) and Table 5-2 (uncorrelated optical and radio) as far as the number of BZRs and OVVs is concerned. However, an interesting result of this study is that most of the objects which show correlated optical and radio events are BL Lacs (6 of the 9 listed in Table 5-1), whereas most of the objects which do not show correlated optical and radio events are QSOs (7 of the 9 listed in Table 5-2). That BL Lacs exhibit correlated optical and radio events is consistent with the relativistic beaming interpretation of BL Lac behavior. With relativistic beaming, the optical and radio continuum flux is due to relativistic bulk motion toward the observer at a small angle to the line of sight. Looking nearly down the jet axis, optical and radio emission is unobstructed. If the jet is not oriented near to the line of sight, as would be the case for the parent populations of BL Lacs and OVV QSOs, optical emission may be obstructed by, for example, a geometrically thick and optically thick accretion disk.

Behavior characteristic of OVV QSOs has also been suggested to be caused by relativistic beaming. There is one OVV QSO listed in Table 5-1 as exhibiting correlated optical and radio events, the object 1921-293. This object has a longer lag time than most of the other objects listed in Table 5-1. Only the Seyfert galaxy, 0007+106 (III Zw 2) has a lag time which is comparable in length (unless, of course, the -14 month lag for the BL Lac object OJ 287 (0851+202) is the proper choice for that object). All of the BL Lacs in Table 5-1 have very short lag times (between -6 and 0 months) except perhaps for OJ 287 which has a lag of either -2 to 0 months or -14 months. This suggests that perhaps opacity effects are more important for QSOs than for BL Lacs or perhaps that the optical emission region is farther away in QSOs than in BL Lacs. Since there is only one OVV QSO in Table 5-1 to compare to the BL Lacs, no firm conclusions should be drawn about differences in the two.

A cautionary remark should also be made concerning the $\sim$1 year lag times found for III Zw 2 (0007+106) and 1921-293. Consider the correlation analysis history of OJ 287. For this object, the large long-term variations in the optical flux and in the radio flux prior to 1974 are offset by roughly one year. This is why Pomphrey et al. (1976) found a lag of -0.875 years and why Valtaoja et al. (1987) found a similar lag for pre-1975 data and a shorter lag for post-1975 data. By including ARO data, short-term events are identified in the radio which are nearly simultaneous with optical events. An analysis of OJ 287 including this ARO data indicates a lag time of -1 to 0 months instead of -14 months. Visual inspection of the III Zw 2 and 1921-293 data suggests that perhaps with more complete sampling, events could be seen which would indicate shorter lag times as was the case for OJ 287.

In Table 5-2 for objects whose optical and radio events are not correlated, 2 of the 9 objects are BL Lacs, 4 are QSOs which have been called blazars in the literature, and

3 are non-OVV QSOs which have not been called blazars in the literature according to Burbidge and Hewitt (1992). One of these non-OVV QSOs, however, does exhibit superluminal motion and so relativistic beaming is suggested. For many objects in Table 5-1 which did exhibit correlated optical and radio events, there were times when the optical and radio were not correlated (3C 120 and BL Lac, for example). Because an object in Table 5-2 did not exhibit correlated optical and radio events in the available light curves does not mean that it never has or never will. So, it is perhaps not valid to draw any conclusions about differences in BL Lacs and QSOs from Table 5-2 since the sample is small and the objects in Table 5-2 may have in the past, or may in the future exhibit correlated optical and radio events.

If opacity effects are more important for QSOs than for BL Lacs, then one might expect the 14.5 GHz - 8.0 GHz lag times to be longer in QSOs than in BL Lacs. However, there is no clear-cut difference seen in the 14.5 GHz - 8.0 GHz lag times for BL Lacs and QSOs. Thirteen BL Lacs had adequate temporal coverage in both the 14.5 GHz and the 8.0 GHz data sets for reliable correlation analysis. All of them had 14.5 GHz - 8.0 GHZ lag times between -4 and 0 months. Of the 15 QSOs for which reliable 14.5 GHz - 8.0 GHz correlation analysis was performed, all but 2 had 14.5 GHz events leading 8.0 GHz events by less than 5 months. One object had a 14.5 GHz - 8.0 GHz lag of -7 to -3 months and the other, a lag of -13 to -11 months. Based on this, it does not appear that opacity effects in the radio emission regions of BL Lacs and QSOs differ. Even fewer objects have adequate 4.8 GHz data to perform reliable 8.0 GHz - 4.8 GHz correlation analysis. Both the BL Lacs and the QSOs have 8.0 GHz - 4.8 GHZ lag times between -5 and 0 months. So, as with the 14.5 GHz - 8.0 GHz correlation analysis, no significant difference between BL Lacs and QSOs is seen in the 8.0 GHz - 4.8 GHz correlation analysis.

The Quality of the Data

Not surprisingly, the objects for which reliable correlation analysis could be performed (those in Tables 5-1 and 5-2) had better temporal coverage than the rest (Table 5-3). The average density of optical observations for objects in Tables 5-1 and 5-2 was 7.4 observations per year compared with 5.2 observations per year for objects in Table 5-3. Even the average density of radio observations is slightly better for all objects in Tables 5-1 and 5-2 (9.6 observations per year) than for those in Table 5-3 (8.2 observations per year). This illustrates one of several shortcomings in the data available for this type of analysis. Some of the shortcomings are described below.

Temporal coverage, especially in the optical, is inadequate.

a.) Optical events have much shorter durations than radio events. Short-term optical events are rarely resolved. Often, only one point defines an optical event (as with 0048-097 and 1921-293).

b.) Optical observations cannot be made for a portion of every month because the moon's position comes too close to the position of the object (i.e., the moon is up during the night when observations would be made). Also, an object cannot be observed optically for a portion of every year because the object's position is too near the position of the sun (i.e., the object is above the horizon during the day).

c.) Ground based optical observations cannot be made during poor weather conditions.

d.) Objects which are not highly variable are not observed as frequently as highly variable ones. This is the reason that 37 of the 46 objects examined in this work are BZRS, OVVs, HPQs, and/or SLSs (see Table 2-2). Objects were not included in this work if their optical temporal coverage was too poor. (As seen in Table 5-3, many objects originally thought to have adequate temporal coverage, did not.)

For the most part, radio observations seem to be adequate as far as temporal coverage is concerned. The shortest variability timescales in the radio are generally on the order of months and so short-term radio events will be well-resolved even if observations are made only once a month. (Notice, however, that this is not true for BL Lac prior to 1978.) Also, radio observers do not have the severe restriction caused by the sun that optical observers have, and therefore, radio light curves are not plagued by yearly gaps in the data as are optical light curves.

An examination of Tables 5-1 through 5-3 shows that the number of data points per year is comparable for the optical and radio light curves. The main reason for this is that the radio observations are monthly averages, with at most, one data point per month in the radio light curve. This is the case for the UMRAO data but not the ARO data. Monthly averages were not used in the optical light curves. Only if more than one observation was made in a given night were the optical data averaged. For some of the more variable objects, optical observations were made two or more times per month whenever possible. This effectively increases the number of data points per year in the optical light curves, making N/year comparable for both optical and radio light curves despite the yearly gaps in the optical light curves.

The gap in frequency between optical and radio is enormous (6 to 7 orders of magnitude). Without information at intermediate frequencies, opacity effects such as those seen when comparing two nearby radio frequencies, when extrapolated into the optical regime, will surely make it difficult, if not impossible, to identify correlated optical and radio events. See, for example, the 14.5 GHz and 8.0 GHz data for 0420-014.

These are all problems that have been recognized since this type of analysis was first attempted. How do we overcome these problems? Some of these problems will be very difficult to completely overcome, poor weather and limitations due to the sun and the moon, for example. Spacebased observations could largely overcome these problems, but the likelihood of getting sufficient temporal coverage from space over the long term are slim, if not none. Also highly desirable would be to open up more of the frequency regime between optical and radio to observations. Monitoring programs for higher frequencies than those observed by UMRAO and ARO do exist. For example, observations have been made for some objects at 22.2 GHz and 36.8 GHz since 1978 (Salonen et al., 1983, 1987) and at 90 GHz since 1965 (Epstein et al., 1982). However, there is still an enormous gap in the observed spectrum between optical and millimeter or even submillimeter wavelengths.

Major improvements can be made in the quality of optical data, even with ground-based observations. The long-term monitoring programs, such as the optical monitoring program of the University of Florida, and the radio monitoring programs of UMRAO and ARO, have proved invaluable in searches for correlated optical and radio events. A dedicated long-term optical monitoring program such as the one at the University of Florida, which concentrates on observations of perhaps a few dozen objects would be beneficial. By observing fewer objects, better temporal coverage is almost guaranteed for those objects than can be obtained with the large program at the University of Florida. Emphasis can be placed on resolving short-term events. Problems associated with the moon can be overcome to some extent by observing into moontime whenever possible. Even problems with the sun can be somewhat alleviated by observing objects which are well away from the ecliptic and high in the mid-summer sky. Such objects can be observed before dawn during the spring and in the early evening in the fall.

Summary

Nine objects were found to show correlated optical and radio events. Another nine objects were found to exhibit no correlated optical and radio behavior. The remaining 28 objects which were examined in this work either did not have adequate temporal coverage in one or both light curves to reliably search for correlated events, or the number and spacing of events in one or both light curves made identification of correlated events impossible.

The objects which exhibited correlated optical and radio events were for the most part BL Lac objects. BL Lacs exhibiting correlated optical and radio events is consistent with the relativistic beaming interpretation of BL Lac behavior. There was one OVV QSO which showed correlated optical and radio events, but with a longer lag time than for the BL Lacs. This suggests that opacity effects may be more important for QSOs than for BL Lacs or that the optical and radio emission region are more widely separated physically in QSOs than in BL Lacs. However, the sample is too small to draw any definitive conclusions about differences between BL Lacs and OVV QSOs. Correlation analysis between two radio frequencies shows no difference in lag times for QSOs and BL Lacs.

As has been emphasized by all researchers who have attempted optical-radio correlation analysis of this kind, better temporal coverage is desperately needed in the optical, and much more of the spectral window between optical and radio frequencies needs to be opened up and monitored to improve our understanding of the relationship between the various wavelength regimes and their associated emission mechanisms.

Table 5-1: Objects Showing Correlated Optical and Radio Events

1	2	3	4	5	6	7	8	9
Object	optical-radio lag (mo)	14.5 - 8.0 GHz lag (mo)	8.0 - 4.8 GHz lag (mo)	Type	Other Designation in Literature	XD or SLS	Optical N/yr	Radio N/yr
0007+106	-13	-3 to 0	-4 to 0	Seyfert			5.6	6.6
0048-097	-6 to 0	0	0	BL Lac	BZR	XD	5.2	8.4
0215+015	-5 to 0	0	0	BL Lac	BZR OVV	XD	7.8	6.0
0235+164	-2 to 0	0	0	BL Lac	BZR OVV	SLS XD	7.4	9.9
0430+052	-4 to 0 (’71.0-’80.0)	0	0	Seyfert	OVV	SLS	7.5	10.2
0851+202	-14 or -2 to 0	0	0	BL Lac	BZR OVV	SLS XD	13.1	12.6
1749+096	-3 to 0	-1 to 0	0	BL Lac	BZR	XD	5.0	10.8
1921-293	-11 to -10	-1 to 0	-1 to 0	QSO	BZR HPQ OVV	XD	3.6	9.2
2200+420	-2 to 0 (pre-1977.0)	0	0	BL Lac	BZR OVV	SLS	16.6	23.4
						Average	8.0	10.8

Table 5-2: Objects whose Optical and Radio Events are Not Correlated

1	2	3	4	5	6	7	8	9
Object	optical-radio lag (mo)	14.5 - 8.0 GHz lag (mo)	8.0 - 4.8 GHz lag (mo)	Type	Other Designations in Literature	SLS or XD	Optical N/yr	Radio N/yr
0229+131	NC	—	—	QSO			3.0	5.0
0735+178	NC	0	0	BL Lac	BZR OVV	SLS XD	9.9	9.6
0829+049	NC	?	?	BL Lac	BZR OVV	XD	6.6	5.3
1156+295	NC	-1 to 0	-3 to 0	QSO	BZR HPQ OVV		16.4	9.0
1226+023	NC	-7 to -3	-5 to 0	QSO		SLS	5.2	10.1
2201+315	NC	?	?	QSO			4.1	9.5
2230+114	NC	-2 to 0	?	QSO	BZR HPQ	SLS XD	4.0	9.7
2251+158	NC	-3 to 0	-3 to 0	QSO	BZR HPQ OVV	SLS XD	5.4	9.8
2345-167	NC	—	—	QSO	BZR HPQ OVV	XD	6.1	7.2
						Average	6.8	8.4

Table 5-3: Objects with Inconclusive Optical-Radio Correlation Analysis

1	2	3	4	5	6	7	8	9
Object	optical-radio lag (mo)	14.5 - 8.0 GHz lag (mo)	8.0 - 4.8 GHz lag (mo)	Type	Other Designations in Literature	SLS or XD	Optical N/yr	Radio N/yr
0333+321	?	-13 to -11	?	QSO			2.9	10.7
0336-019	?	-2 to 0	-1 to 0	QSO	BZR HPQ	XD	3.9	9.6
0420-014	?	-1 to 0	-4 to 0	QSO	BZR HPQ OVV	XD	6.9	11.5
0422+004	?	0	0	BL Lac	BZR OVV	XD	3.9	9.3
0440-003	?	—	—	QSO	BZR OVV	XD	4.9	4.4
0723-008	?	?	?	NSO			4.8	6.6
0736+017	?	-2 to 0	-2 to 0	QSO	BZR HPQ	XD	5.3	7.1
0754+100	?	-2 to 0	-2 to 0	BL Lac	BZR	XD	4.8	7.5
0953+254	?	—	—	QSO			4.4	5.4
1101+384	?	?	?	BL Lac	BZR	XD	4.5	7.6
1148-001	?	?	?	QSO			1.4	4.6
1219+285	?	-1 to 0	?	BL Lac	BZR OVV	XD	7.8	8.2
1253-055	?	0	0	QSO	BZR HPQ OVV	SLS XD	4.4	9.6
1308+326	?	-4 to 0	-3 to 0	BL Lac	BZR HPQ OVV	XD	7.8	11.2
1418+546	?	0	0	BL Lac	BZR	XD	2.9	11.2
1510-089	?	-1 to 0	-2 to 0	QSO	BZR HPQ	XD	4.0	10.5
1514-241	?	?	?	BL Lac	BZR OVV	XD	6.1	5.2
1611+343	?	0	-3 to 0	QSO			3.4	9.4
1641+399	?	0	0	QSO	BZR HPQ OVV	SLS XD	11.4	9.9
1652+398	?	?	?	BL Lac	BZR	XD	6.1	7.6
1730-130	?	-4 to 0	-3 to 0	QSO	OVV		3.1	8.4

Table 5-3: (Continued)

1	2	3	4	5	6	7	8	9
Object	optical-radio lag (mo)	14.5 - 8.0 GHz lag (mo)	8.0 - 4.8 GHz lag (mo)	Type	Other Designations in Literature	SLS or XD	Optical N/yr	Radio N/yr
1749+701	?	?	?	BL Lac	BZR	SLS XD	3.6	8.4
1807+698	?	?	?	BL Lac	BZR OVV	SLS XD	7.9	7.5
1901+319	?	?	?	QSO		SLS	5.0	6.4
2134+004	?	?	?	QSO			2.7	7.3
2144+092	?	?	?	QSO	OVV		7.2	6.7
2145+067	?	-5 to +1	?	QSO			4.0	9.5
2223-052	?	-1 to 0	-4 to 0	BL Lac	BZR HPQ OVV	SLS XD	9.9	9.3
						Average	5.2	8.2

BIBLIOGRAPHY

Aller, H. D., Aller, M. F., Latimer, G. E., and Hodge, P. E. (1985). Astrophys. J. Suppl. 59, 513.

Aller, H. D., Hughes, P. A., and Aller, M. F. (1991) In Variability of active galactic nuclei, edited by H. R. Miller and P. J. Witta (Cambridge University Press, Cambridge), p. 172.

Andrew, B. H., MacLeod, J. M., Harvey, G. A., and Medd, W. J. (1978). Astron. J. 83, 863.

Andrew, B. H., MacLeod, and Feldman, P. A. (1981). Astron. Ap. 99, 36.

Balonek, T. J. (1982). Ph. D. dissertation, University of Massachusetts.

Blandford, R. D., and Königl, A. (1979). Astrophys. J. 232, 34.

Blandford, R. D., and Rees, M. J. (1974). Mon. Not. R. Astron. Soc. 169, 395.

Bregman, J. N., and Hufnagel, B. R. (1989). In BL Lac Objects, edited by L. Maraschi, T. Maccacaro, and M.-H. Ulrich (Springer-Verlag, Berlin), p. 159.

Brown, L. M. J., Robson, E. I., Gear, W. K., Hughes, D. H., Griffin, M. J., Geldzahler, B. J., Schwartz, P. R., Smith, M. G., Smith, A. G., Shepherd, D. W., Webb, J. R., Valtaoja, E., Terasranta, H., and Salonen, E. (1989). Astrophys. J. 340, 129.

Burbidge, G., and Hewitt, A. (1992). In Variability of Blazars, edited by E. Valtaoja and M. Valtonen (Cambridge University Press, Cambridge), p. 4.

Dent, W. A. (1968). Astrophys. J. Lett. 153, L29.

Edelson, R. A., and Krolik, J. H. (1988). Astrophys. J. 333, 646.

Edelson, R. A., and Malkan, M. A. (1986). Astrophys. J. 308, 59.

Epstein, E. E., Fogarty, W. G., Mottmann, J., and Schneider, E. (1982). Astron. J. 87, 449.

Ghisellini, G., Maraschi, L., and Treves, A. (1985). Astron. Astrophys. 146, 204.

Hayes, D. S., and Latham, D. W. (1975). Astrophys. J. 197, 593.

Hewitt, A., and Burbidge, G. (1987). Astrophys. J. Suppl. 63, 1.

Hughes, P. A., Aller, H. D., and Aller, M. F. (1989a). Astrophys. J. 341, 54.

Hughes, P. A., Aller, H. D., and Aller, M. F. (1989b). Astrophys. J. 341, 68.

Hutter, D. J., and Mufson, S. L. (1986). Astrophys. J. 301, 50.

Jones, T. W., O'Dell, S. L., and Stein, W. A. (1974). Astrophys. J. 188, 353.

Kellerman, K. I., and Pauliny-Toth, I. I. K. (1969). Astrophys. J. Lett. 155, L71.

Königl, A. (1981). Astrophys. J. 243, 700.

Leqeuex, J. (1962). Ann. Astrophys. 25, 221.

Lü, P. K. (1972). Astron. J. 77, 829.

Marscher, A. P. (1980). Astrophys. J. 235, 386.

Medd, W. J., Andrew, B. H., Harvey, G. A., and Locke, J. L. (1972). Mem. R. Astron. Soc. 77, 109.

Pauliny-Toth, I. I. K., and Kellerman, K. I. (1966). Astrophys. J. 146, 634.

Pearson, T. J., and Zensus, J. A. (1987). In Superluminal Radio Sources, edited by J. A. Zensus and T. J. Pearson (Cambridge University Press, Cambridge), p. 1.

Penston, M. J., and Cannon, R. (1970). R. Obs. Bull. No. 159.

Peterson, F. W., and Dent, W. A. (1973). Astrophys. J. 186, 421.

Peterson, F. W., and King, C., III (1975). Astrophys. J. 195, 753.

Pica, A. J., Smith, A. G., Webb, J. R., Leacock, J. L., Clements, S., and Gombola, P. P. (1988). Astron. J. 96, 1215.

Pollock, J. T., Pica, A. J., Smith, A. G., Leacock, R. J., Edwards, P. L., and Scott, R. J. (1979). Astron. J. 84, 1658.

Pomphrey, R. B. (1977). Ph. D. dissertation, University of Florida.

Pomphrey, R. B., Smith, A. G., Leacock, R. J., Olsson, C. N., Scott, R. L., Pollock, J. T., Edwards, P., and Dent, W. A. (1976). Astron. J. 81, 489.

Rees, M. J. (1966). Nature 211, 468.

Rees, M. J. (1967). Mon. Not. R. Astron. Soc. 135, 345.

Reynolds, S. P. (1982). Astrophys. J. 256, 38.

Salonen, E., Lehto, H., Urpo, S., Teerikorpi, P., Teräsranta, H., Haarala, S., Valtaojo, E., Tähtinen, L., Sillanpää, A., Tiuri, M., and Valtonen, M. (1983). 51, 47.

Salonen, E., Teräsranta, H., Urpo, S., Tiuri, M., Moiseev, I. G., Nesterov, N. S., Valtaoja, E., Haarala, S., Lehto, H., Valtaoja, L., Teerikorpi, P., and Valtonen, M. (1987). 70, 409.

Seielstad, G. A. (1974). Astrophys. J. 193, 55.

Shklovskii, I. S. (1960). Soviet Astron. – Astron. J. 4, 243.

Strittmatter, P. A., Carswell, R. F., Gilbert, G., and Burbidge, E. M. (1974). 190, 509.

Urry, C. M. (1988). In Multiwavelength Astrophysics, edited by F. Cordóva (Cambridge University Press, Cambridge), p. 279.

Usher, P. D. (1979) Astron. J. 84, 1253.

Valtaoja, L., Sillanpää, A., and Valtaoja, E. (1987). Astron. Astrophys. 184, 57.

van der Laan, H. (1962). Mon. Not. R. Astron. Soc. 124, 125.

Walker, R. C., Benson, J. M., and Unwin, S. C. (1987). In Superluminal Radio Sources, edited by J. A. Zensus and T. J. Pearson (Cambridge University Press, Cambridge), p. 48.

Webb, J. R., Smith, A. G., Leacock, R. J., Fitzgibbons, G. L., Gombola, P. P., and Shepherd, D. W. (1988). Astron. J. 95, 374.

BIOGRAPHICAL SKETCH

Sandra Denise Clements was born on April 23, 1963, in Birmingham, Alabama. She graduated from Huffman High School in June of 1981. A physics major at Auburn University in Auburn, Alabama, she graduated with a Bachelor of Science degree in June of 1985. She then moved to Baltimore, Maryland, to work for a year as a Research Assistant at the Space Telescope Science Institute. In August of 1986, she entered the Graduate School of the University of Florida where she worked as a graduate teaching assistant in the Department of Astronomy. The following year, she joined the AGN-monitoring program as a graduate research assistant and has been an observer with that program for the rest of her graduate school career. During that time, she earned her Master of Science degree in astronomy and has completed the research requirements for the degree of Doctor of Philosophy in astronomy.

I certify that I have read this study and that in my opinion it conforms to acceptable standards of scholarly presentation and is fully adequate, in scope and quality, as a dissertation for the degree of Doctor of Philosophy.

Alex G. Smith

Alex G. Smith, Chair
Distinguished Service Professor
of Astronomy

I certify that I have read this study and that in my opinion it conforms to acceptable standards of scholarly presentation and is fully adequate, in scope and quality, as a dissertation for the degree of Doctor of Philosophy.

Robert J. Leacock

Robert J. Leacock, Cochair
Associate Professor of Astronomy

I certify that I have read this study and that in my opinion it conforms to acceptable standards of scholarly presentation and is fully adequate, in scope and quality, as a dissertation for the degree of Doctor of Philosophy.

James H. Hunter

James H. Hunter
Professor of Astronomy

I certify that I have read this study and that in my opinion it conforms to acceptable standards of scholarly presentation and is fully adequate, in scope and quality, as a dissertation for the degree of Doctor of Philosophy.

Thomas D. Carr

Thomas D. Carr
Professor of Physics and
Astronomy

I certify that I have read this study and that in my opinion it conforms to acceptable standards of scholarly presentation and is fully adequate, in scope and quality, as a dissertation for the degree of Doctor of Philosophy.

Neil S. Sullivan
Professor of Physics

This dissertation was submitted to the Graduate Faculty of the Department of Astronomy in the College of Liberal Arts and Sciences and to the Graduate School and was accepted as partial fulfillment of the requirements for the degree of Doctor of Philosophy.

August 1992

Dean, Graduate School